

ET  
1417

Engineering  
Library

INVESTIGATION OF BOND IN BEAMS  
WITH TOR STEEL REINFORCEMENT

By

GEORGE J. UBAJI

Submitted to the School of Engineering, American University of Beirut, in partial fulfilment of requirements for the degree of Master of Engineering, Major in Civil Engineering.

Adviser: Prof. Hanna M. MAKHLOUF

Beirut, Republic of Lebanon  
September 1966

## ACKNOWLEDGEMENTS

The author wishes to express his sincerest appreciation to Professor Hanna M. Makhlouf, Assistant Professor of Civil Engineering, under whose direction this research was performed, for his invaluable assistance and encouragement in all of its phases; to Professors: Robert W. Sloane, Professor of Engineering Sciences; Raja A. Iliya, Associate Professor of Civil Engineering; and Terence R. Searle Assistant Professor of Civil Engineering, for their assistance.

The author wishes to express his thanks to the School of Engineering which sponsored this research.

The author wishes to thank his wife for her assistance.

## TABLE OF CONTENTS

Page

LIST OF TABLES . . . . .	i
LIST OF FIGURES . . . . .	iii
LIST OF PHOTOGRAPHS . . . . .	v
LIST OF SYMBOLS . . . . .	vi
ABSTRACT . . . . .	vii
INTRODUCTION . . . . .	1
I: THEORETICAL BACKGROUND . . . . .	3
II. EXPERIMENTAL WORK	
a) Description of Beams . . . . .	9
b) Description of Steel . . . . .	18
c) Loading of the Beams . . . . .	19
d) Reactions . . . . .	30
e) Testing Procedure . . . . .	30
f) Behavior under Test . . . . .	33
III. DATA ANALYSIS	
a) Development Length . . . . .	34
b) The Effect of Cracking upon Development Length . . . . .	40
c) Bond Wave . . . . .	44
d) Concrete Cover . . . . .	44
IV. SUMMARY AND CONCLUSIONS . . . . .	49
APPENDIX A . . . . .	50
APPENDIX B . . . . .	57
APPENDIX C . . . . .	58
APPENDIX D . . . . .	81
BIBLIOGRAPHY . . . . .	95

## LIST OF TABLES

Table	Page
I Description of Beams Batch 1 . . . . .	10
II Description of Beams Batch 2 . . . . .	10
III Description of Beams Batch 3 . . . . .	11
1A Concrete Strength Batch 1 . . . . .	51
2A Concrete Strength Batch 2 . . . . .	52
3A Concrete Strength Batch 3 . . . . .	53
C1 Beam D <sub>8-4-1</sub> Test Data . . . . .	60
C2 Beam D <sub>12-2-1</sub> " " . . . . .	61
C3 Beam D <sub>12-1-1</sub> " " . . . . .	62
C4 Beam D <sub>12-4-1</sub> " " . . . . .	63
C5 Beam D <sub>15-4-1</sub> " " . . . . .	64
C6 Beam D <sub>17-4-1</sub> " " . . . . .	65
C7 Beam D <sub>20-4-1</sub> " " . . . . .	66
C8 Beam D <sub>8-4-2</sub> " " . . . . .	67
C9 Beam D <sub>12-4-2</sub> " " . . . . .	68
C10 Beam D <sub>12-2-2</sub> " " . . . . .	69
C11 Beam D <sub>12-1-2</sub> " " . . . . .	70
C12 Beam D <sub>15-4-2</sub> " " . . . . .	71
C13 Beam D <sub>20-4-2</sub> " " . . . . .	72
C14 Beam D <sub>8-4-3</sub> " " . . . . .	73
C15 Beam D <sub>10-4-3</sub> " " . . . . .	74
C16 Beam D <sub>10-2-3</sub> " " . . . . .	75
	76

LIST OF TABLES (Cont'd.)

Table					Page
C17	Beam D <sub>12-4-3</sub>	Test Data	.	.	77
C18	Beam S <sub>1</sub>	" "	.	.	78
C19	Beam S <sub>1</sub>	" "	.	.	79
C20	Beam S <sub>2</sub>	" "	.	.	80

## LIST OF FIGURES

Figure	Page
1 . . . . .	4
2 Wedge Action . . . . .	6
3 Reinforcement Details. Batches 1 and 2 . . . . .	12
4 Reinforcement Details. Batch 3 . . . . .	13
5 Reinforcement Details. Beams $S_1$ and $S_2$ . . . . .	14
6 Test Bar for Beams $S_1$ and $S_2$ . . . . .	16
7 Position of Strain Gages for Beams $S_1$ and $S_2$ . . . . .	17
8 Load v. Strain for Type I Steel . . . . .	20
9 Load v. Strain for Type II Steel . . . . .	21
10 Calibration Curve for Beam $S_1$ . . . . .	22
11 Calibration Curve for Beam $S_2$ . . . . .	23
12 Shear and Moment Diagrams for Beams $D_8$ . . . . .	24
13 Shear and Moment Diagrams for Beams $D_{10}$ . . . . .	25
14 Shear and Moment Diagrams for Beams $D_{12}$ . . . . .	26
15 Shear and Moment Diagrams for Beams $D_{15}$ . . . . .	27
16 Shear and Moment Diagrams for Beam $D_{17}$ . . . . .	28
17 Shear and Moment Diagrams for Beams $D_{20}$ . . . . .	29
18 Bond Stress v. Machine Load. Batch 1 . . . . .	35
19 Bond Stress v. Machine Load. Batch 2 . . . . .	36
20 Bond Stress v. Machine Load. Batch 3 . . . . .	37
21 Bond Stress v. Development Length . . . . .	38
22 Force v. Development Length . . . . .	39
23a . Functioning Strain Gages Beam $S_1$ . . . . .	42
23b Force v. Machine Load Beam $S_1$ . . . . .	42
24a Functioning Strain Gages Beam $S_2$ . . . . .	43
24b Force v. Machine Load Beam $S_2$ . . . . .	43

LIST OF FIGURES (Cont'd).

Figure		Page
25	Bond Wave. Beam S <sub>1</sub> . . . . .	45
26	Bond Stress v. Machine Load for Different Concrete Covers. Batch 1 . . . . .	46
27	Bond Stress v. Machine Load for Different Concrete Covers. Batch 2 . . . . .	47
28	Bond Stress v. Machine Load for Different Concrete Covers. Batch 3 . . . . .	48
A1	Cross Section of Top Steel . . . . .	56
C1	Position of major flexural cracks . . . . .	59

# LIST OF PHOTOGRAPHS

	Page
Testing Machine . . . . .	31
Reinforcements in Formwork . . . . .	31
Reaction . . . . .	32
Load . . . . .	32
Beams at Failure	
Beam D <sub>8-4-1</sub> . . . . .	83
Beam D <sub>12-4-1</sub> . . . . .	84
Beam D <sub>15-4-1</sub> . . . . .	85
Beam D <sub>17-4-1</sub> . . . . .	86
Beam D <sub>20-4-1</sub> . . . . .	87
Beam D <sub>8-4-2</sub> . . . . .	88
Beam D <sub>12-1-2</sub> . . . . .	89
Beam D <sub>12-4-2</sub> . . . . .	90
Beam D <sub>15-4-2</sub> . . . . .	91
Beam D <sub>20-4-2</sub> . . . . .	92
Beam S <sub>1</sub> . . . . .	93
Beam S <sub>2</sub> . . . . .	94



## LIST OF SYMBOLS

- $A_s$  = area of tension reinforcement
- $C$  = compression force
- $d$  = distance from extreme compression fiber to centroid of tension reinforcements
- $f_c$  = compression strength of concrete
- $f_s$  = stress in reinforcements
- $F$  = force in reinforcement
- $j$  = ratio of distance between centroid of compression and centroid of tension to depth,  $d$
- $L_d$  = development length
- $P$  = load
- $R$  = reaction
- $T$  = tension in reinforcement
- $u$  = bond stress
- $u_u$  = ultimate bond stress
- $U_u$  = ultimate average bond force per unit length
- $V$  = total shear at section
- $X$  = distance
- $\sum_o$  = sum of perimeters of all effective bars crossing the section on the tension side

## ABSTRACT

According to the ACI 1963 Building Code, bond failure does not occur if the length between the free end of a reinforcing bar and the point of maximum stress along the bar is greater than a certain minimum length called the "development length". To apply this concept in the design of reinforced concrete members, the concrete cover is specified to be at least 1.5 inches and the steel reinforcing bars should comply with ASTM 305A specifications.

This research program aims at the following three objectives:

1. To verify the ACI Code recommendations on development length using Tor steel which does not conform to ASTM specifications.
2. To investigate the effect of different concrete covers (namely 1.5  $\frac{3}{4}$  and  $\frac{3}{8}$  inches) on development length requirements.
3. To investigate the effect of the cracking pattern on development length.

Twenty-one beams were designed and tested for this purpose. Although this limited number of beams will not allow definite conclusions to be made, the results indicate the following:

1. Tor steel may be treated as deformed bars complying with ASTM 305A specifications.
2. A Tor steel bar 20 mm. in diameter with 1.5 inches of clear concrete cover will develop more force than a similar bar with  $\frac{3}{8}$  inch of clear concrete cover.
3. The cracking pattern influences to a great extent the minimum required development length.

## INTRODUCTION

Bond between steel bars and concrete in reinforced concrete members is an important factor that makes these members stand, and act as a unit. When plain bars are used, bond is provided only by the surface adherence of the concrete to the steel bar, while with deformed bars, it is mostly the wedge action of the lugs (deformation) that provides this bond between the two materials.

Until recently the only criterion to check against bond failure was to ensure that the flexural bond stresses determined by the expression  $u = \frac{V}{\sum o jd}$  were below the allowable stresses, which are based mainly on experimental results from pullout tests and beam tests combined.

In the past 30 years, a great amount of research has been conducted on the mechanics of bond stresses in reinforced concrete beams. Some of the most fruitful studies were made at the University of Texas<sup>1\*</sup> and the Bureau of Standards<sup>2</sup>, where, by means of a thorough testing program, it was established that bond failure does not occur if the length between the free end of a reinforcing bar and the point of maximum stress along the bar is greater than a certain minimum length called the "development length". The reinforcing bars used in the above mentioned studies were deformed bars complying with ASTM 305A specifications.

---

\*The superscripts appearing in this statement and elsewhere in this work refer to the number of the reference listed under Bibliography.

This basic and new concept of checking against bond failure was adopted by the ACI Building Code (1963 edition) wherein it is stated that if the development length of a reinforcing bar is more than the minimum length established in the above mentioned research, there is no need to check for local bond stresses even though locally they may exceed the allowable stresses.

No doubt that this new concept is quite advantageous. To apply it to Tor steel, which is much used in this part of the world, and which does not comply with ASTM 305A specifications needs verification.

In order to verify this, and to investigate the effect of cover over the bars, as well as the effect of crack occurrence on the development bond theory at large, as explained in Chapter I, this study was initiated.

## I. THEORETICAL BACKGROUND

Flexural bond stresses along a reinforcing bar are developed due to the rate of change of tensile forces along the bar as determined by the moment diagram. Isolating an element of a reinforced concrete beam bounded by two sections at a distance  $dx$  away from each other, as shown in Fig. 1a and taking moments of all the forces acting on this free body diagram about point  $a$ , and reducing terms, the following classical bond formula is derived:

$$u = \frac{V}{\sum_o jd} \quad (1)$$

where  $u$  = bond stress

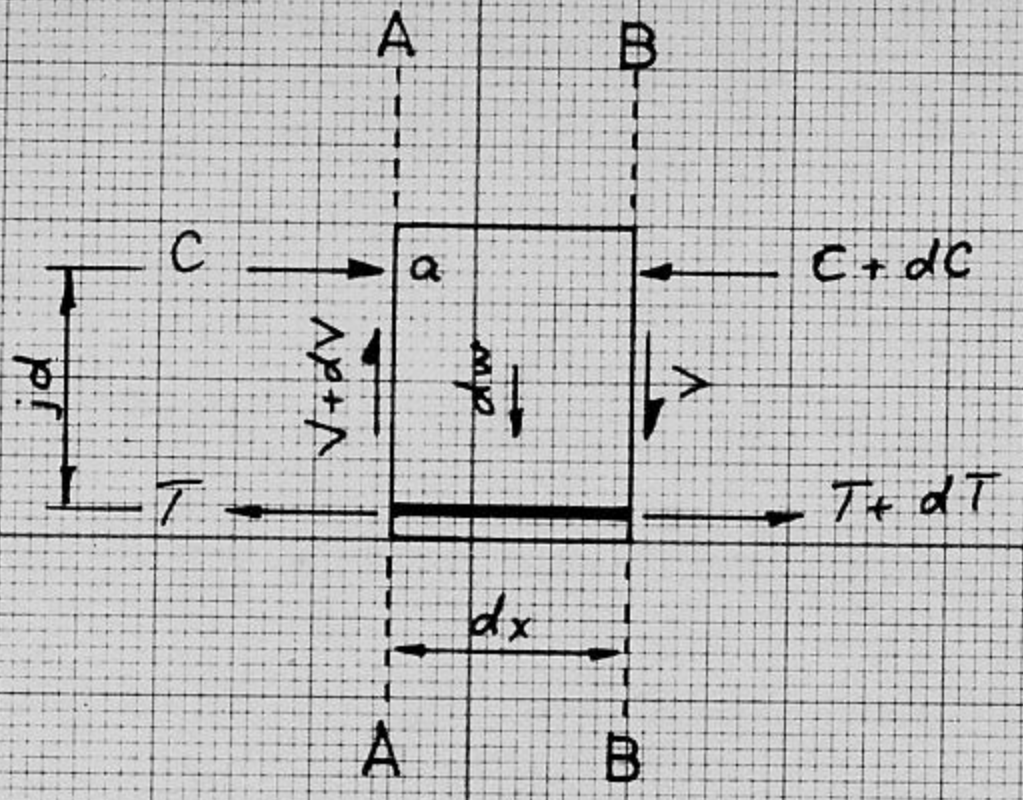
$V$  = total shear at section

$\sum_o$  = sum of perimeters of all effective bars crossing the section on the tension side.

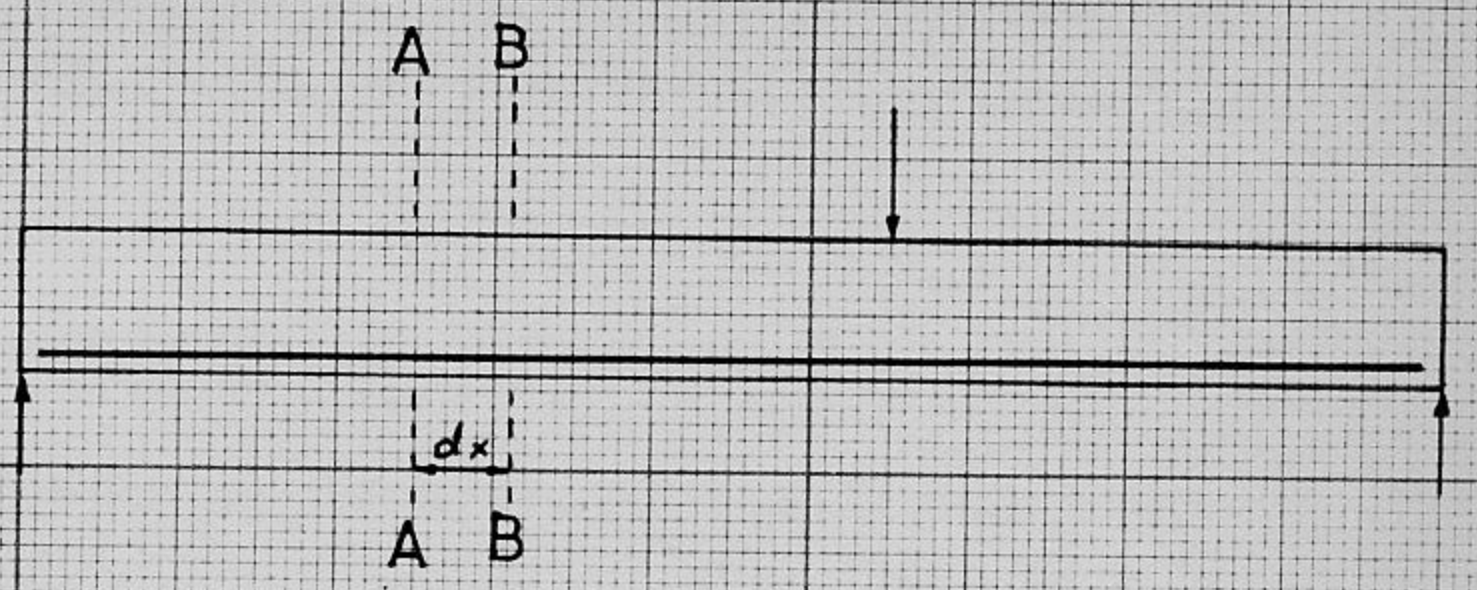
$j$  = ratio of distance between centroid of compression and centroid of tension to depth,  $d$

$d$  = distance from extreme compression fiber to centroid of tension reinforcement.

A bar cut off at any point along the beam will have the tendency to pull out due to the unbalanced tension between its free end and any other section along its length. This phenomenon develops bond stresses, known as anchorage bond, that prevents this slippage between the reinforcing bar and the concrete. To develop the full tensile capacity of the bar, therefore, a certain minimum length called the development length is necessary.

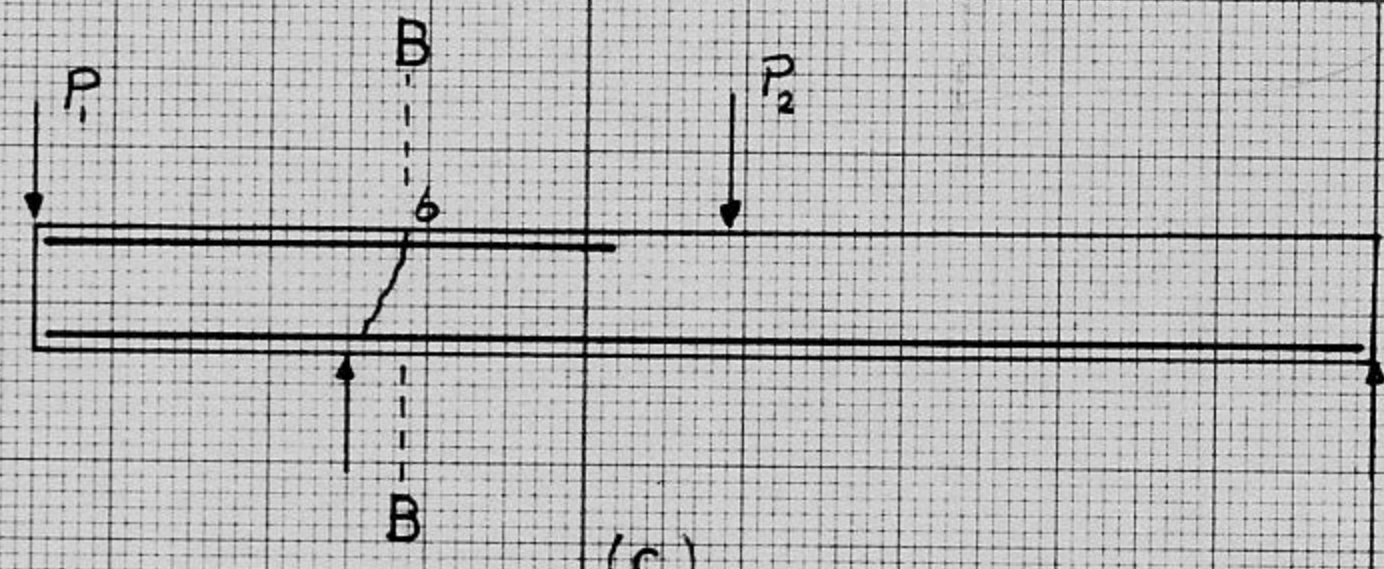


(a)

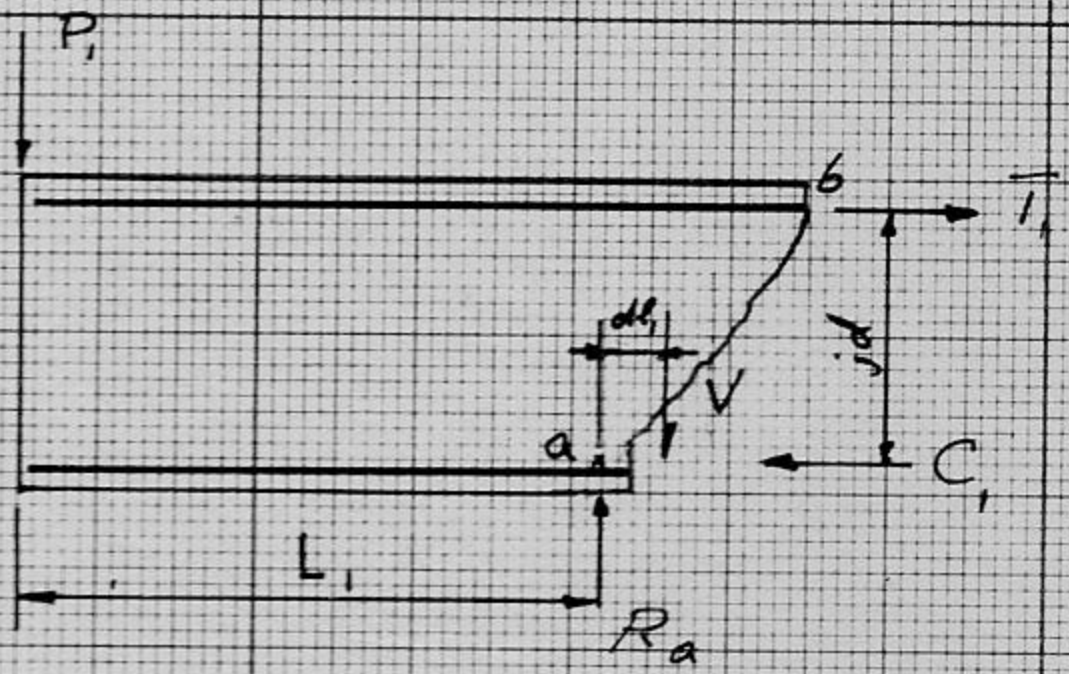


(b)

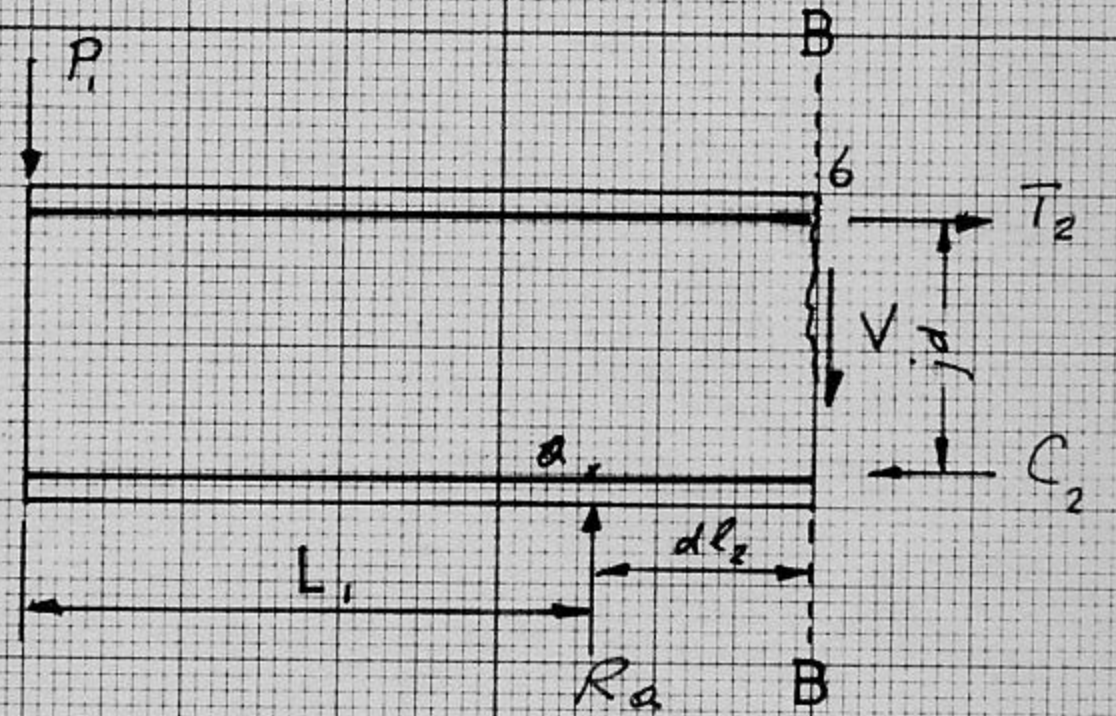
FIG.



(c)



(d)



(e)

FIG.1

Lately a research program at the University of Texas<sup>1</sup> was done, where it was shown that, the bond force (anchorage bond) per inch of bar is constant for any bar diameter; in other words, it is not the bar diameter that determines resistance to slippage, as much as, the mechanical interlock between the concrete and the steel lugs (herein referred to as wedge action) as shown in Fig. 2.

This finding renders the following expression:

$$L_d = \frac{A_s f_s}{U_u} \quad (2a)$$

where  $L_d$  = development length

$A_s$  = area of tension reinforcement

$f_s$  = stress in reinforcement

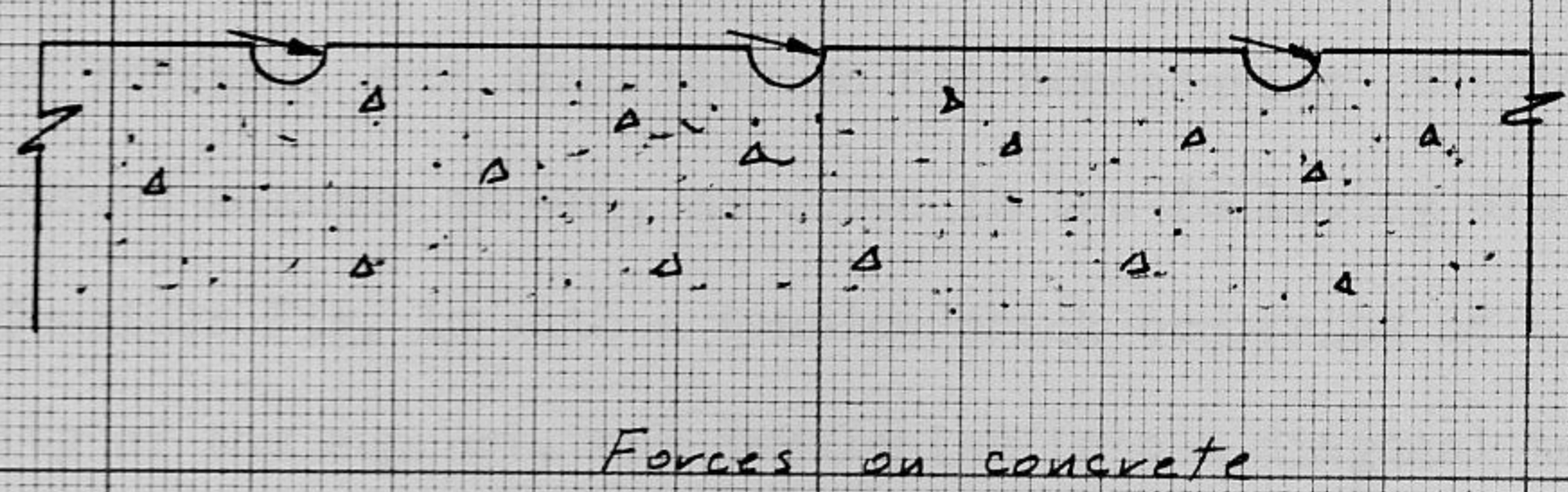
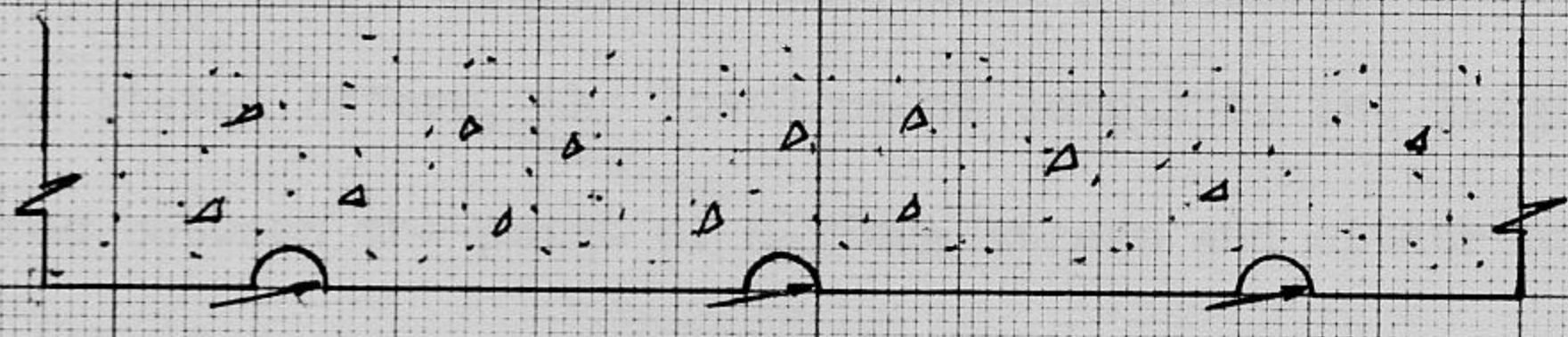
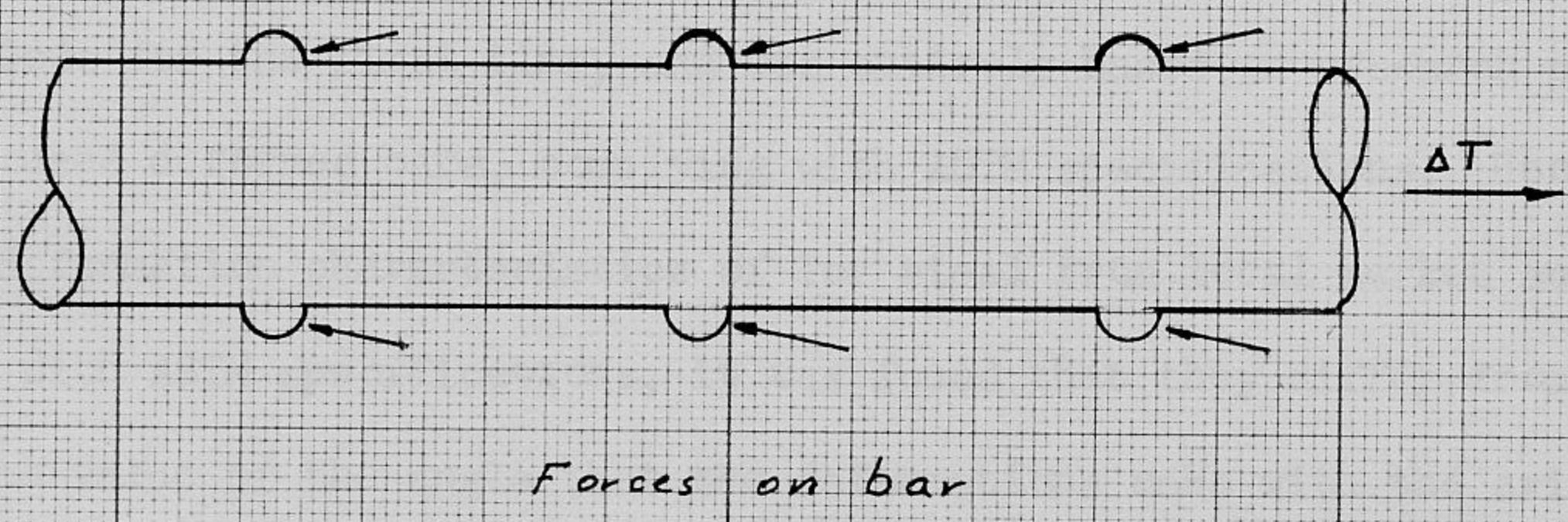
$U_u$  = ultimate average bond force per unit length

The ultimate average bond force per inch of length of bar  $U_u$ , varies from  $30 \sqrt{f'_c}$  to  $35 \sqrt{f'_c}$  as reported in "Design of Concrete Structures"<sup>5</sup>.

Using equation 2a and replacing  $U_u$  by its equivalent  $\sum_o u$  one can also express  $L_d$  in terms of the bar perimeter and an average bond stress around the bar, as follows:

$$L_d = \frac{A_s f_s}{\sum_o u} \quad \text{or} \quad u = \frac{A_s f_s}{L_d \sum_o} \quad (2b)$$

Equations (1) and (2b), both giving a measure of bond stresses along the bar, are derived from two different considerations.



Forces on concrete

FIG. 2 WEDGE ACTION



According to the ACI 1963 Building Code, the flexural bond stress Eq. (1) need not be considered in those cases of tension where anchorage bond is less than 0.8 of the permissible, or in other words, the development or anchorage length is more than 1.25 the permissible.

This new concept of checking for bond stresses was introduced by the ACI Code for the first time, and was entirely based on research programs that used deformed bars, complying with ASTM specifications. Upon checking the deformation characteristics of Tor steel from local market and comparing them with ASTM specifications, it was found that they differ from the latter by the value of the angle that the deformations make with the axis of the bar as well as the non-reversing of direction of the deformations (for details see Appendix A). Therefore research work directed at verifying whether Tor steel exhibits a similar performance as American deformed bars in its resistance to slippage was deemed necessary.

As stated before, the development length is the length along the bar measured between the point of maximum stress and either end. Theoretically the point of maximum stress coincides with the point of maximum moment. There are cases, however, where the cracking pattern in a beam influences the bar stresses such that they do not necessarily coincide with points of theoretical maximum moment, as shown in the following discussion.

Consider Fig. 1c with a tension crack occurring at b, within the vicinity of the support, and developing into a diagonal tension crack as shown. Theoretically the stress in the top bar at point b is governed by the moment at section B-B while, due to the shape of the crack the stress at point b is governed by a greater moment at some inner section between the support and section B-B, this can be proved by comparing Fig. 1d with Fig. 1e, where the crack in Fig. 1e is vertical rather than inclined.

Taking moments about point a in Figs. 1d and 1e respectively one obtains the following two equations:

$$T_1 jd = P_1 L_1 - V dl_1$$

$$T_2 jd = P_1 L_1 - V dl_2$$

but  $dl_2$  is greater than  $dl_1$ , therefore  $T_1$  is greater than  $T_2$ .

To verify this effect of the cracking pattern on development length two beams were designed accordingly, as explained in Chapter II.

## II. EXPERIMENTAL WORK

### a)) Description of Beams

The cross-section of the beams were chosen so that the beam would be large enough to be considered a structural member in an actual building and not too large to fit in the testing machine available in the material testing lab.

The development lengths in the various beams were chosen to vary between the values of 20 inches required by the Code for a 20 mm. deformed bar and 8 inches. This was done in order to ensure that bond failure would take place.

The design of the beams was based upon a value of  $f'_c = 2500$  psi. Using ready mixed concrete, the strength attained was in the order of 5000 psi. This has affected the results, as will be seen later, in the sense that many of the beams that are designed to fail by bond have failed either by yielding of the longitudinal steel or by yielding of the web reinforcement.

There were 21 beams distributed evenly into three batches,\* 7 beam each, poured at different dates. The pouring of the seven beams in each batch was achieved in less than 45 minutes. The procedure was to pour, rod, and vibrate one beam at a time; simultaneously three cylinders were poured with each beam. The dimensions of all the beams are given in the following tables and the reinforcement details are shown in figures 3, 4 and 5.

---

\* The reason for pouring three batches at different dates was the necessity of reusing the same formwork.

Table I

Batch 1.  $f'_c = 4760$  psi

Beam Notation	Development Length (in)	Concrete Cover (in)	Width (in)	Effective Depth d (in)	Total Length of Beam (ft)
D <sub>12-4-1</sub> **	12	1.5	8	12	7.5
D <sub>8-4-1</sub>	8	1.5	8	12	7.5
D <sub>12-2-1</sub>	12	3/4	8	12	7.5
D <sub>12-1-1</sub>	12	3/8	8	12	7.5
D <sub>15-4-1</sub>	15	1.5	8	12	7.5
D <sub>17-4-1</sub>	17	1.5	8	12	7.5
D <sub>20-4-1</sub>	20	1.5	8	12	7.5

Table II

Batch 2.  $f'_c = 5650$  psi

Beam Notation	Development Length (in)	Concrete Cover (in)	Width (in)	Effective Depth d (in)	Total Length (ft)
D <sub>8-4-2</sub>	8	1.5	8	12	7.5
D <sub>12-4-2</sub>	12	1.5	8	12	7.5
D <sub>12-4-2</sub> <sup>+</sup>	12	1.5	8	12	7.5
D <sub>12-2-2</sub>	12	3/4	8	12	7.5
D <sub>12-1-2</sub>	12	3/8	8	12	7.5
D <sub>15-4-2</sub>	15	1.5	8	12	7.5
D <sub>20-4-2</sub>	20	1.5	8	12	7.5

\*Details about the concrete strength are given in Appendix A.

\*\*In the beam notation the first subscript is the development length; the second subscript stands for the cover (4 means a cover of 1.5 inches (4 cm.), 2 means a cover of 3/4 inch (2 cms.), 1 means a cover of 3/8 inch (1 cm.)) and the last subscript is the batch number.

<sup>+</sup>Disregard. see page 3/.

Table III

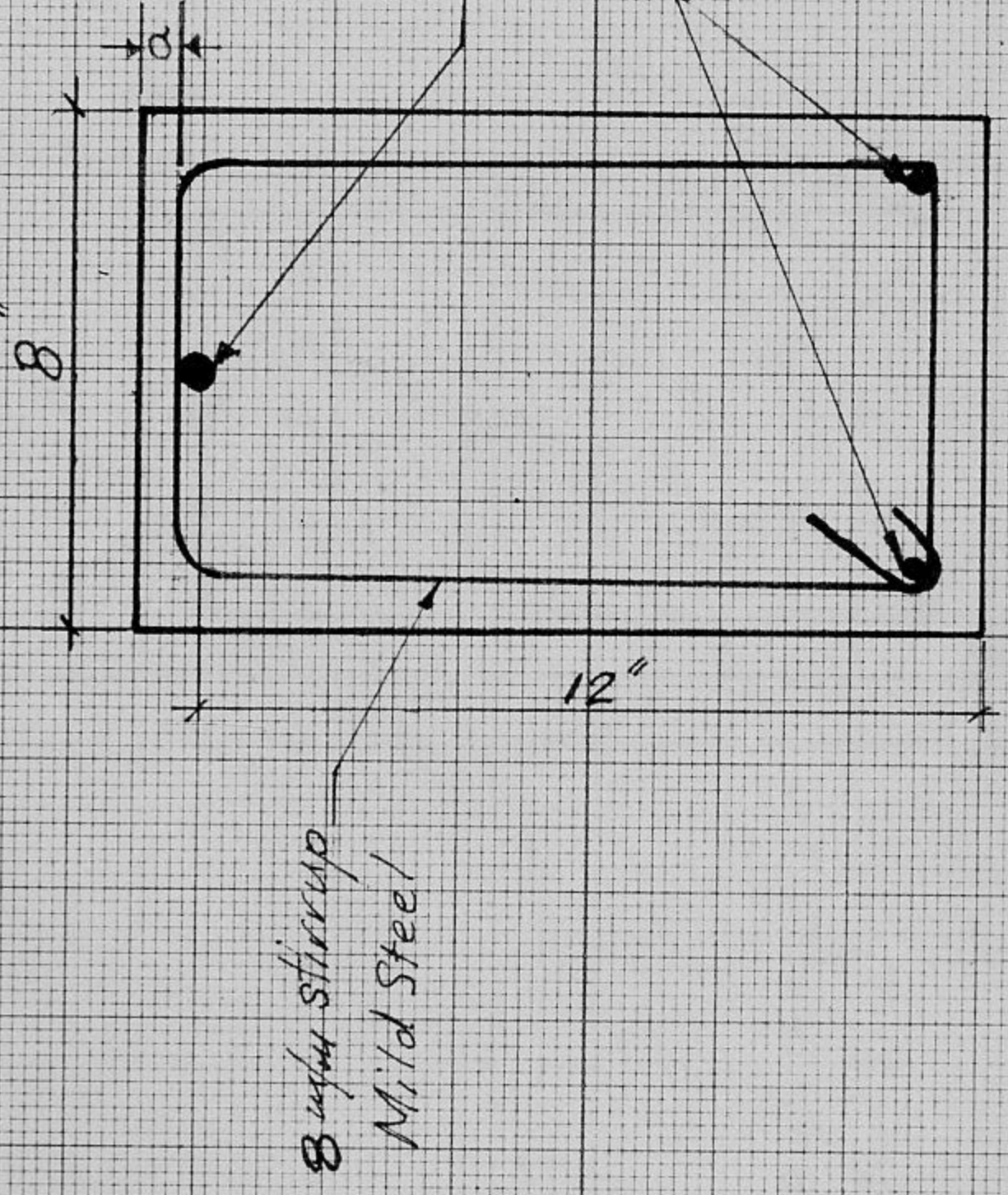
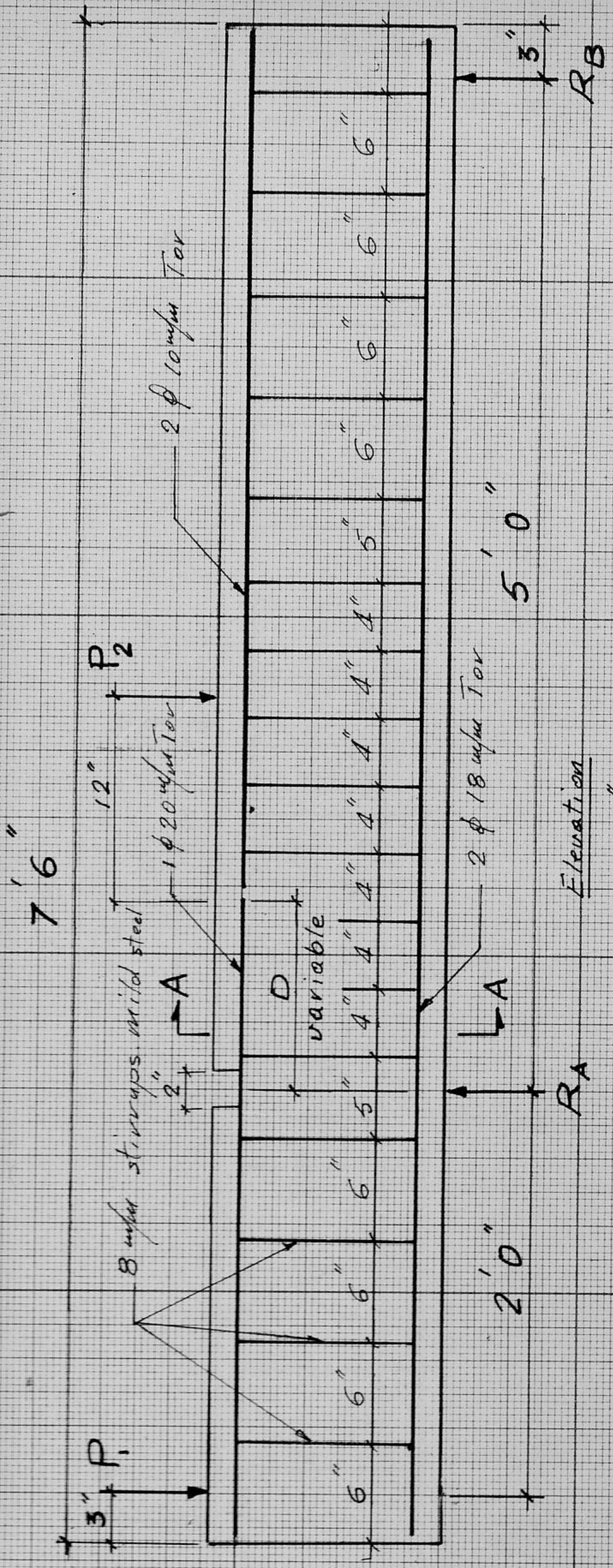
Batch 3.  $f'_c = 4480$  psi

Beam Notation	Development Length (in)	Concrete Cover (in)	Width (in)	Effective Depth d (in)	Total Length (ft)
D <sub>8-4-3</sub>	8	1.5	8	12	7.5
D <sub>12-4-3</sub>	12	1.5	8	12	7.5
D <sub>10-4-3</sub>	10	1.5	8	12	7.5
D <sub>10-2-3</sub>	10	3/4	8	12	7.5
D <sub>10-1-3</sub> *	10	3/8	8	12	7.5
S <sub>1</sub>	10	1.5	8	12	7.5
S <sub>2</sub>	10	1.5	8	12	7.5

As shown in the details of the beams, Figs. 3 and 4, the  $\phi$  20 mm. bar is the one on which anchorage bond stress is measured. This was achieved by mounting a strain gage at the test bar over the reaction  $R_a$ , and that provided the measurement of the tensile force. The anchorage bond stress was obtained by substituting this force, and the length of the bar between this point and the nearest free end of the bar in equation (2).

Moreover, two special beams ( $S_1$  and  $S_2$  shown in Fig. 5) were designed and instrumented to verify the effect of the cracking pattern upon development length, as well as to measure the bar strain at various points along its development length. The test reinforcement in these beams is composed of two

\*The beam was not tested because of excessive honeycombing.



Section A-A

**FIG. 3 REINFORCEMENT  
DETAILS. BATCHES  
I and II**

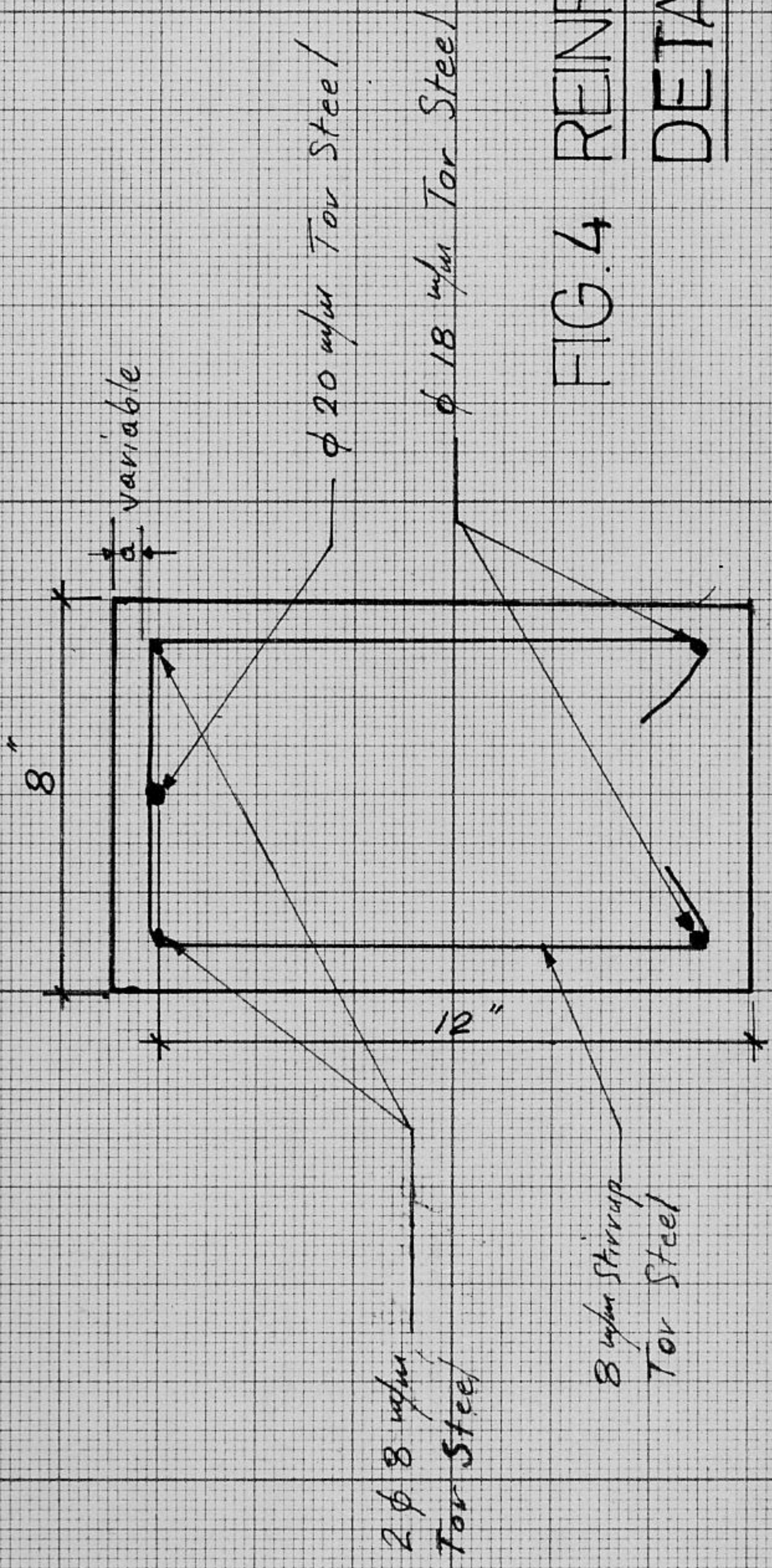
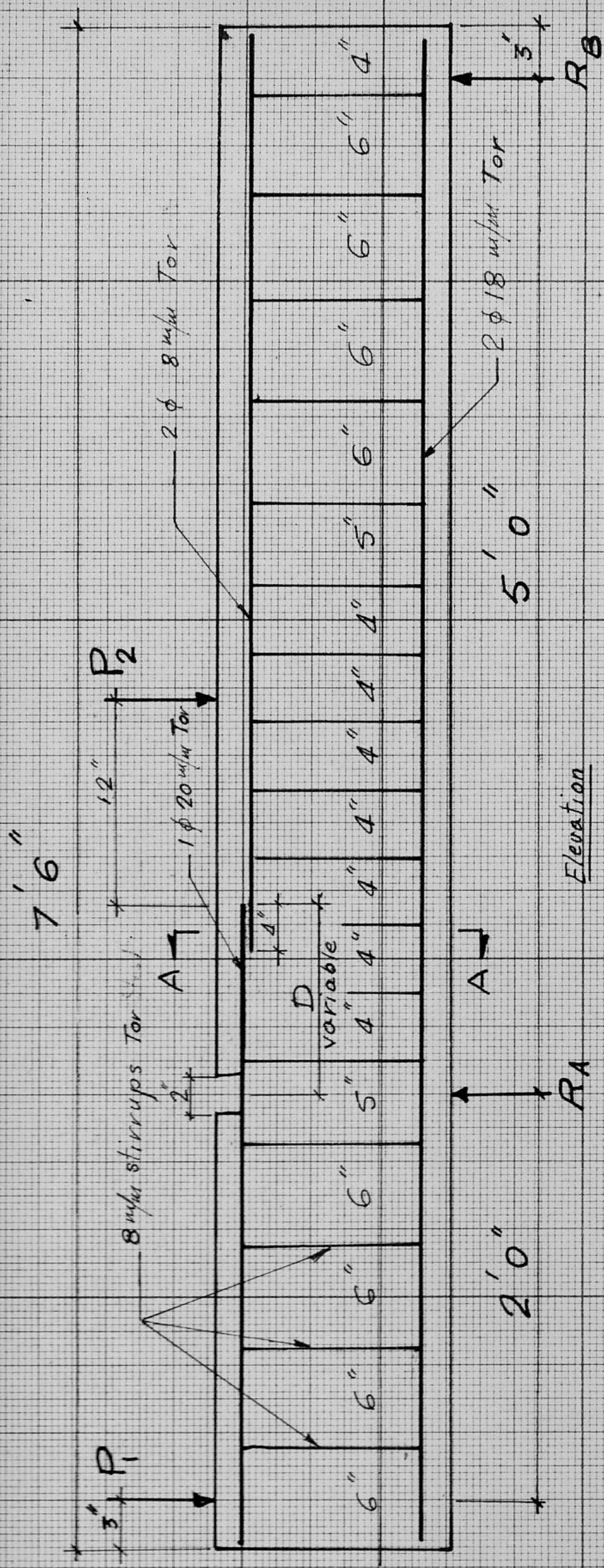


**FIG. 4 REINFORCEMENT  
DETAILS BATCH III**

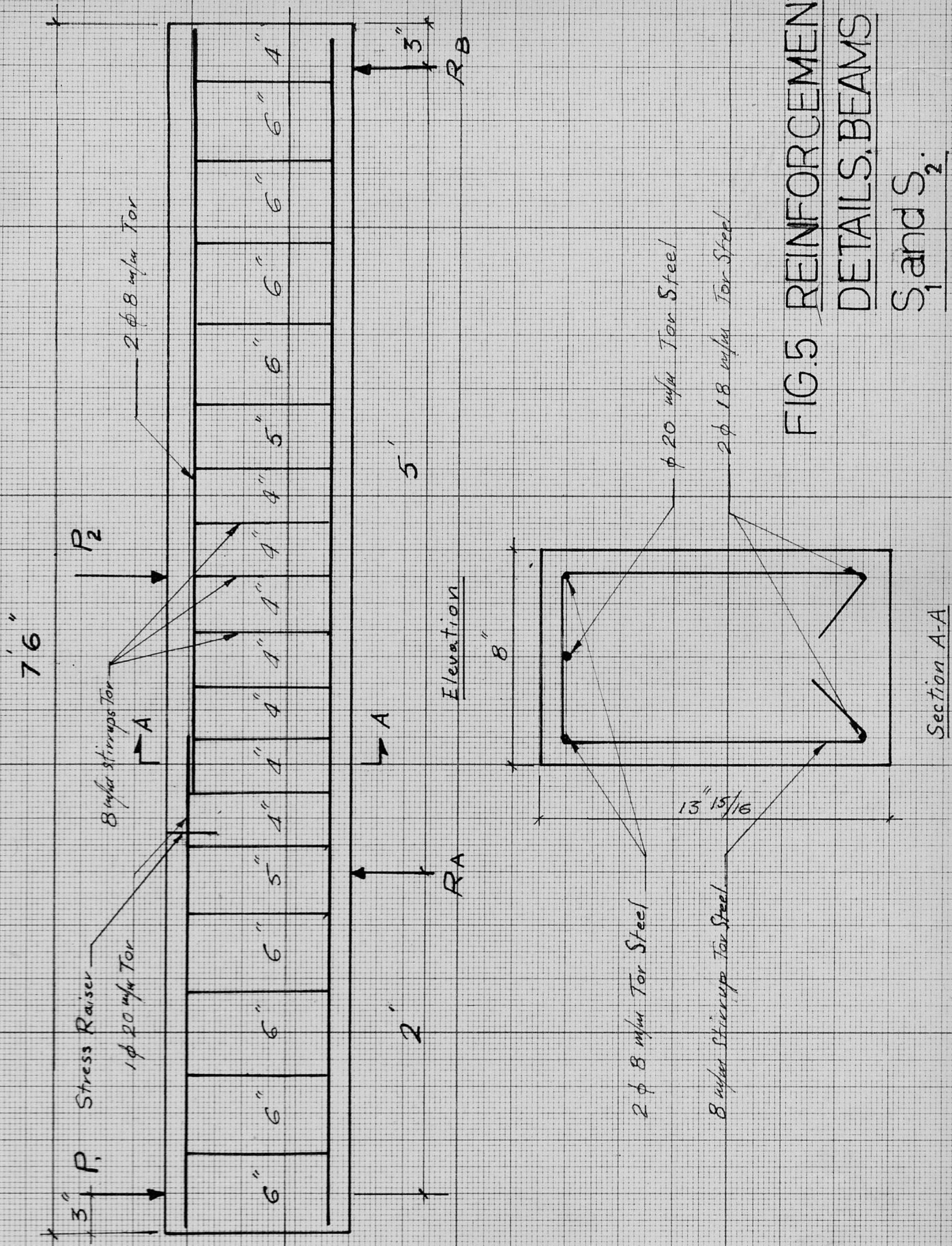


**FIG.5 REINFORCEMENT  
DETAILS. BEAMS  
S<sub>1</sub> and S<sub>2</sub>.**



halves of 20 mm.<sup>+</sup> bar where one half has a groove 10 x 1 mm. along the development length as shown in Fig. 6. Ten strain gages spaced 1 inch center<sup>\*\*</sup> were mounted on the half which does not contain the groove, starting from the inside end of the bar\*.

Thin coated wires were soldered to the terminals of the strain gages and the leads were gathered up and taken out from the inside end of the bar. The wires were then fitted into the groove, the two halves assembled and spot welded at every 4 inches in the depressions made by the continuous deformation and the bar proper, so that the deformations on the bar were barely changed. The resistances of most strain gages were the same before and after welding. Then the bar was fitted in the testing machine and the strain gages calibrated to a stress equal to approximately 0.4 of the yield stress.<sup>++</sup> So that the jaws of the testing machine would not damage the strain gages, the bar was made longer by 10 cms. from the inside end. This extra length was cut after the calibration of the strain gages was performed. Dupont cement was used to fill the thin groove which was left between the halves. Enough care was taken to prevent the adherence of any excess cement to the surface of the bar.

---

\* The inside end of the bar is the end that falls in the span and not at the cantilever part, see Fig. 5

\*\* See Fig. 7

+ See Fig. 6

++ See Figs. 10 and 11

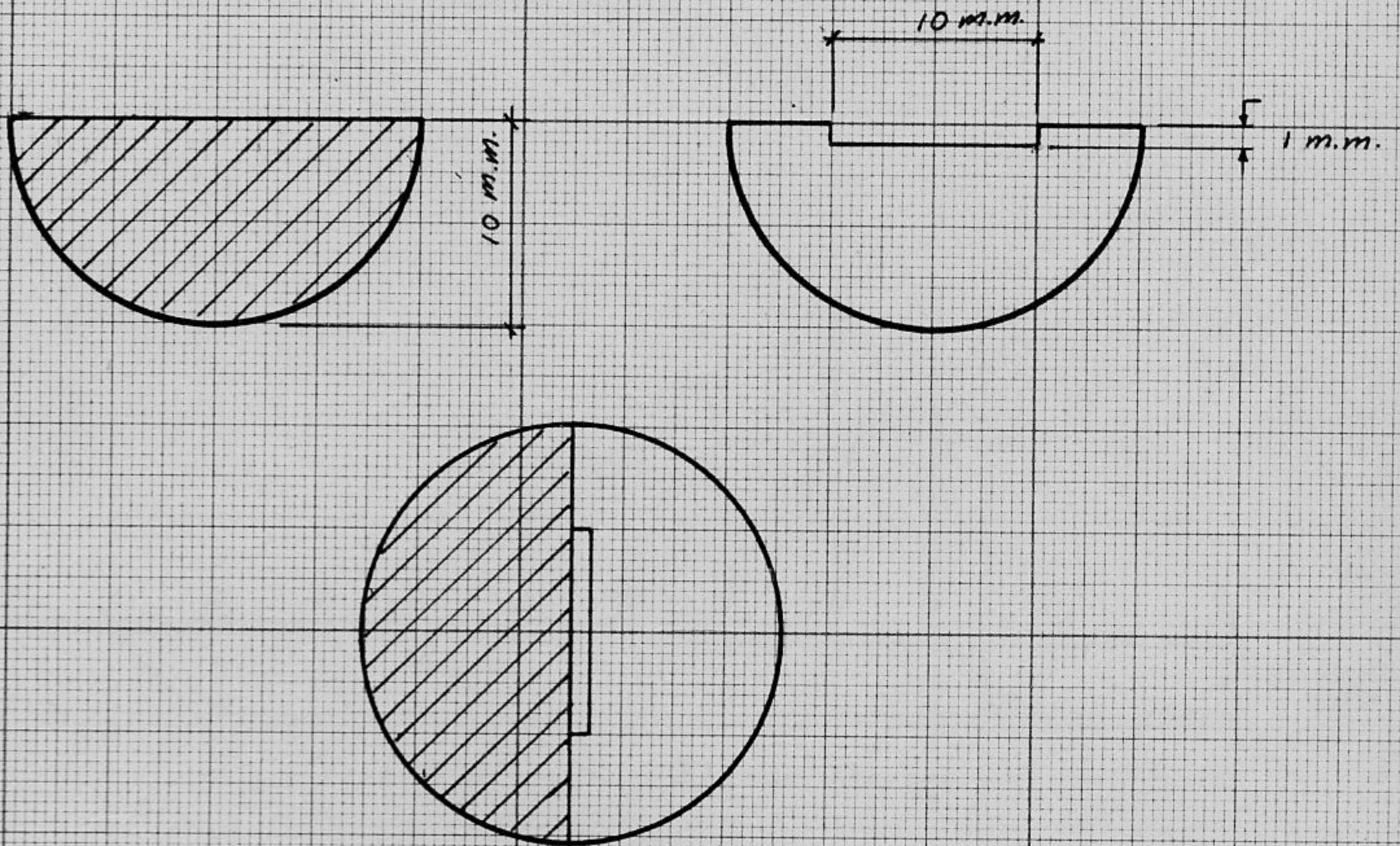


FIG.6 TEST BAR FOR BEAM S<sub>1</sub> AND S<sub>2</sub>

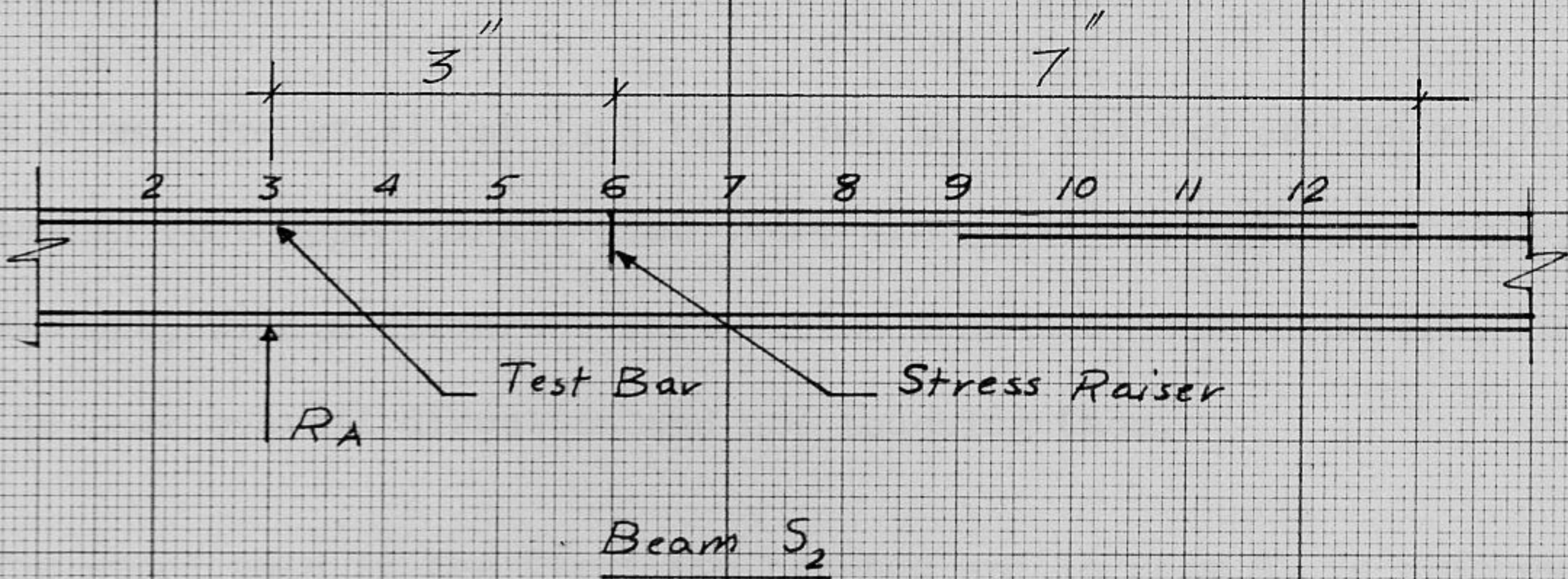
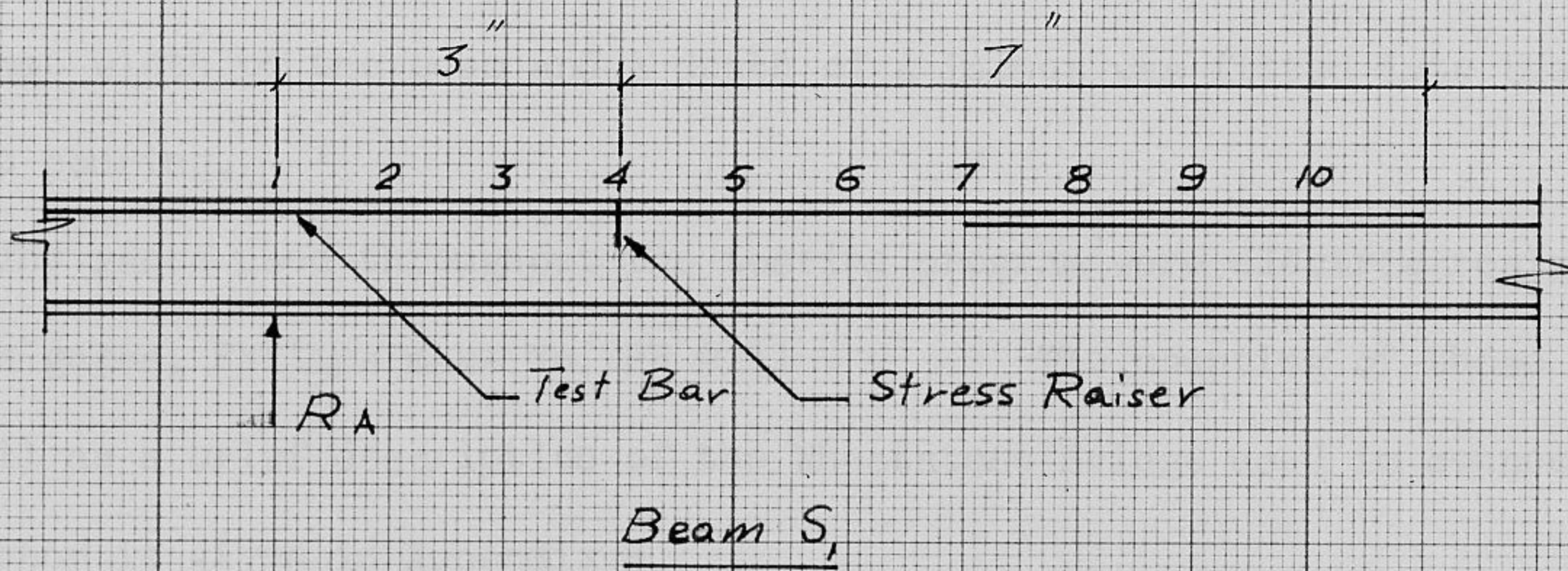


FIG. 7 POSITION OF STRAIN GAGES FOR BEAMS  $S_1$  AND  $S_2$ .

These two beams have no notches over the support. To initiate a crack in the beam at a distance from the support (in this case 3 inches to the right of  $R_a$ ) a hard piece of cardboard coated with grease, having the same width of the beam and a depth of 4 inches was fitted into the forms before pouring.

The gages used throughout the testing program were electric resistance strain gages, Philips make No. PR 9211 . The mounting of these gages as well as a brief description of the Wheatstone Bridge used in connection with them is given in Appendix B.

b) Description of Steel

The steel used in this research is Tor steel whose load v. strain diagram shown in Figs. 8 and 9, and its deformation properties are given below. All the test bars are 20 mm. in diameter.

A 20 mm. Tor steel bar is a round bar which has two continuous helical deformation (see Appendix A); also there are small discontinuous oblique deformations, with a different inclination than the continuous one, but with the same overall direction and not touching them.

The steel used in the first two batches and in Beam  $S_1$  is somehow different in its stress-strain curve and in the sizes and the spacing of deformations than the steel used in the third batch. Although both types satisfy the ASTM specifications as far as the size of the deformations and their spacing are concerned, they both fail to meet these requirements in the angle of inclination of the deformations with respect to the axis of the bar as explained in Appendix A. For identification the steel used in

the first two batches and in beam  $S_1$  from the third batch, is referred to as type I, and the steel used in the third batch including beam  $S_2$  is referred to as type II.

For each type a calibration curve, load v. strain averaged for three bars was drawn as shown in Figs. 8 and 9. The strain was measured by strain gages (described on page 57) and an extensometer was attached to the bar for checking purposes. For the same load the strain gage showed a somewhat larger strain than that given by the extensometer which is due to the filing of the deformation where the strain gage was mounted.

According to the ASTM the yield strength shall be determined by the drop of the beam or halt in the gage of the testing machine. This was not possible in our case as seen from Fig. 8 on page 20. According to European<sup>3</sup> practice, for high strength steel, the yield point is determined by the intersection of a parallel to the linear portion of the curve from 0.2% strain, and the curve proper. In our case this point is far in the plastic range, which prompted an arbitrary choice of the yield point, that takes into account the non-linear properties of the stress-strain curve, yet does not allow the yield point to fall in the plastic range. The yield point was taken as the point of intersection of parallel to the straight portion of the curve from .05% strain and the curve proper. This was at 0.238% strain for type I and at 0.272% strain for type II.

### c) Loading of the Beams

The beams were loaded with two concentrated loads in a manner so that the inflection point coincides with the inside end of the bar, see Figs. 12 to 17. This has insured the reinforcement of the tension zone, yet did not allow the bar to continue into the compression zone.

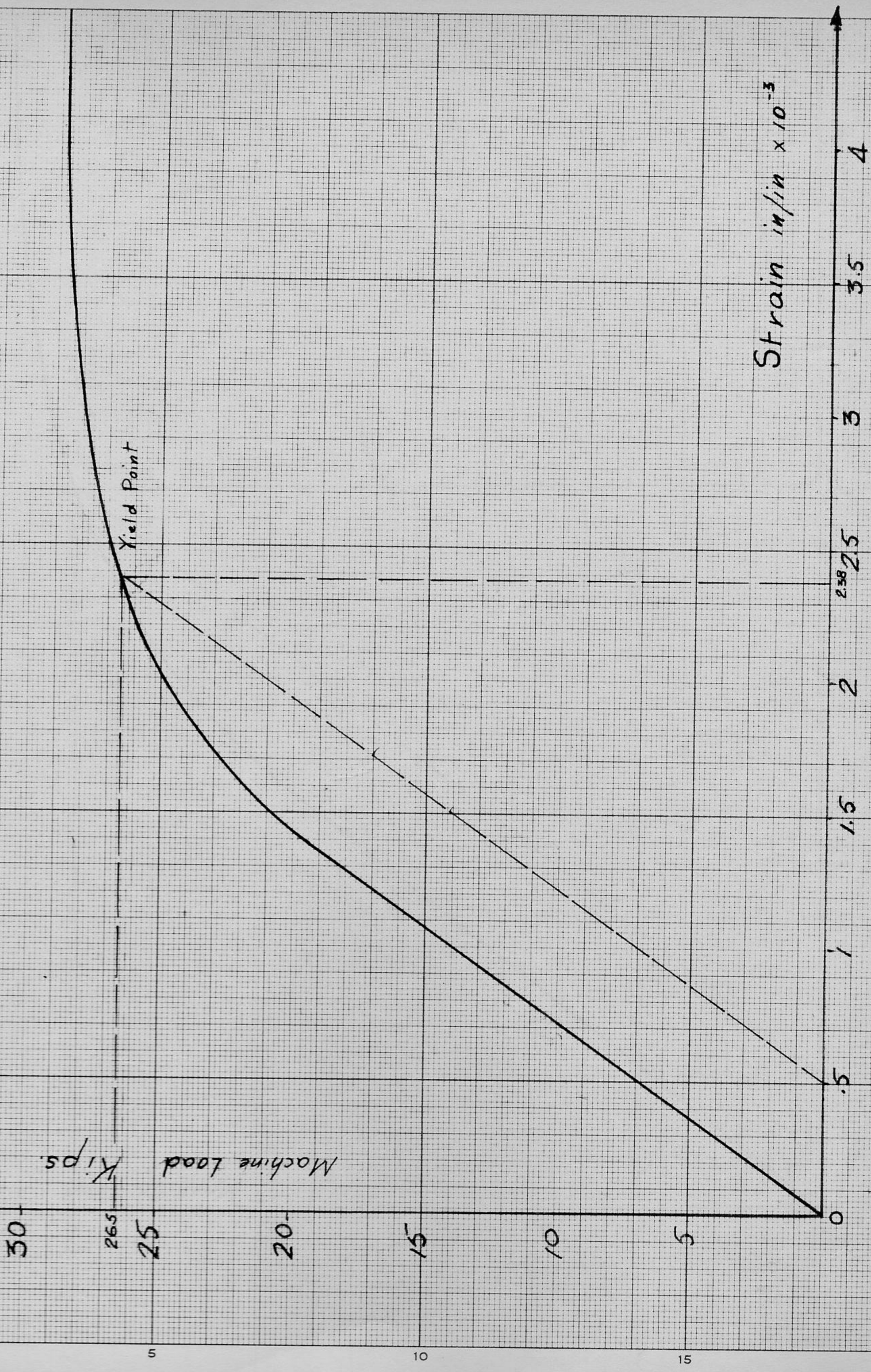


FIG.8 LOAD V. STRAIN FOR TYPE I STEEL

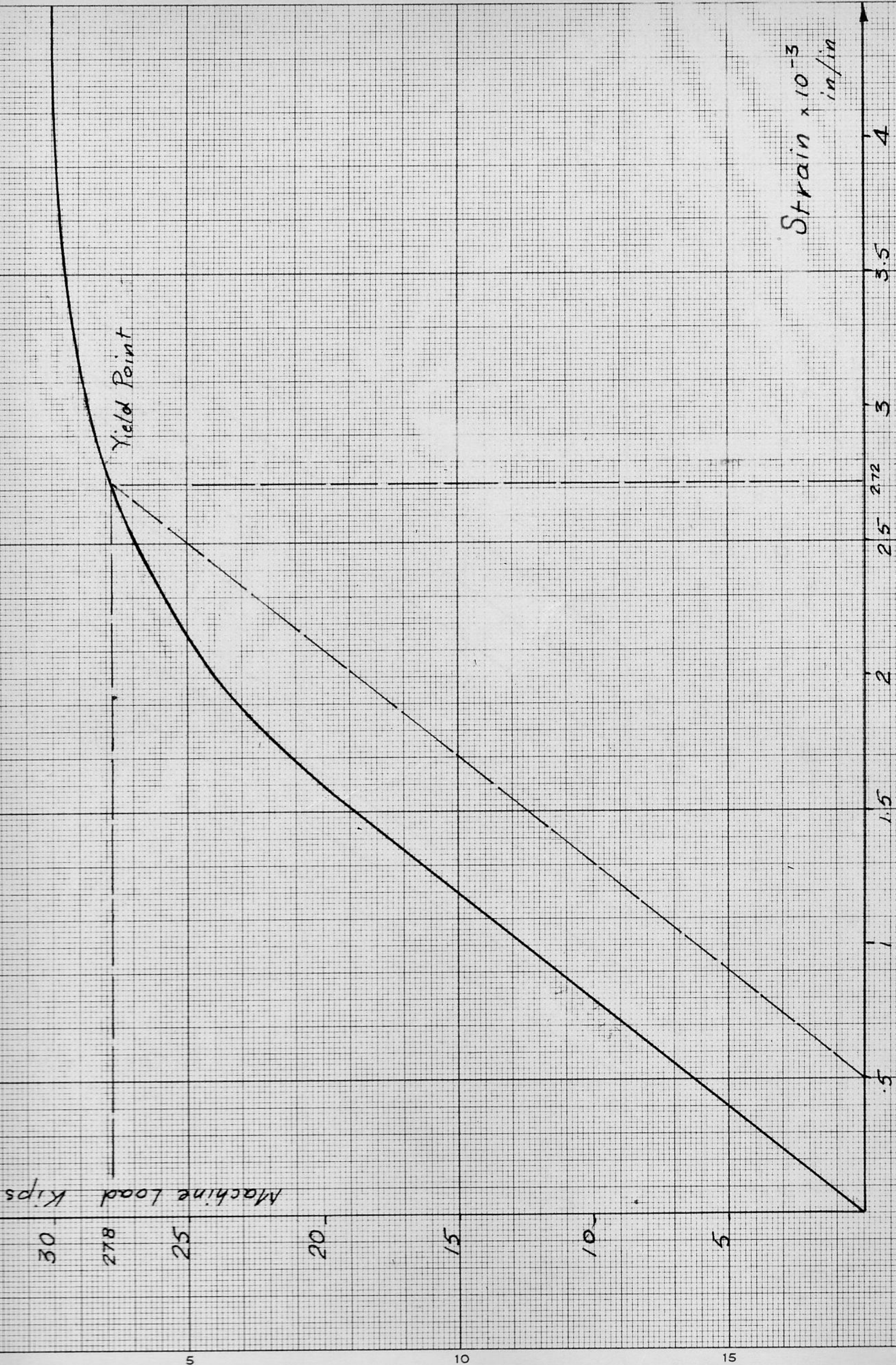


FIG. 9 LOAD VS. STRAIN FOR TYPE II STEEL

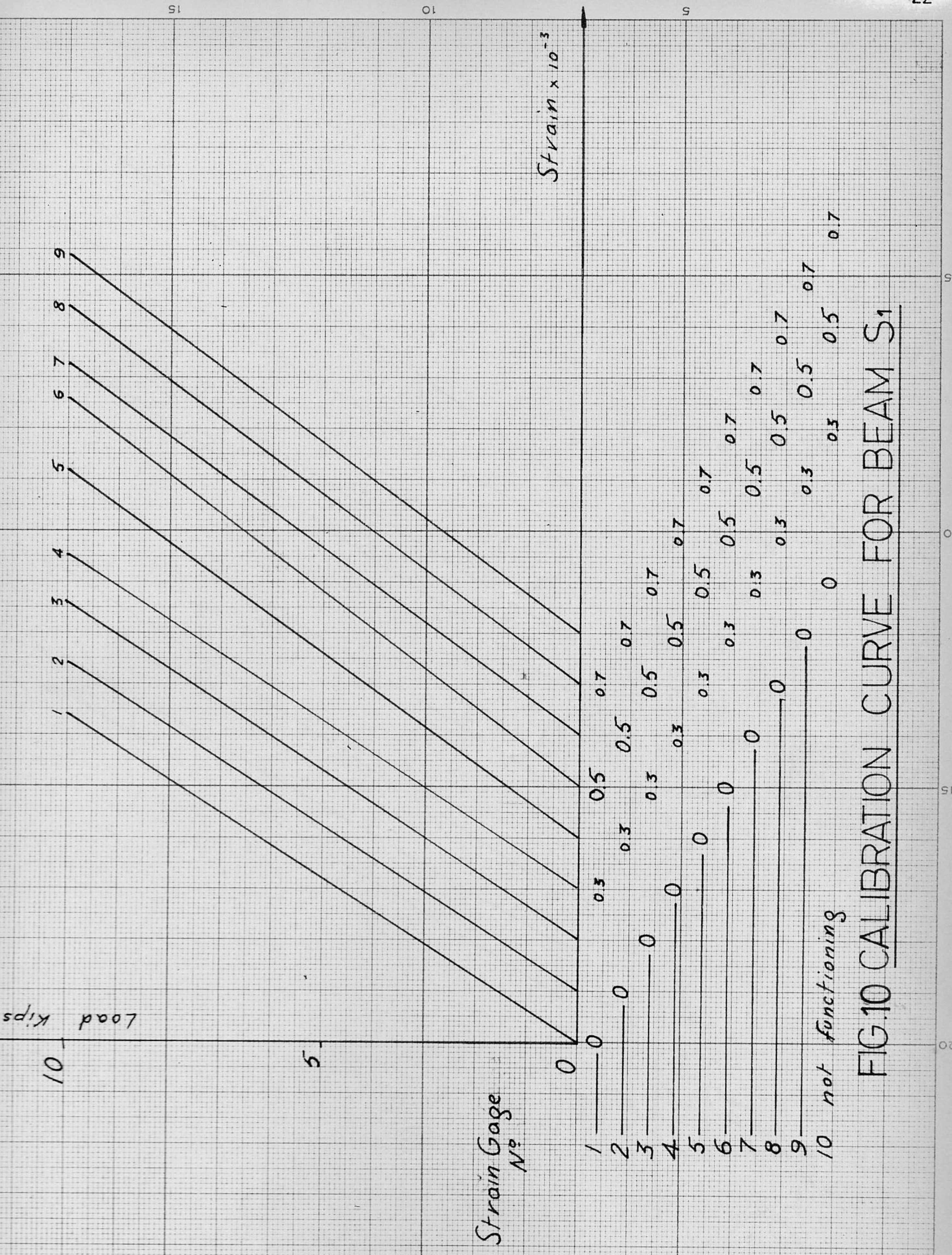


FIG.10 CALIBRATION CURVE FOR BEAM S1



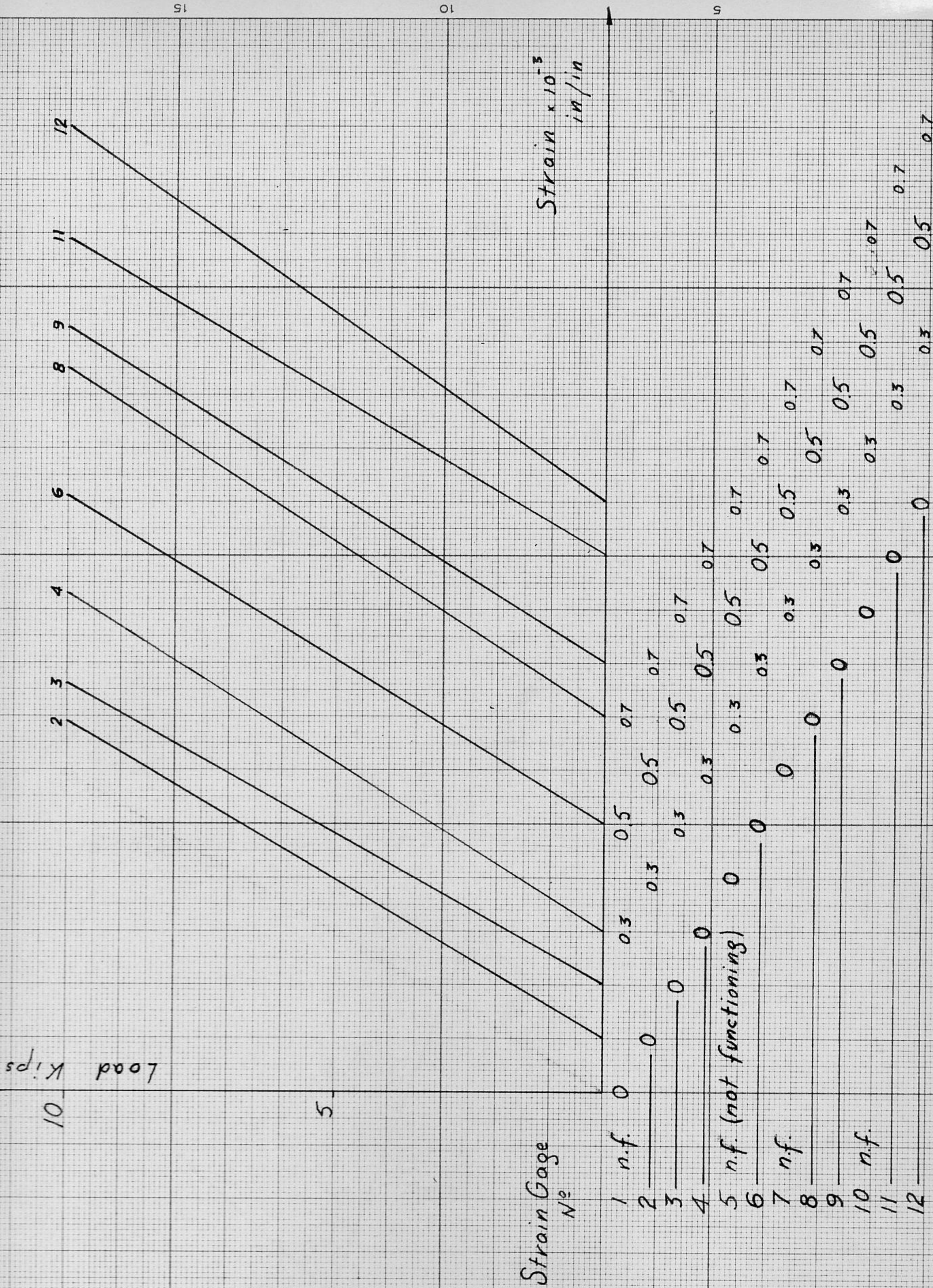


FIG.11 CALIBRATION CURVE FOR BEAM S<sub>2</sub>

# Beams D8

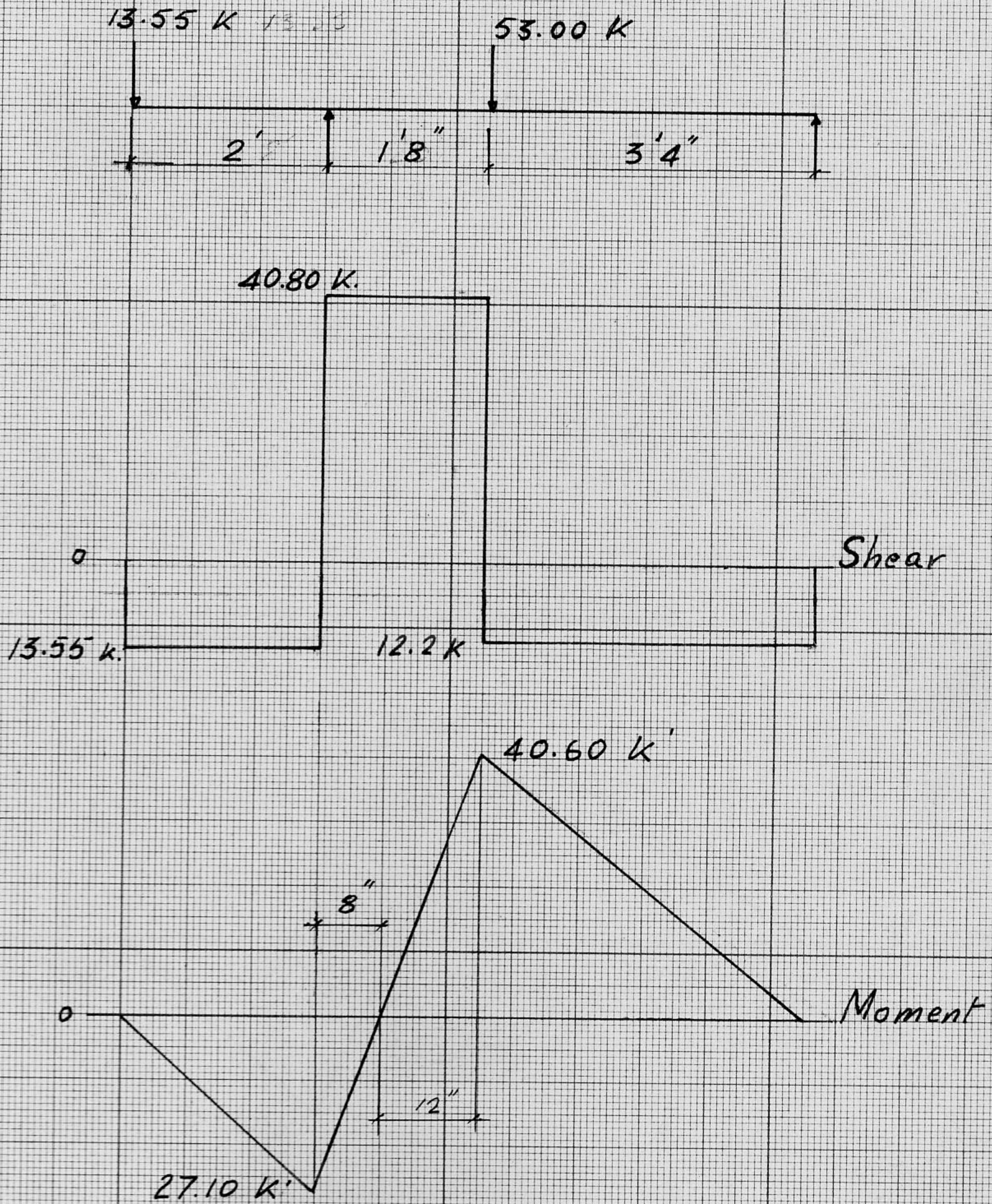


FIG.12

Beams D<sub>10</sub>

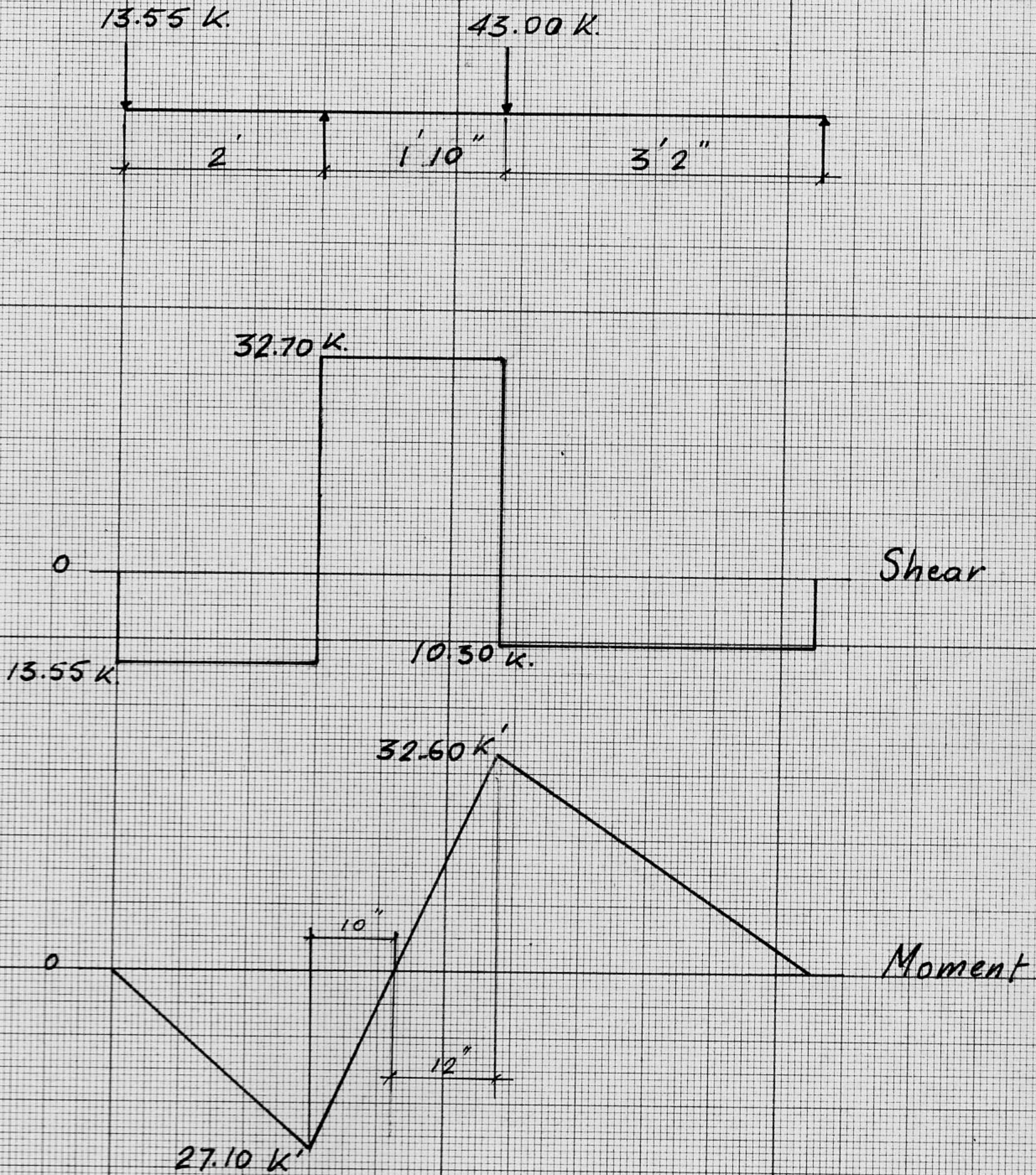


FIG. 13

Beams D<sub>12</sub>

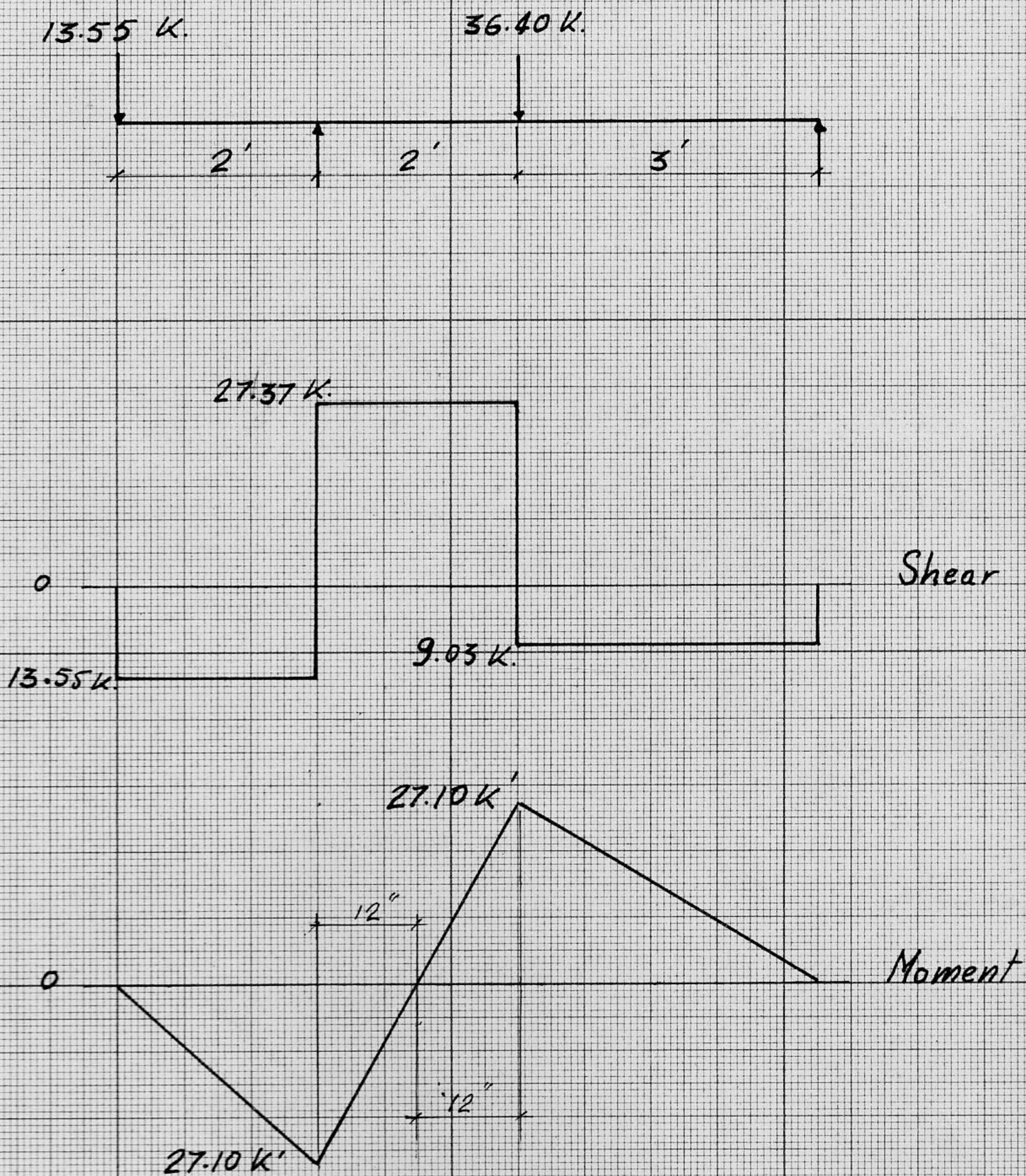


FIG. 14

# Beams D15

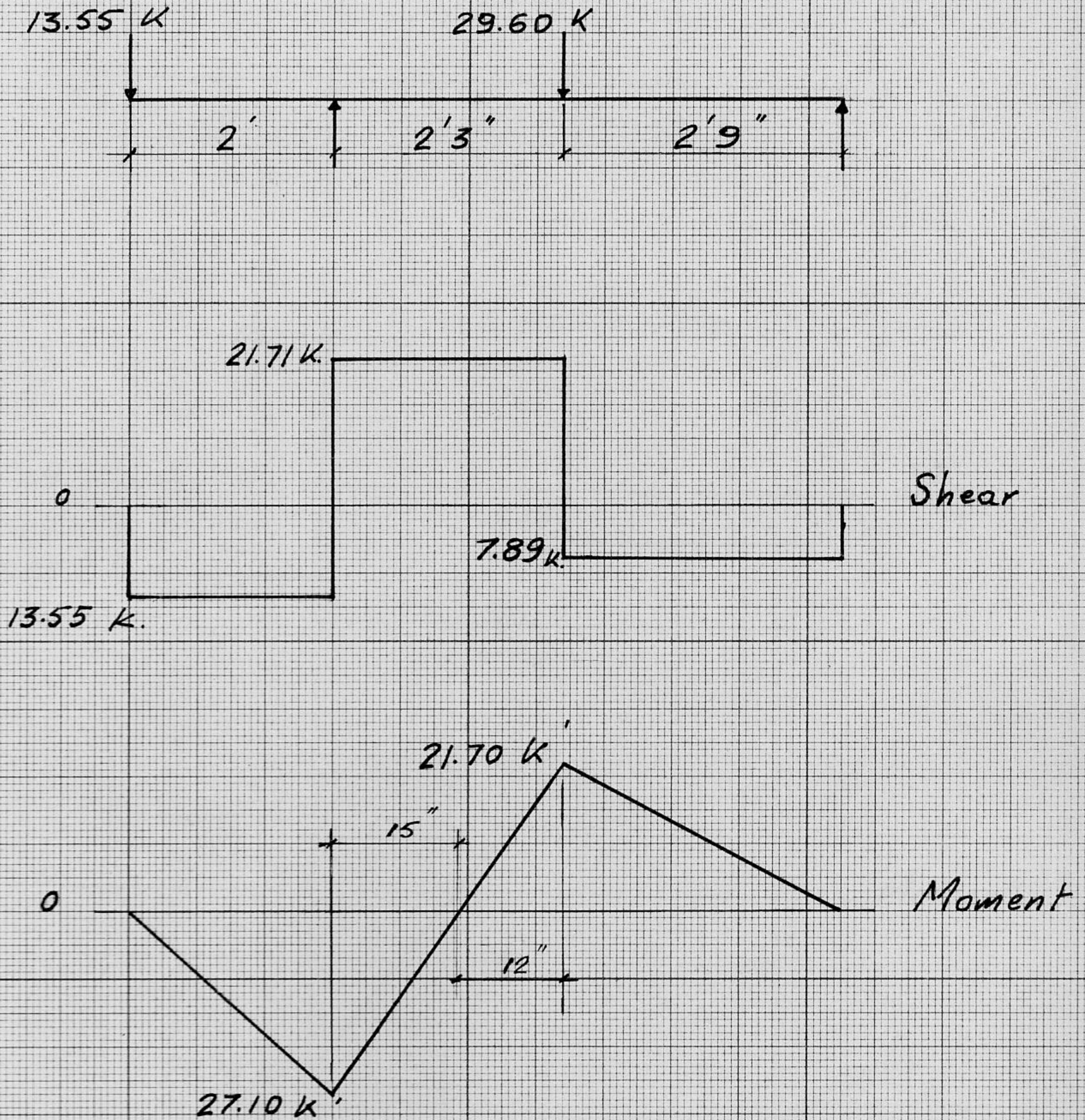


FIG.15

# Beam D17

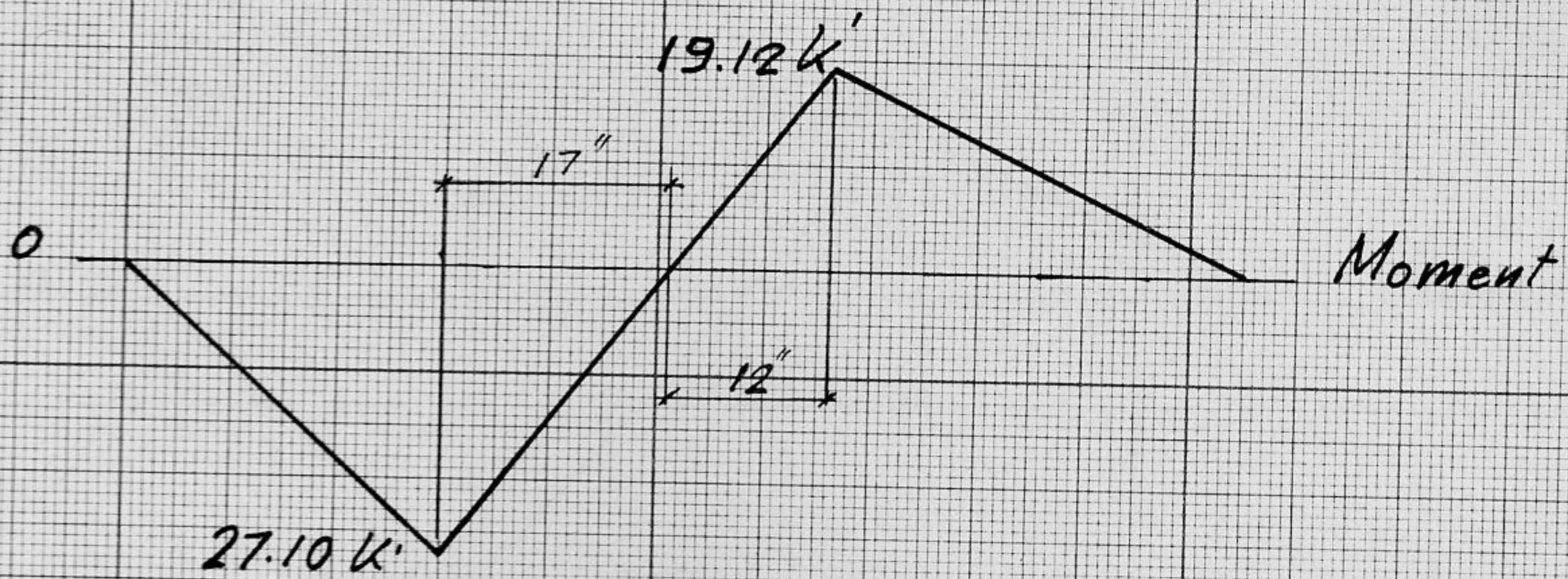
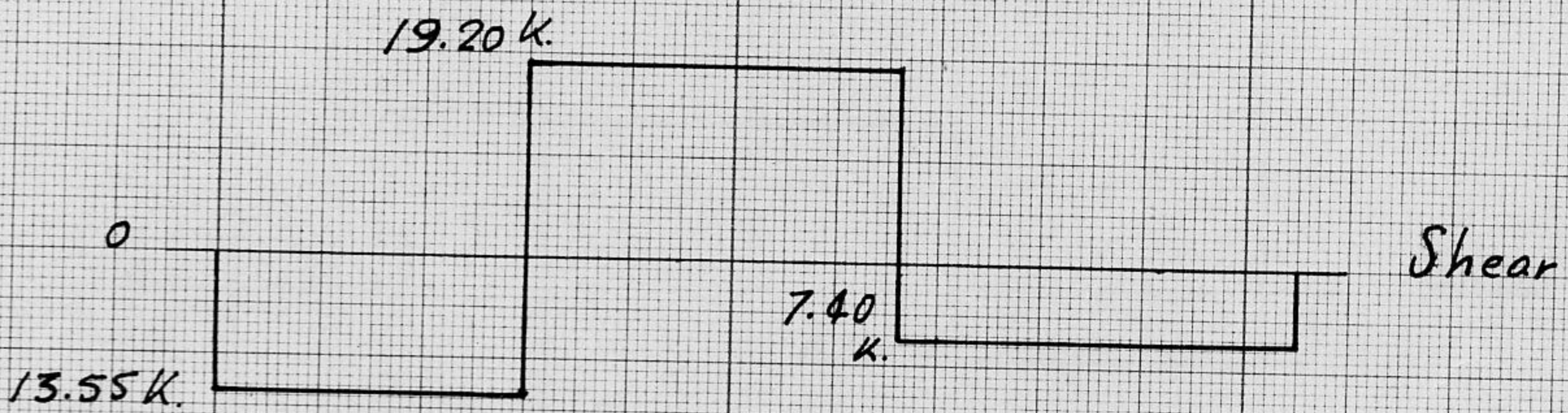
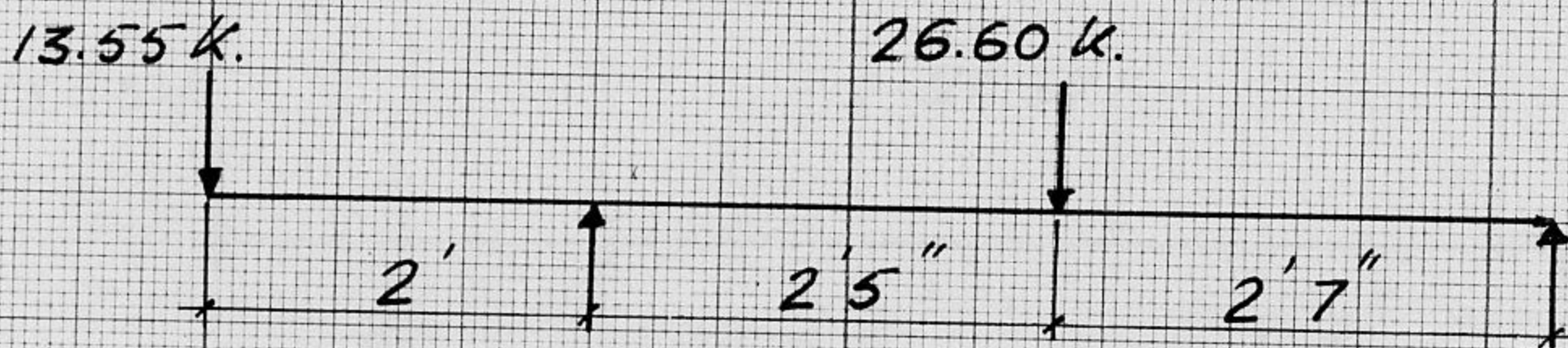


FIG 16

# Beams D<sub>20</sub>

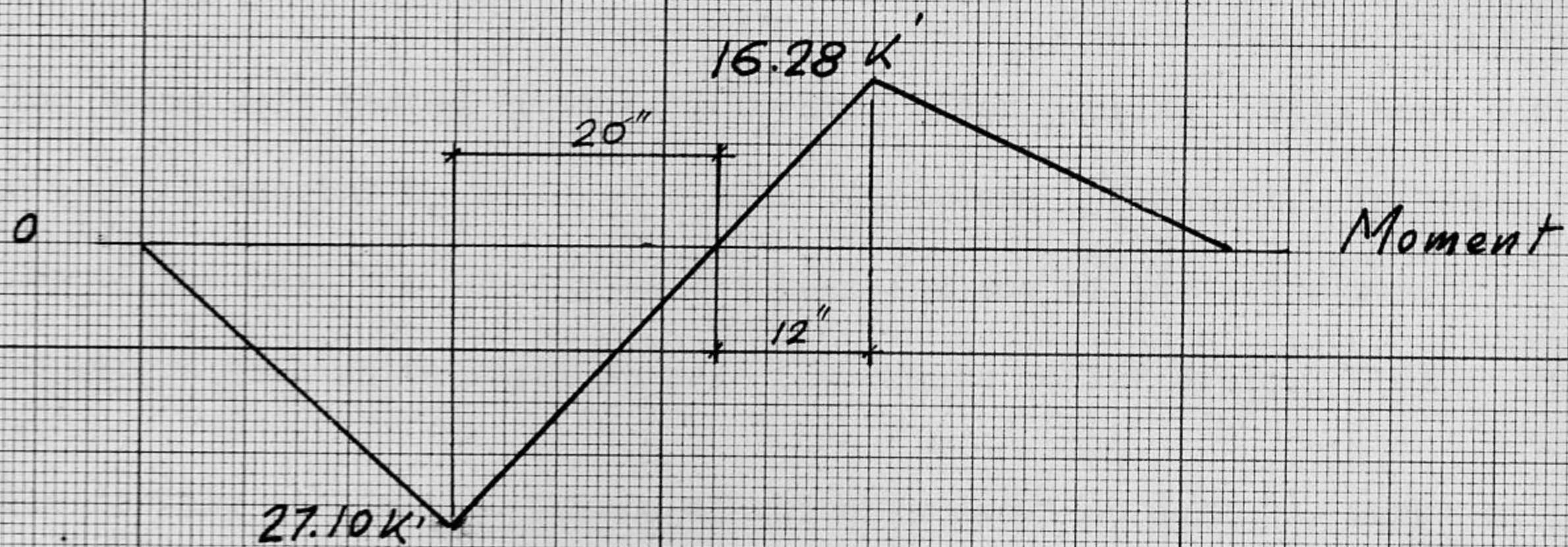
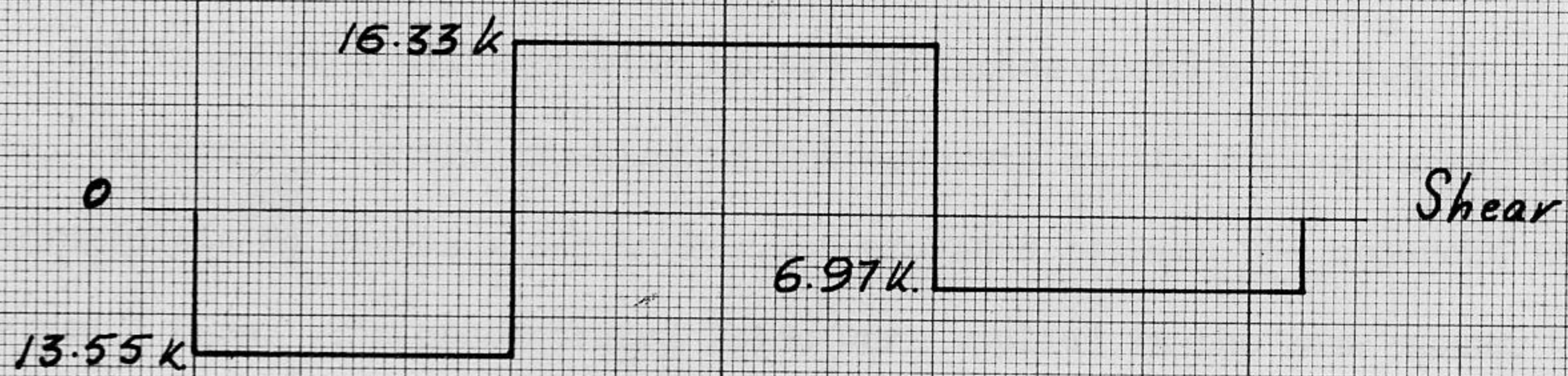
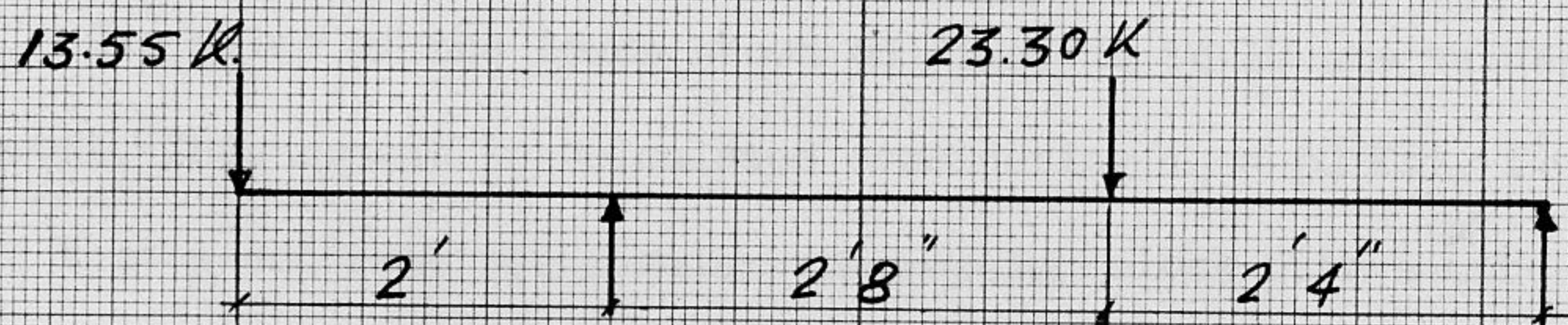


FIG. 17

The inside concentrated load was always 12 inches away from the end of the bar so that the bar will be far from the influence of local compression stresses due to this concentrated load.

The value of the loads shown on Figs. 12 to 17 are values at ultimate moment. This moment is calculated considering  $f_y = 60$  Ksi,  $f'_c = 2500$  psi, and that a concrete rectangular compression block with a stress equal to  $0.85 f'_c$  (Whitney's method) is taking the compression. In all calculations, the weight of the beams (0.1 Kip per foot), is neglected.

#### d) Reactions

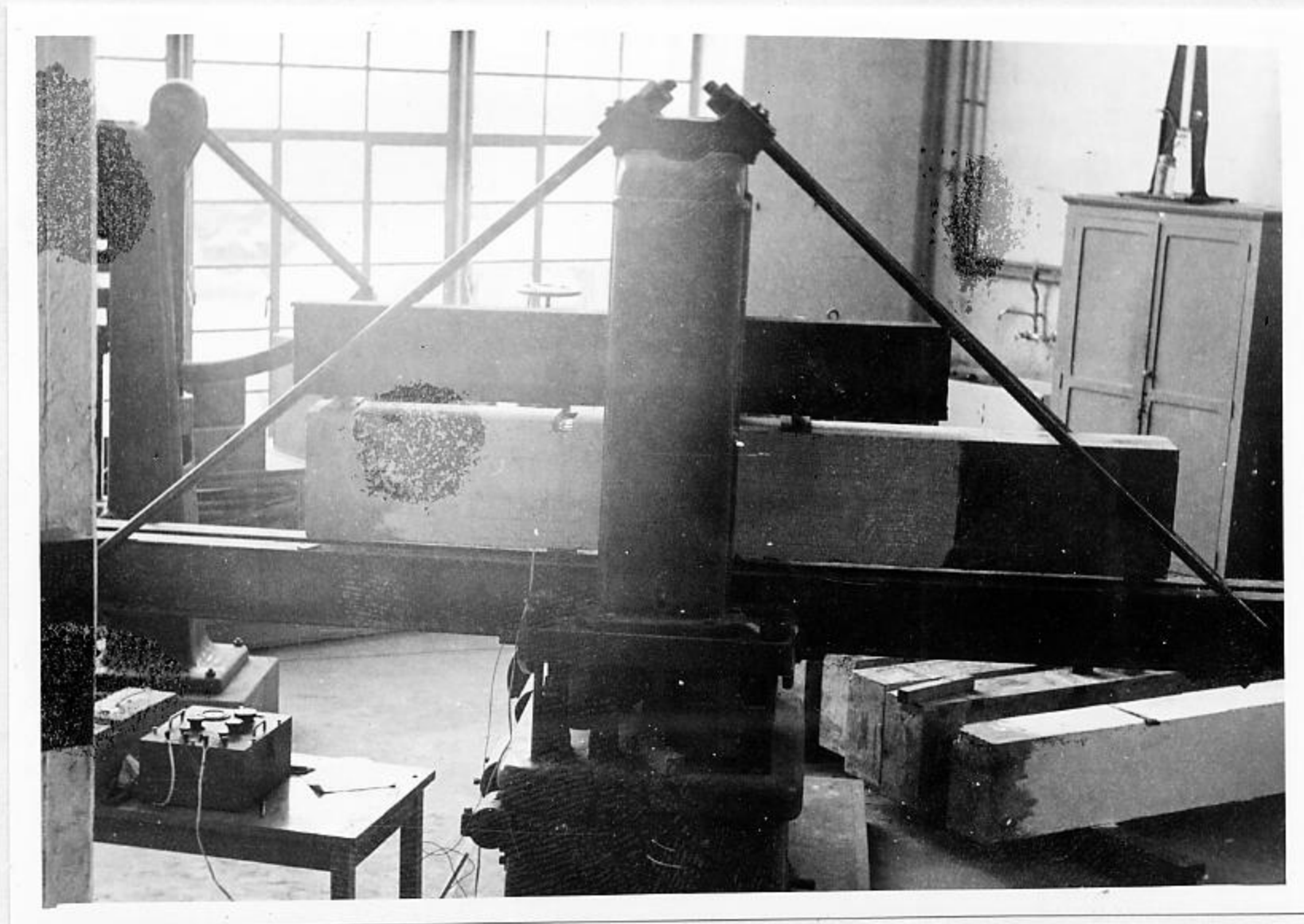
The beams were all supported on two  $1\frac{1}{4}$  inches round bars, 8.5 inches long. In order to avoid crushing of the concrete at the contact area, a metal bearing plate  $8\frac{1}{2}$  inches x  $3/8$  inches was provided between the concrete and the round bars. The concentrated loads were applied in the same manner (See page 32).

#### e) Testing Procedure

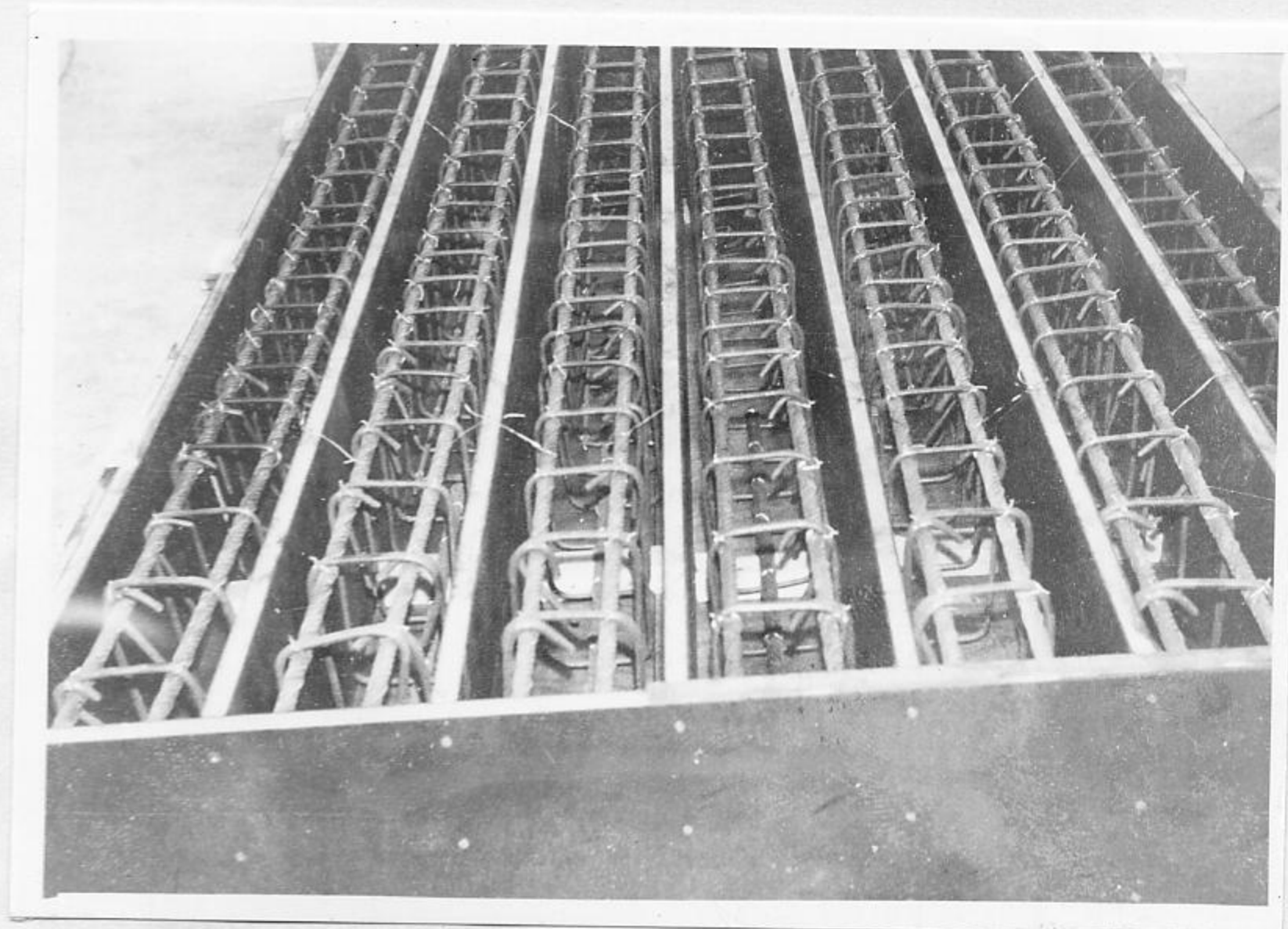
The beams were tested at 28 days or more after pouring. They were put on the testing machine by means of a steel cable and a forklift. In the vicinity of the test bar the top of the beam and one of its sides were painted with a thin white layer to make the cracks more visible.

The testing machine, a picture of which is shown on page 31, works on D.C. current, and the application of the load is mechanical rather than hydraulic. The single machine load was distributed into two concentrated

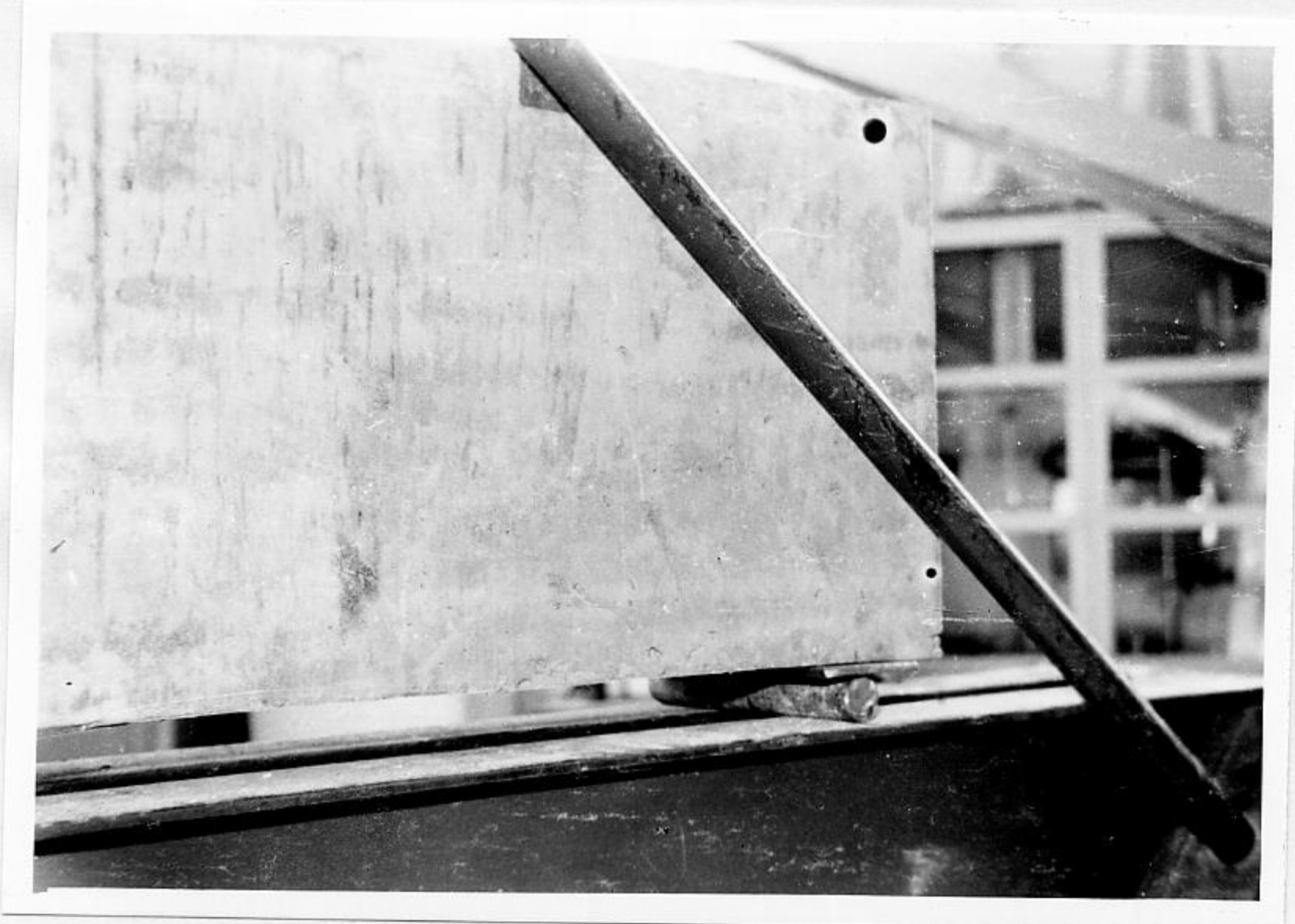




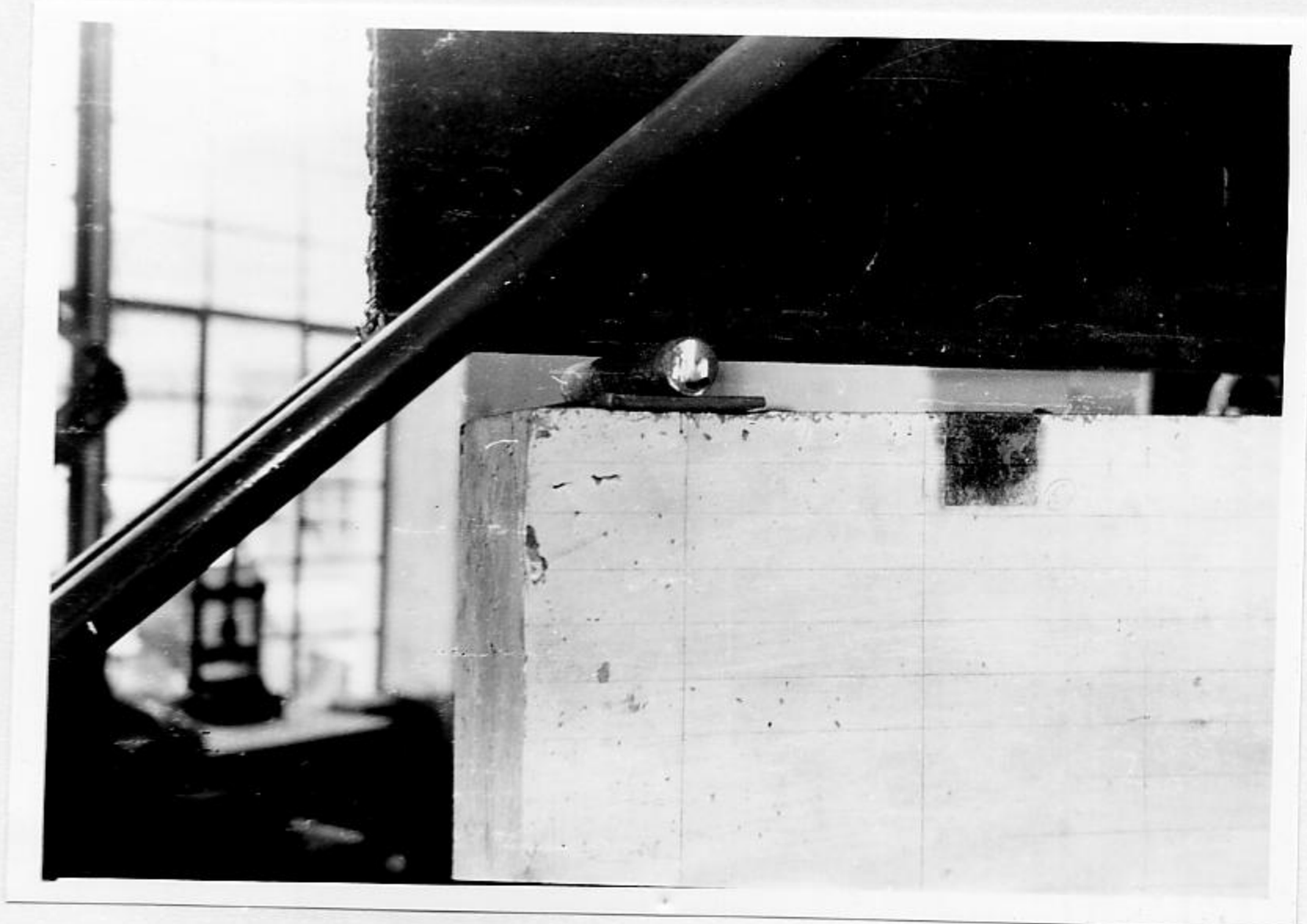
Testing Machine



Reinforcements in form work



Reaction



Load

loads by a steel I beam. The machine was stopped at each reading to enable the observation of cracks. The rate of application of the load was about 500 lbs per minute.

f) Behaviour under Test

In all beams two flexural cracks occurred in the vicinity of the development length of the bar. A record of the propagation of these cracks v. load was taken and entered in the tables on test data given in Appendix C. Splitting occurred in almost all beams, and it started by a single split on the top along the bar.

The mode of failure, however, may not be classified as pure bond failure except in few beams (where pure bond failure is exhibited by severe splitting of the concrete along the bar by a combination of longitudinal and transversal cracks). Although mild splitting has occurred in all cases, most beams failed by a combination of splitting and diagonal tension cracks. Pictures of these beams as well as their respective modes of failure appear in Appendix D.

III. DATA ANALYSIS

a) Development Length

For every beam the development or anchorage bond stress  $u = \frac{A_s f_s}{\sum_o L_d}$

plotted against machine load;  $L_d$  was taken as the development length minus half an inch; because over the length of one inch of the bar where the gage was mounted, only half the bar was covered. The curves pertaining to beams of the same batch were drawn on the same sheet. Referring to page 35 all curves start with a gentle slope; this is due to the uncracked section of the concrete which was helping in resisting the tension when the flexural crack started, over the support A, the force in the steel bar increased rapidly as the crack propagated downward.

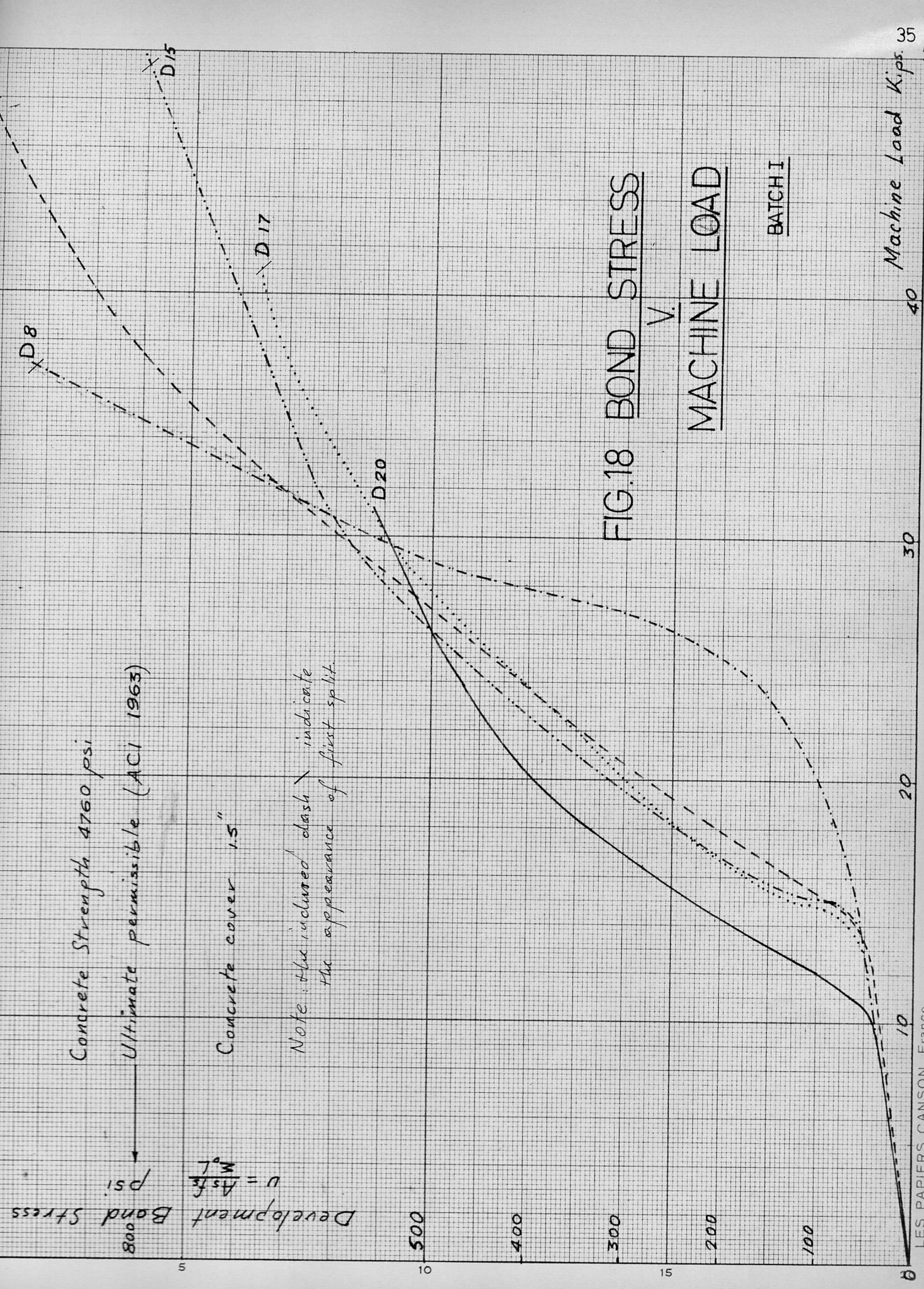
Beam D20-4-1 failed by tension at the end of development length due to a mistake in loading, which caused a shift of the inflection point. In all beams the force in the test bar is not increasing linearly with machine load or moment; this is due to the increase of the moment arm  $jd$  as the machine load was increasing.

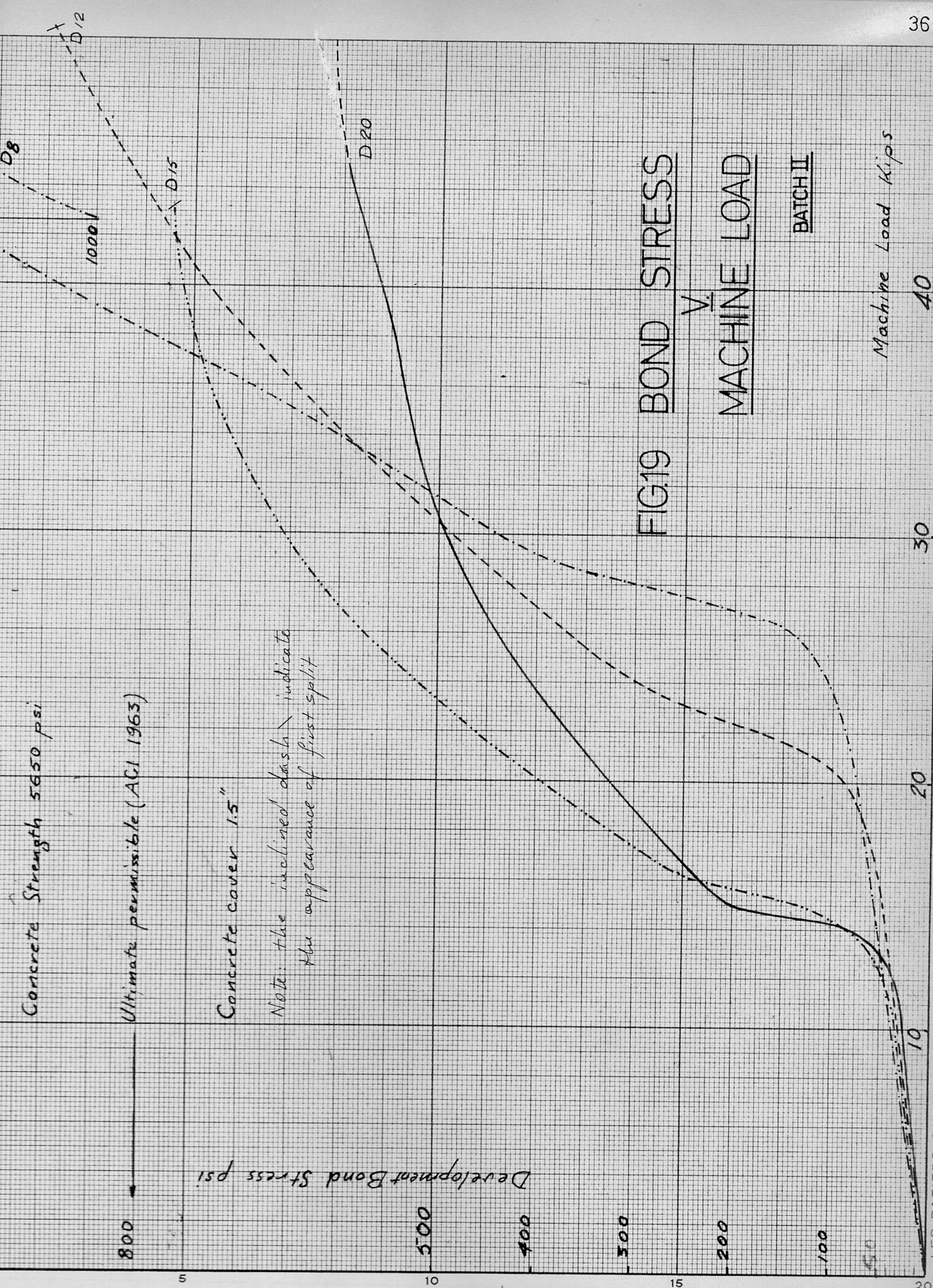
The curve of the beam D12-4-2 was not drawn because toward the end of the experiment the strain gage measuring bridge was out of order.

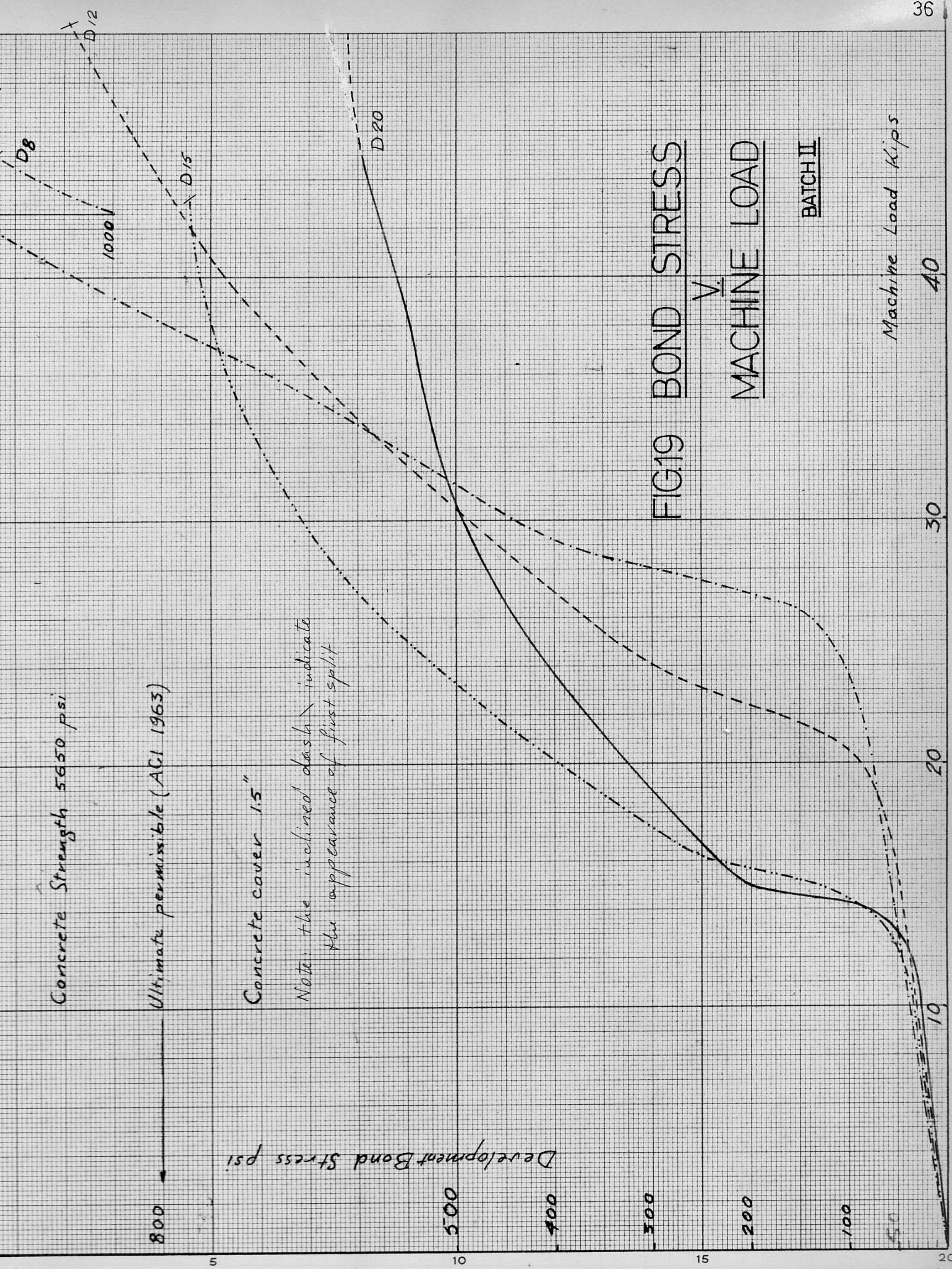
In Fig. 21\* the bond stress (at the appearance of the first split and at yield) v. development length are shown. In most of the beams the bond stress (at the appearance of the first split) approached the bond stress at yield and in some beams exceeded it. This shows that the appearance of a crack along a reinforcing bar (split) in a beam is an indication and a warning against a very near bond failure. On the other hand the appearance of flexural crack is not dangerous.

---

\*In Figs. 21 and 22 the concrete strength was reduced or increased to 5000 psi by multiplying the bond stress or the force by a factor equal to  $\sqrt{\frac{5000}{f'_c}}$







Concrete Strength 5650 psi

Ultimate permissible (ACI 1963)

Concrete cover 1.5"

Note: the inclined dash indicate the appearance of first split

FIG 19 BOND STRESS V. MACHINE LOAD BATCH II

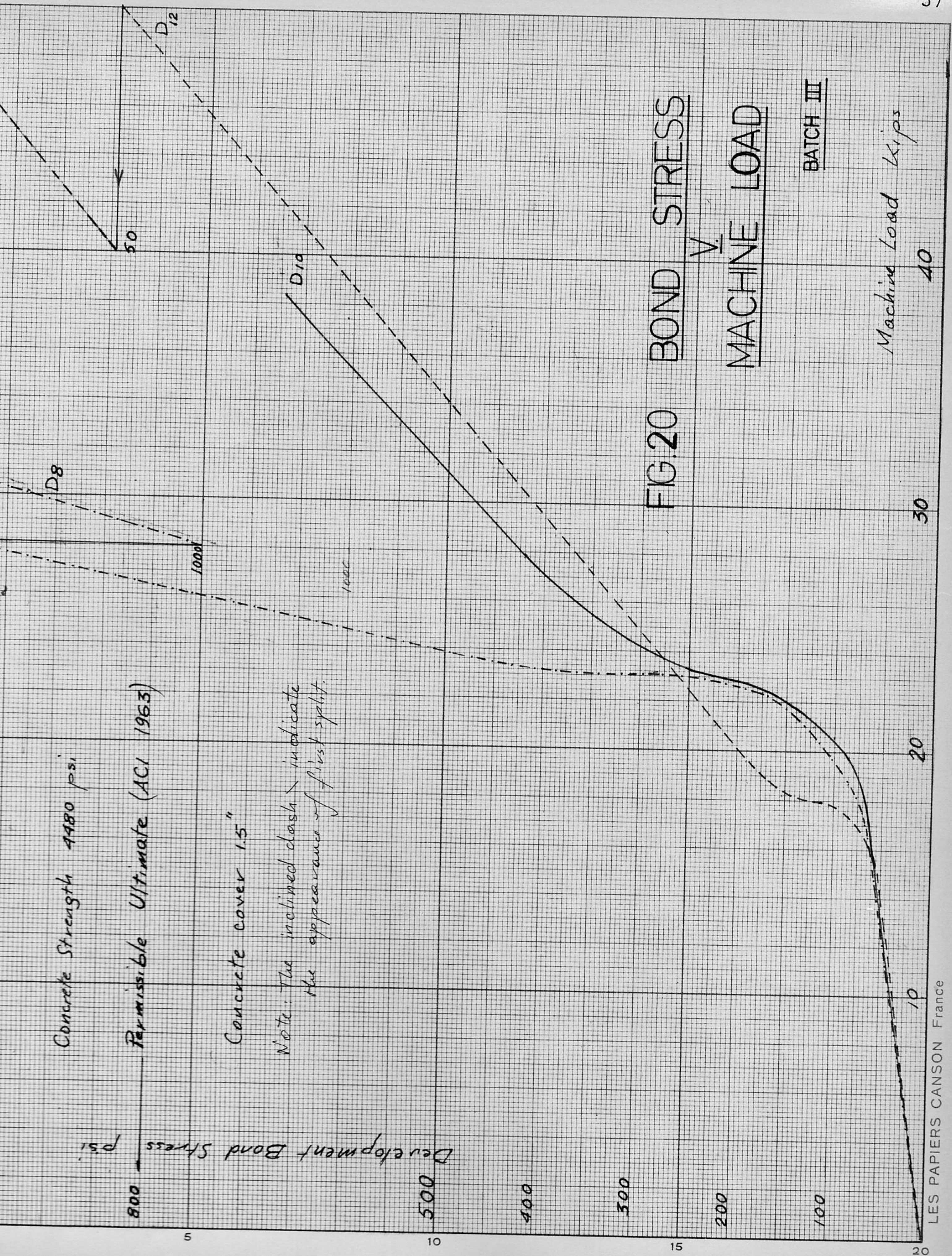
Machine Load Kips

40

30

20

10





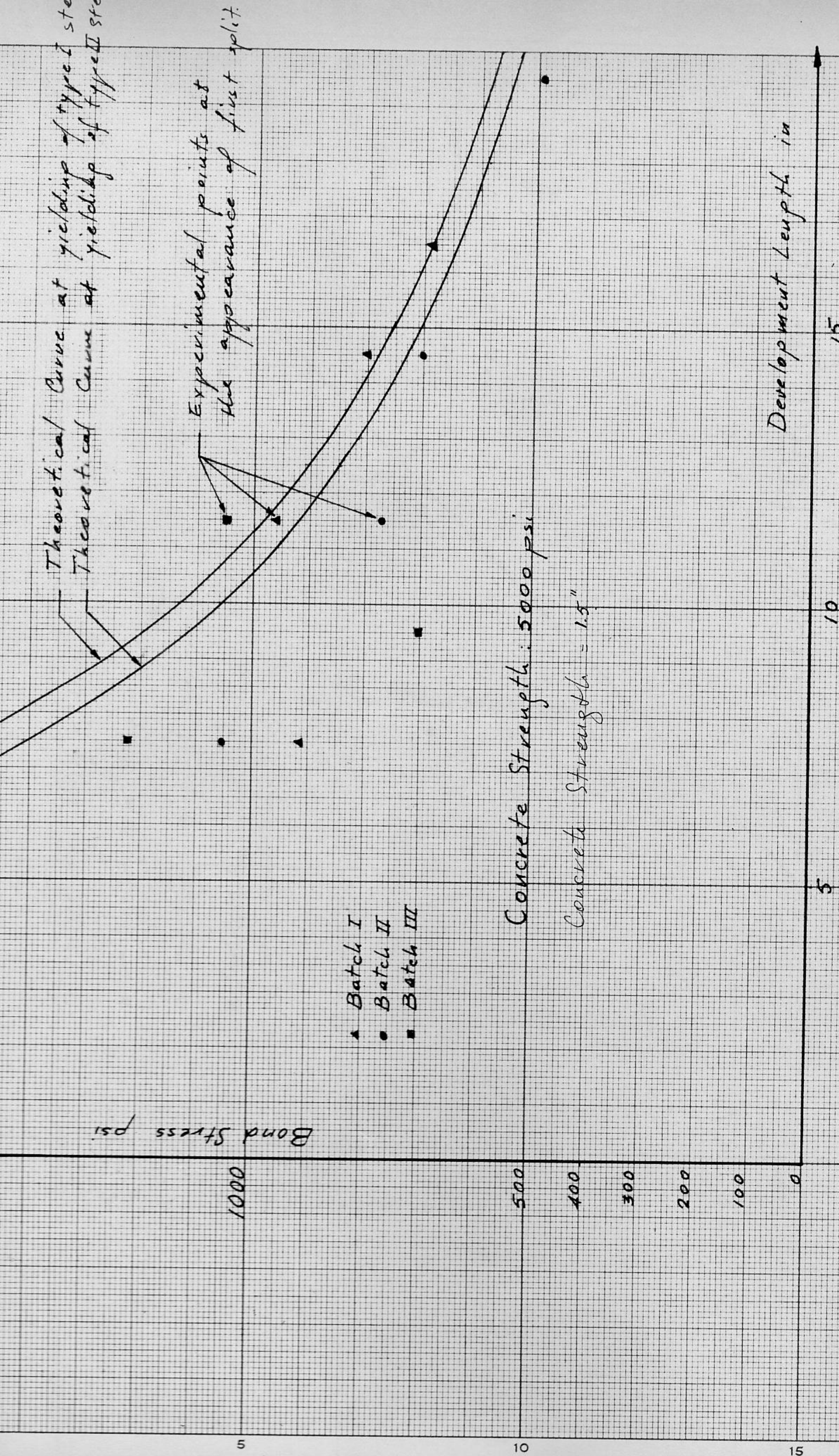


FIG. 21 BOND STRESS V. DEVELOPMENT LENGTH



The test results indicate that the bond carrying capacity of Tor steel is as good as deformed bars conforming to ASTM specifications. This may be concluded from the results depicted in Fig. 22, where a theoretical and an experimental plot of the tensile force in the reinforcing bar  $v$ , the development length is shown. The straight solid line is a theoretical curve representing eq. 2b, and using the ACI code permissible ultimate bond stress for a 20 mm. deformed bar and an  $f'_c = 5000$  psi.

Due to the high strength of concrete few beams failed by bond while the rest failed by yielding of steel and/or by diagonal tension. Although it is not definite how much of a bond force could have been generated in the beams that failed by other than bond failure, it is safe to assume that the full bond capacity of the bar was not attained. For this reason the experimental points plotted in Fig. 22 are divided into four categories, denoting the four modes of failure that are indicated on the figure. It is seen that in the two cases of pure bond failure the bond force attained was more than the ultimate recommended by the code. In most of the other cases, although the full bond carrying capacity was not achieved the points indicate values that are either close to the theoretical curve or exceeding it. This enable one to draw the afore mentioned conclusion about the bond resisting properties of Tor steel.

#### b) The Effect of Cracking upon Development Length.

As mentioned earlier the strain gages mounted on the reinforcement of the special beams  $S_1$  and  $S_2$  were spaced at 1 inch center to center. In the process of spot welding of the bars and pouring of concrete, some of the strain gages were damaged. The following sketch, Fig. 23a show the relative position of the functioning strain gages with respect to the induced crack.

In the case of  $S_1$  the gages offered an excellent means of computing the bar strain along the length of the bar and consequently the bond stress distribution, hereby referred to as the bond wave. The bond stresses were found from the expression:

$$u = \frac{F}{\sum_0 X}$$

where  $F$  = change in the force between two sections on the bar a distance  $X$  apart

In  $S_2$  however, the functioning strain gages were so far apart that an evaluation of the bond wave from those gages was quite approximate and therefore misleading.

Figs. 23b and 24b show that the stress over the support in  $S_1$  or 1 inch to the right in  $S_2$  is less than the stress at the induced crack, while theoretically the reverse is true. On the other hand the development length measured between the induced crack and the end of the bar is less than the theoretical development length by 3 inches. It is logical to assume, therefore, that beams  $S_1$  and  $S_2$  with the induced cracks may fail by bond at a lesser load than their twin beam  $D_{10-4-3}$ , which had no induced crack (For clarity on the geometry of beams  $S_1$ ,  $S_2$  and  $D_{10-4-3}$  refer to figures 4 and 5). The test results support strongly the above mentioned hypothesis. As listed in tables C15, C18 and C20 in Appendix C. Beam  $S_1$  failed by splitting at a machine load of 28550 lbs,  $S_2$  at 23500 lbs, while  $D_{10-4-3}$  failed by splitting at 41000 lbs.

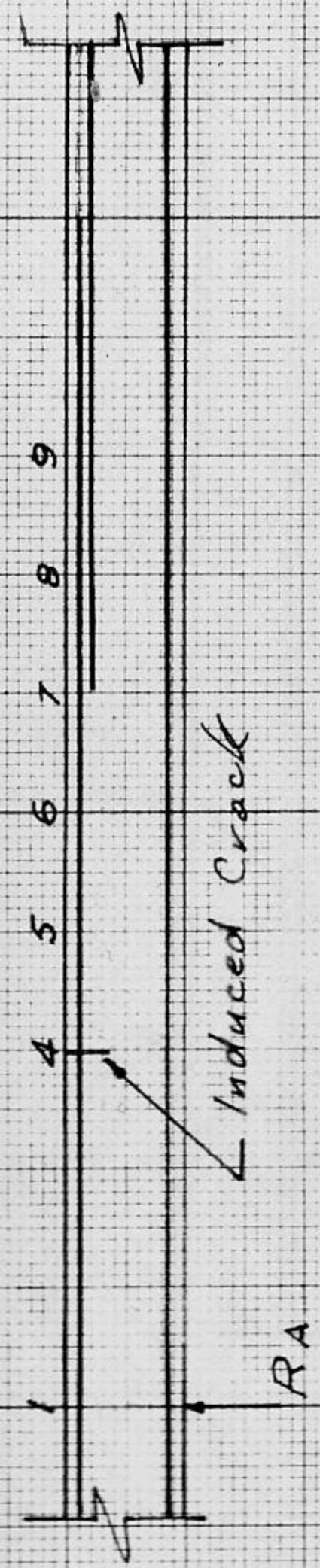
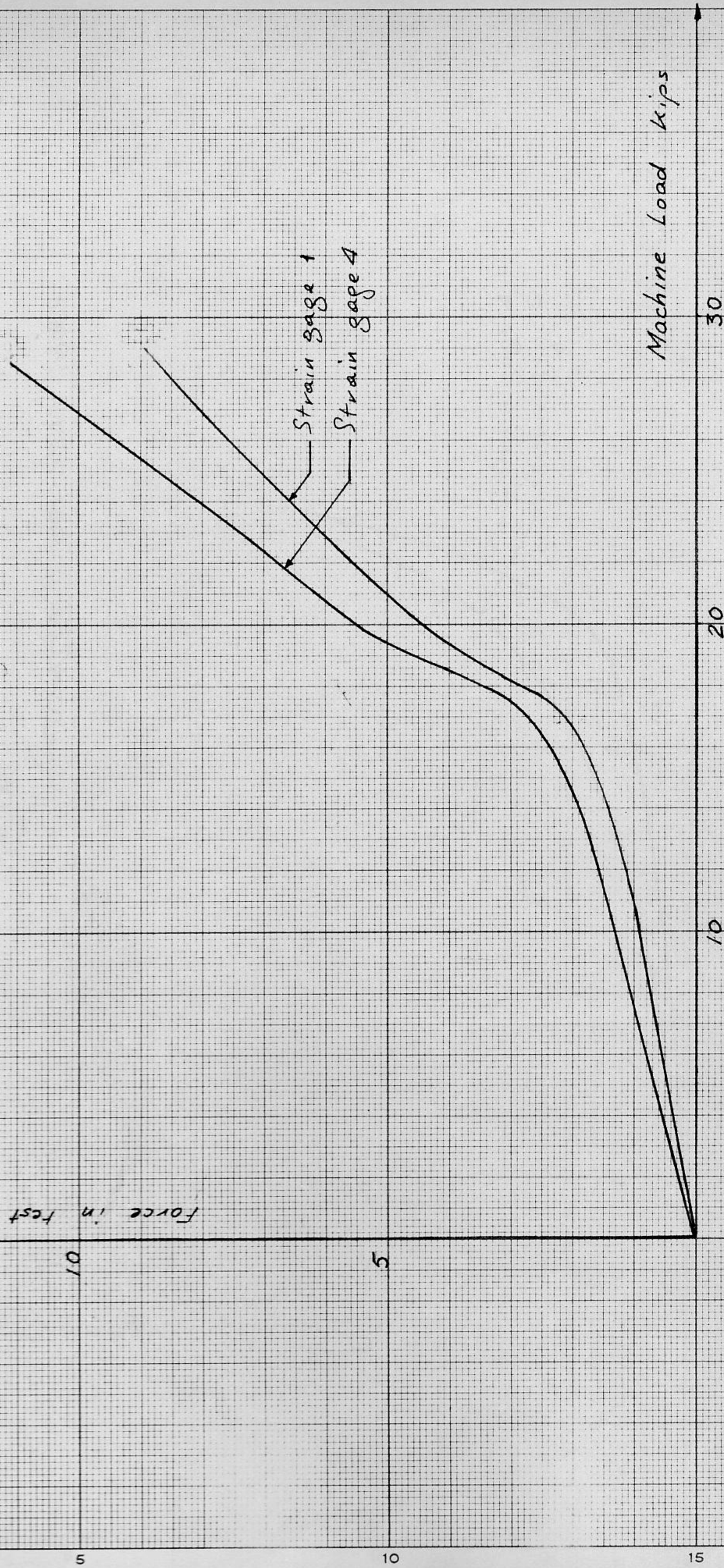


FIG. 23a FUNCTIONING STRAIN GAGES

Force in test bar kips



Machine Load kips

FIG. 23b FORCE V. MACHINE LOAD. BEAM S<sub>1</sub>

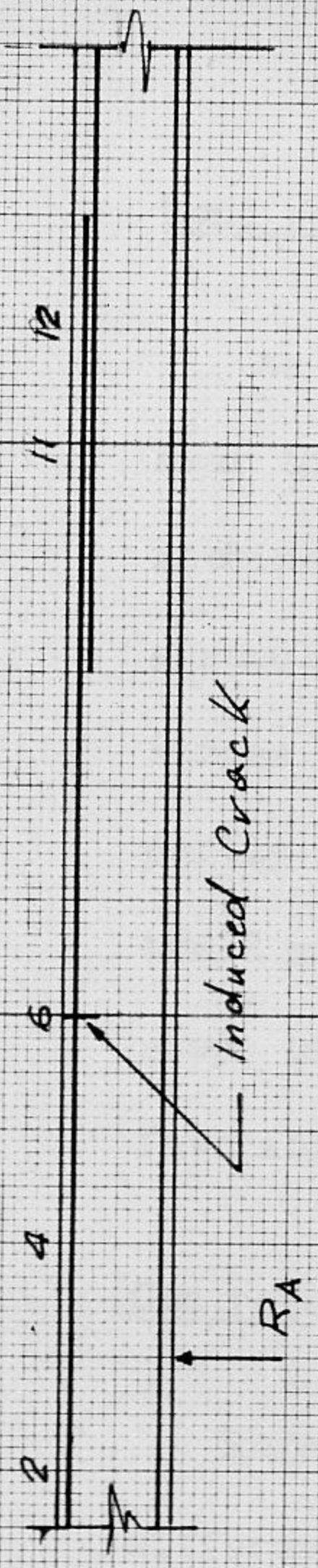


FIG. 24a FUNCTIONING STRAIN GAGES

Force Kips

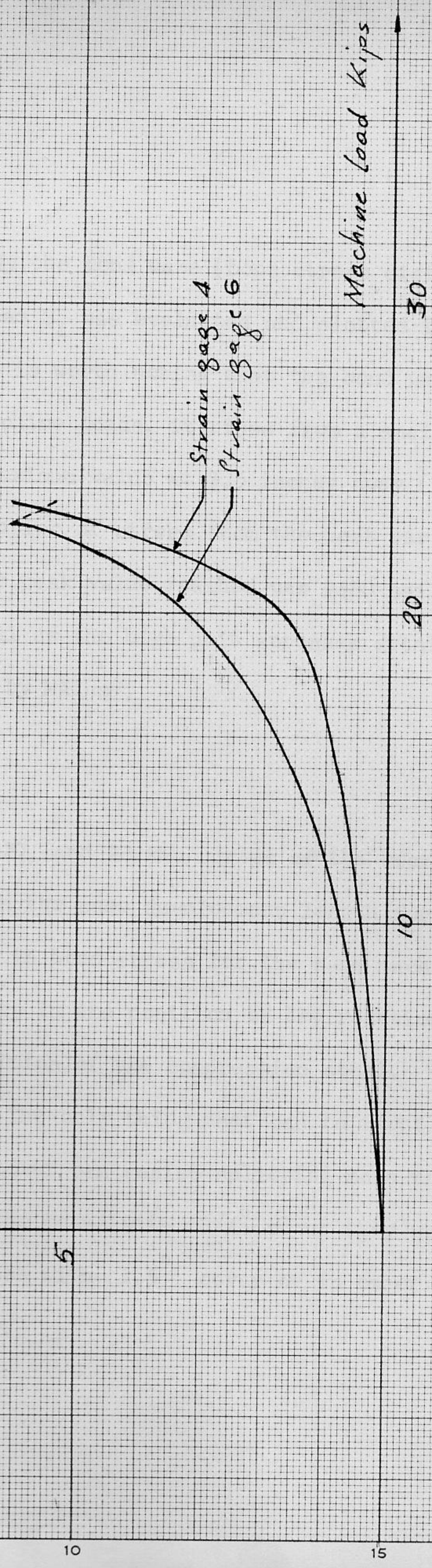


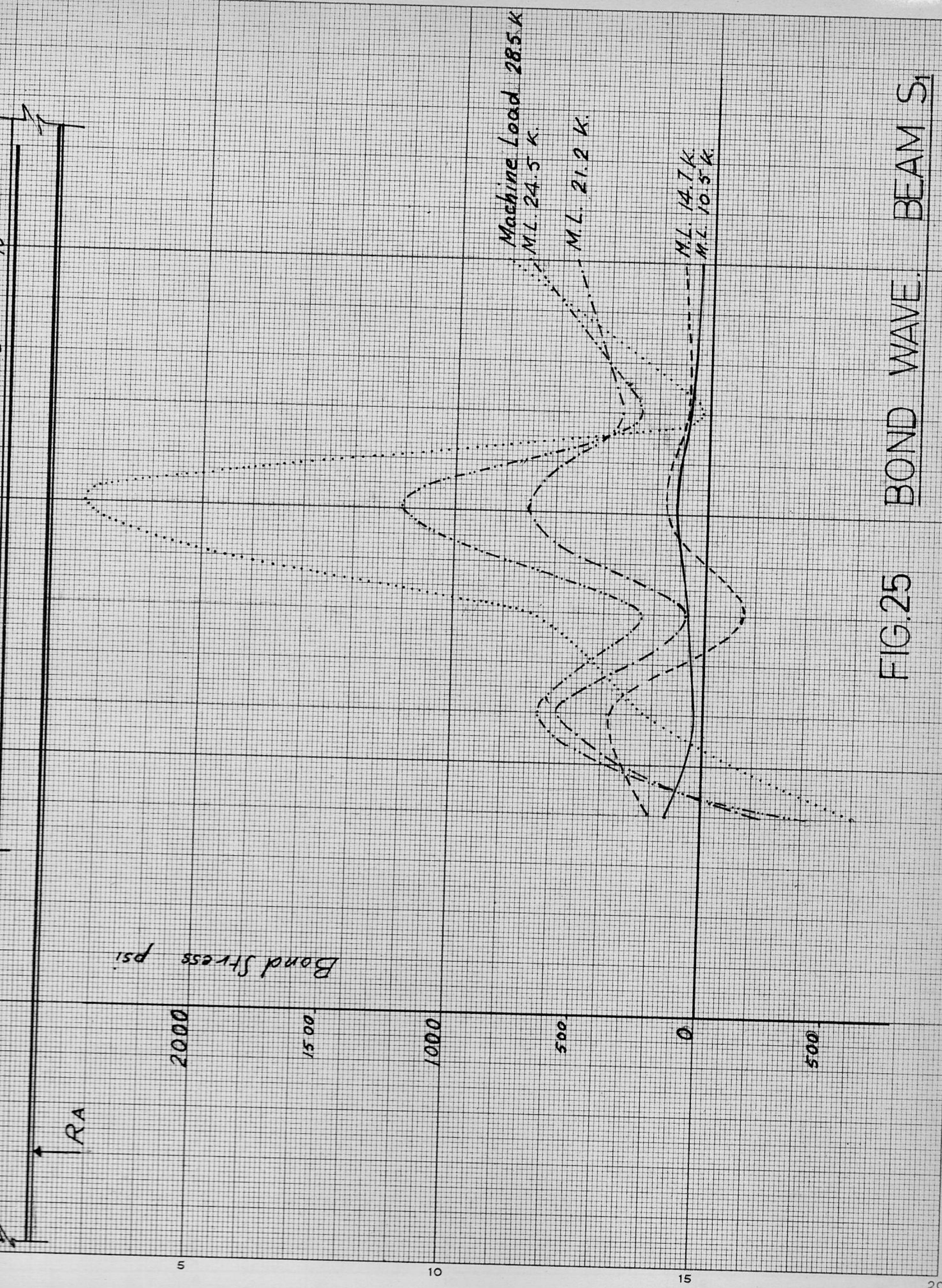
FIG. 24b FORCE V. MACHINE LOAD. BEAM  $S_2$

Bond Wave:

As a result of this study the bond wave (bond stress distribution) near the induced crack in beam  $S_1$  was evaluated and plotted for various machine loads (Fig. 25). It is worth noting that the bond wave follows a regular pattern for all machine loads, it rises from a small value of stress near the crack to a maximum value at 3.5 inches away (This may be partly attributed to the transfer of stress from the test bar to the adjacent two 8 mm. bars). The maximum peak value reached was 2480 psi. The overall shape of the bond wave as well as the high unit stresses attained agree favorably with the work done by Mains<sup>4</sup>.

Concrete Cover:

Referring to figures 26, 27, and 28 the curves of the beams of different concrete covers with the same development length for every batch were plotted. The difference in bond stress for the same machine load can be attributed to the inaccuracy in the position of the reactions or loads and the difference in the position of the compression steel. However, the results were not conclusive. The only thing that can be rightly concluded is that the beam with 1.5" cover can resist splitting more than the beams with 3/8" cover. As far as the beams with 3/4" cover they were in some cases as strong in bond as those with 1.5" cover or in other cases as weak as those with 3/8" cover.







Note: The inclined dash indicates the appearance of first split.

FIG. 26 BOND STRESS  
V.  
MACHINE LOAD

FOR DIFFERENT CONCRETE COVERS. BATCH I

Machine Load Kips

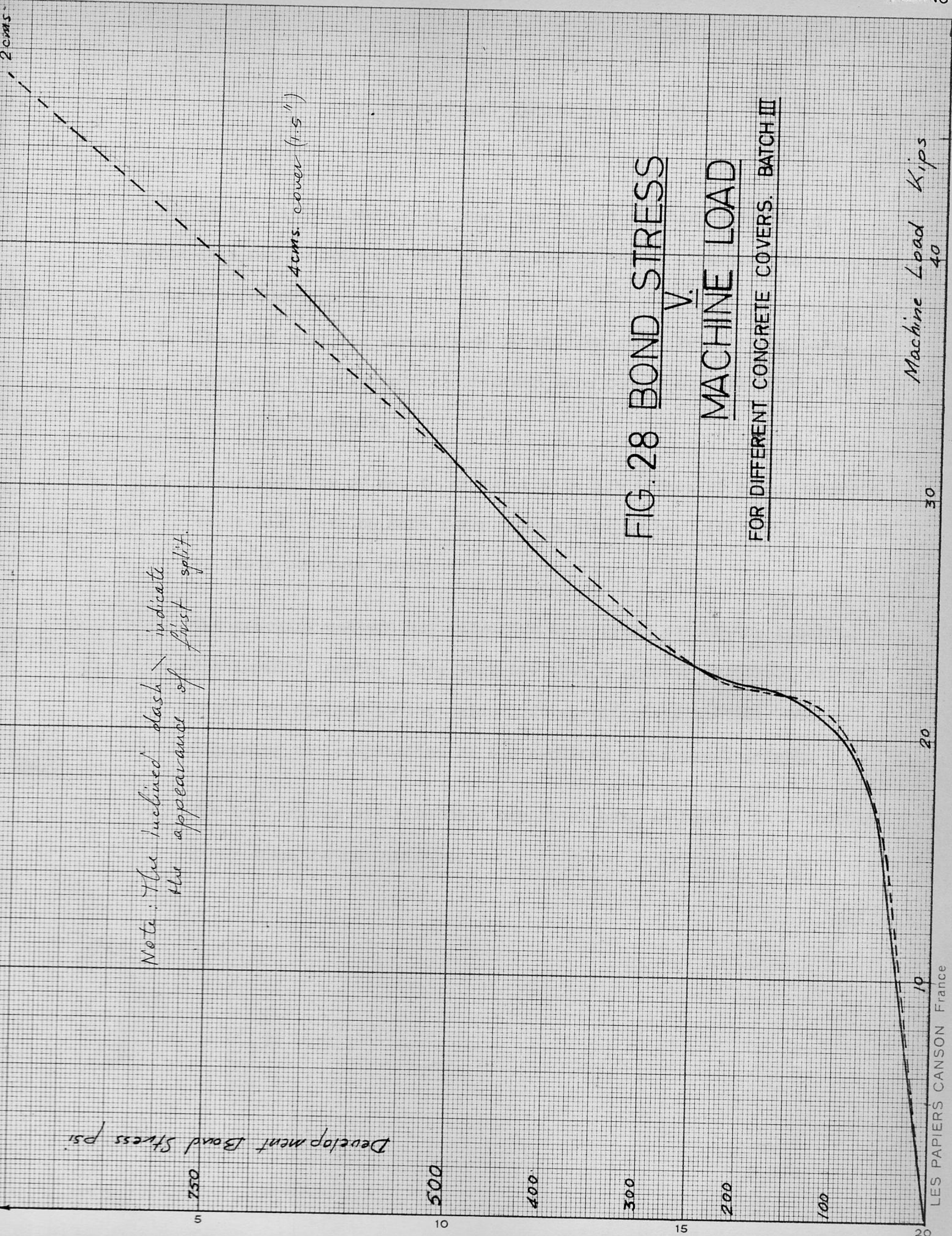
Development Bond Stress psi



FIG. 27 BOND STRESS  
V.  
MACHINE LOAD

FOR DIFFERENT CONCRETE COVERS. BATCH II

(4)



#### IV . SUMMARY AND CONCLUSIONS

Due to the limited number of beams tested and the high strength of concrete attained no definite conclusions may be drawn. The results, however, indicate the following:

1. The bond carrying capacity of 20 mm. Tor steel reinforcing bars appeared to be as good as deformed bars complying with ASTM 305A 56T specifications.
2. A deformed bar 20 mm. in diameter with 1.5 inches of clear concrete cover will develop more force than a similar bar with  $\frac{3}{8}$  of an inch of clear concrete cover.
3. The cracking pattern may influence to a great extent the required development length. This suggests that a greater factor of safety should be applied to the value 1.25 specified by the ACI Code, regarding the computation of the required development length.
4. The bond stress distribution along steel bars in beams, in a constant shear span, is not uniform.

## APPENDIX A

### Concrete Strength:

Concrete strength was taken as a constant value for a batch because all the beams were tested after 28 days and there was no trend.

A correction was made for the strength of the first batch because the cylinders were not capped; two cardboard were put under and over the cylinders under test.

For the second and the third batches the strength was taken as the average of capped cylinders. The average difference between capped and uncapped cylinders was found and this average difference was used to correct the strength of the first batch.

The average difference between capped and uncapped cylinders tested in this program was found to be 19%.

<u>Batch Number</u>	<u>Concrete Strength</u>
1	4760 psi
2	5650 psi
3	4480 psi

(For details see following pages.)

Table 1A, Batch I, Concrete Strength

Beam Notation	Days between pouring and testing	Strength of uncapped cylinders  psi	Av. Strength of uncapped cylinders  psi
D <sub>12-1</sub>	33	4280 4860 3710	4280
D <sub>20-4</sub>	34	4320 3940 3200	3800
D <sub>17-4</sub>	35	3960 4740 3470	4050
D <sub>15-4</sub>	37	4630 3150 3500	3750
D <sub>12-4</sub>	44	4460 3960 3200	3850
D <sub>8-4</sub>	46	4960 5240 4100	4750
D <sub>12-2</sub>	48	3110 3110 4040	3410

Table 2A. Batch II, Concrete Strength

Beam Notation	Days between pouring and testing	Strength of capped cylinders psi	Av. strength of capped cylinders psi	Strength of uncapped cylinders psi	Difference between capped & uncapped cylinders %
D <sub>12-1-2</sub>	35			3900 2900 2750	
D <sub>8-4-2</sub>	37			3250 4100 3180	
D <sub>12-4-2</sub>	39	5500 5500	5500	5250	4.5%
D <sub>12-4-2</sub>	46	5600 5800	5700	4200	27%
D <sub>15-4-2</sub>	97				
D <sub>20-4-2</sub>	98	750 6250	6000	3900	35%
D <sub>12-2-2</sub>	101	5500 5300	5400	4400	19%

Table 3A Batch III, Concrete Strength

Beam Notation	Days between pouring and testing	Strength of capped cylinders psi	Average strength of capped cylinders psi	Strength of uncapped cylinders psi	Difference between capped & uncapped cylinders %
D <sub>10-2</sub>	28	4440 3680	4060	3620	11%
D <sub>10-4</sub>	28	3950 4170	4060	3300	19%
D <sub>12-4</sub>	34	4450 4670	4560	3820	16%
D <sub>8-4</sub>	35	4670 4450	4560	3600	21%
S <sub>1</sub>	40	5020 5020 4460	4820		
S <sub>2</sub>	41	4880 4880 4960	4900		



### Deformations on Tor Steel

Description of the deformations of Tor steel used, is shown on page 56. The one requirement of the ASTM, A305 56T, which the Tor steel does not meet is found in item b of these specifications as quoted below:

The deformation shall be placed with respect to the axis of the bar so that the included angle is not less than 45 deg, where the line of deformations form an included angle with the axis of the bar of from 45 to and including 70 deg, the deformations shall alternately reverse in direction on each side, or those on one side shall be reversed in direction from those on the opposite side.

In Tor steel the angle which the continuous deformation form with the axis of the bar is from 17 to 21 deg, and the angle which the discontinuous deformations form with the axis of the bar is from 41 to 45 deg. These deformations do not reverse direction in any way.

However, the two types of Tor steel used conform to the requirements for minimum height and average spacing, given in items c and e of the ASTM specifications as quoted below:

The average spacing or distance between deformations on each side of the bar shall not exceed seven-tenth of the nominal diameter of the bar.

The average height of deformations shall be not less than the following percentages.

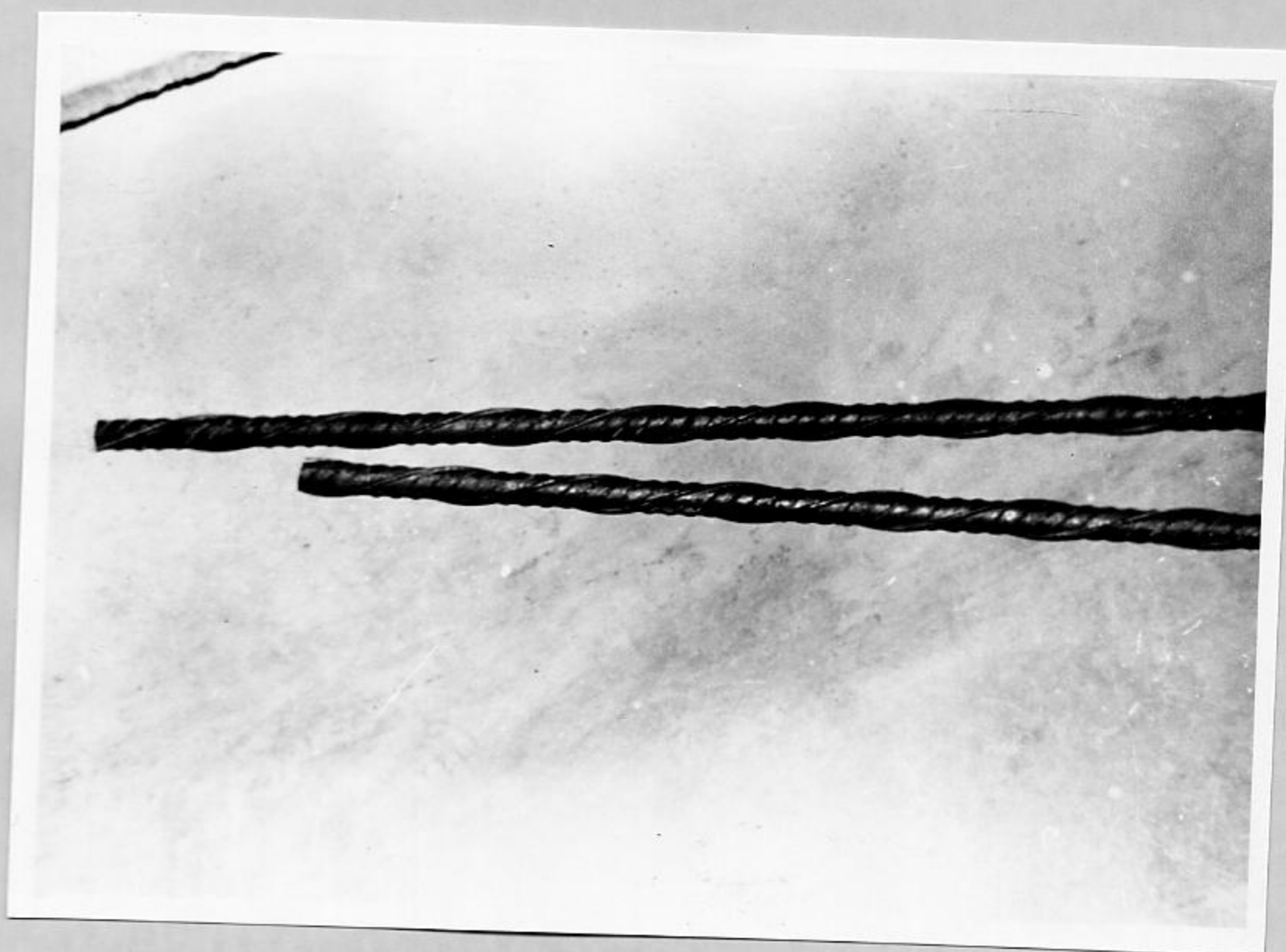
Deformed Bar Designation Number	Percent of Nominal Diameter
6 to 11	5

For 20 mm. steel bar the average height of deformations must be  $20 \times 0.05 = 1$  mm. which is available in the two types of steel used (see page 56).



	TYPE I	TYPE II
A	25.6m.m.	22.6 m.m.
B	19.7	19.5
C	2.4	3.1
D	2.0	3.4
E	1.2	1.4
F	13.5	14.0

FIG.A1 CROSS SECTION OF TOR STEEL

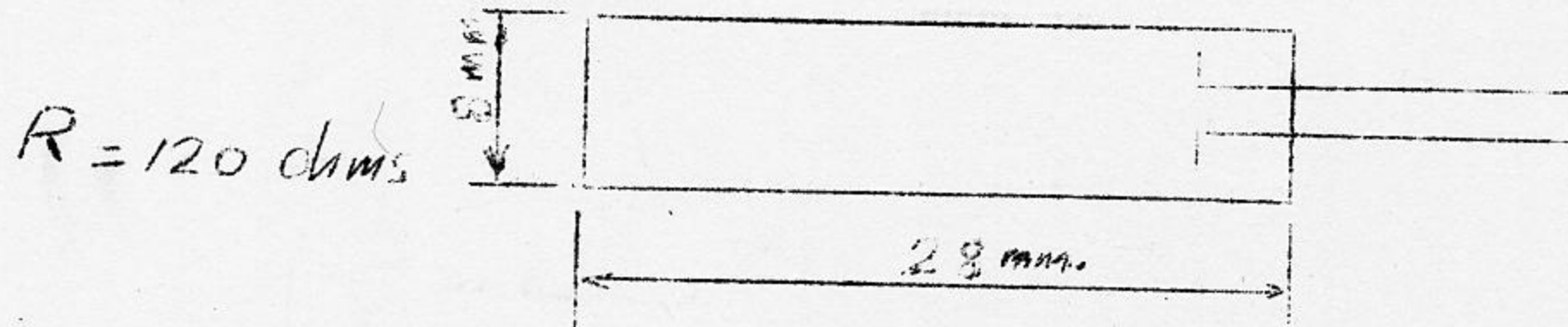


TOR STEEL

## APPENDIX B

### Strain Gages

Strain gages used are paper strain gages (Philips make) PR 9211



For mounting the strain gages a surface area of approximately  $6 \text{ cm}^2$  of the bar was filed to remove the deformation only, then this area was smoothed with emery cloth, and wiped with pure acetone. A small drop of Dupont cement was wiped energetically with the finger, applying pressure to fill the irregularities of this surface. A sufficient amount of this cement was then put on the surface and the strain gage was stuck onto it. A piece of soft rubber was placed on the strain gage followed by another piece of hard rubber. This setup was loaded with 3 Kgs. of weight and left for twenty four hours. A compensating gage was prepared always in similar manner, and used throughout the testing program.

### Measuring Bridge

The measuring bridge, used for taking static strain measurements with strain gages, consists in principle of a Wheatstone bridge.

Strain measurements are in essence measurements of the resistance alterations at strain. It is possible to measure a resistance variation of 0.0006 ohm, consequently a diagonal tension of the bridge arising from a strain of  $0.005 \text{ } \text{‰}$ .

APPENDIX C

Experimental Results

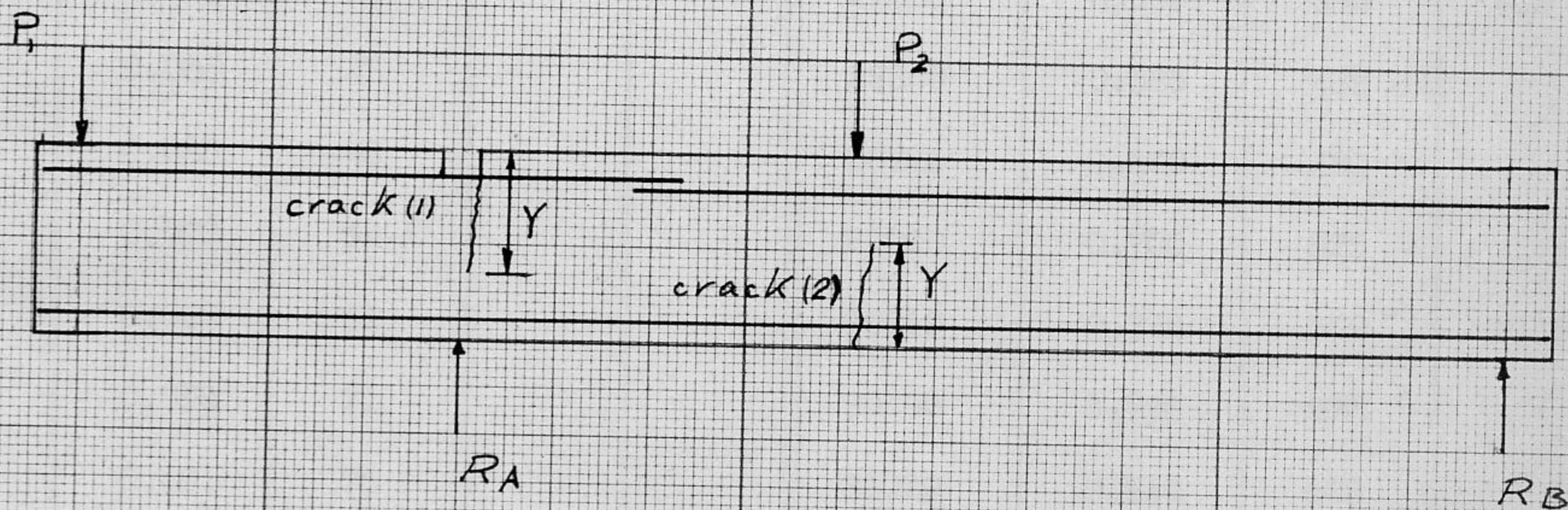


FIG.C1 POSITION OF MAJOR FLEXURAL CRACKS.

Beam D<sub>8-4-1</sub>

Table C 1

Machine Load Lbs	Strain ‰	Development Bond Stress Psi	Crack (1) Dist. Y in.	Crack (2) Dist. Y in.	Machine Load Lbs	Strain ‰	Development Bond Stress Psi	Crack (1) Dist. Y in.	Crack (2) Dist. Y in.
3670	0.018	13			25210	0.281	211	4.5	
5720	0.029	22			26010	0.325	244		
7040	0.031	23			26360	0.356	267		
7790	0.038	29			27030	0.391	293	5.5	
8860	0.044	33			27650	0.450	336		
10030	0.051	38			27650	0.530	396	9.5	
10880	0.058	43			28340	0.585	438		
11960	0.060	48			28720	0.640	480		
13220	0.072	54			29020	0.700	525		8
14710	0.082	61			29710	0.725	542	10.5	
16020	0.095	71			30490	0.770	576		
17240	0.101	76			31020	0.810	608		
18260	0.115	86			31770	0.850	638		
19670	0.130	98			32550	0.898	674		
20380	0.140	105			33240	0.941	706		
21640	0.156	117			34230	0.980	735		
2050	0.171	136			34440	1.080	809		
3010	0.190	142		4.5	34820	1.128	846		
3760	0.207	155		6	35430	1.160	869		
4430	0.230	172			36280	1.190	890		
4830	0.255	191			37170	1.230	921		
					37480 **				

\* See fig CI.

\*\* Appearance of first split.

Table C 2

Machine Load Lbs	Strain %	Development Bond Stress Psi	Crack (1) Dist. Y* in.	Crack (2) Dist. Y in.	Machine Load Lbs	Strain %	Development Bond Stress Psi	Crack (1) Dist. Y in.	Crack (2) Dist. Y in.
1370	0.009	4			20120	0.770	376		
2230	0.015	7			20860	0.828	405		
3260	0.020	10			21800	0.905	443		5
4180	0.030	15			22510	0.975	479	9.5	
5170	0.034	17			23350	1.030	403		
6360	0.042	21			24070	1.075	525		
7520	0.051	25			24930	1.110	539	10	
8860	0.061	30			25820	1.160	569		
9730	0.071	35			26780	1.205	590		
10950	0.078	38			27820	1.250	611		
11940	0.104	51			28600	1.280	625		
13090	0.144	71			29410	1.325	650		
13880	0.156	76			30270	1.350	661		
14750	0.178	83			30830	1.375	673		8.5
15350	0.230	112			31940	1.420	660		
15700	0.500	196	4.5		32790	1.460	715		
15870	0.440	215			33700**	1.480	725		
16440	0.462	226	5.5		33920	1.482	725		
17180	0.525	256			34220	1.495	731		
17950	0.592	290	7		34660	1.495	731		
18390	0.655	320		2					
19200	0.705	346	8.5						

\* See fig CI

\*\* Appearance of first split



Beam D<sub>12-1-1</sub>

Table C 3

Machine Load Lbs	Strain ‰	Development Bond Stress Psi	Crack (1) Dist. Y in.	Crack (2) Dist. Y in.	Machine Load Lbs	Strain ‰	Development Bond Stress Psi	Crack (1) Dist. Y in.	Crack (1) Dist. Y in.
1000	0.002	1							
1500	0.005	3			35760	1.427	700		
2000	0.009	4			36980	1.473	720		
2500	0.012	6			37790	1.512	731		
3000	0.015	7			39330	1.567	760		
3500	0.019	9			40395	1.623	771	10.5	
4000	0.021	10			41345	1.677	790		
5000	0.026	13			42155	1.722	806		
6000	0.031	15			42890	1.763	818		
7000	0.037	18			44050	1.817	830		
8000	0.042	20			44780	1.858	845	11	
9000	0.049	24			45325 **				
10000	0.053	26							
11000	0.061	30							
11970	0.067	33							
13240	0.077	37							
14375	0.084	41							
15250	0.092	45							
16070	0.120	59							
17200	0.242	119	3.5						
17630	0.292	143							
18210	0.352	173	4.5						
18785	0.522	257							
19810	0.562	277							
20720	0.627	306	5.5						
21180	0.717	350							
23175	0.782	384							
24020	0.832	407							
25120	0.900	440	8						
26350	0.980	490							
27255	1.037	508							
28780	1.110	541	9.5						
29970	1.172	575		9					
30490	1.202	590							
30740	1.253	612							
30000	1.303	640							
30090	1.353	661							
30900	1.388	680							

\* See fig CI.

\*\* Appearance of first split

Table C 4

Machine Load Lbs	Strain ‰	Development Bond Stress Psi	Crack (1) Dist. Y in.	Crack (2) Dist. Y in.	Machine Load Lbs	Strain ‰	Development Bond Stress Psi	Crack (1) Dist. Y in.	Crack (2) Dist. Y in.
95	0.008	4							
80	0.011	5			34870	1.510	736		
70	0.020	10			35610	1.555	751	11	
40	0.030	15			36130	1.595	768		
20	0.039	19			36920	1.642	778		
20	0.047	23			37180	1.690	798		
30	0.055	27			37450	1.710	803		
0	0.065	32			38120	1.750	812		10.5
0	0.076	37			38690	1.775	816		
0	0.090	44			38760	1.790	824		
0	0.102	50			39140	1.812	830		
0	0.150	71			39770	1.850	838		
0	0.215	105	4.5		40250	1.890	849		
0	0.260	128	5.5		40700	1.920	854		
0	0.378	185	6.5		41090	1.955	864		
0	0.430	211			41720	2.010	874		
0	0.458	225			42140	2.050	883		
0	0.498	244			42920	2.105	891		
0	0.546	267	8.5		43410	2.165	901		
0	0.610	299			43910	2.220	911		
0	0.650	319			44340	2.260	919		
0	0.680	334	9		44920	2.318	921		
0	0.710	349			45340	2.370	927		
0	0.748	366		5	45870	2.430	939		
0	0.782	384			46260	2.480	942		
0	0.825	405	10		46460	2.530	949		
0	0.870	428		7	46850	2.570	951		
0	0.905	445			47240	2.640	958		
0	0.948	465			47580	2.698	960		
0	0.998	490			47820 **	2.752	964	12	
0	1.050	415							
0	1.090	434	10.5		48220	2.810	969		
0	1.121	551							
0	1.175	575							
0	1.210	593							
0	1.240	619							
0	1.265	621							
0	1.280	629							
0	1.365	670							
0	1.400	686		9.5					
0	1.437	704							
0	1.480	724							

Machine Load Lbs	Strain o/oo	Development Bond Stress Psi	Crack (1) Dist. Y* in.	Crack (2) Dist. Y in.	Machine Load Lbs	Strain o/oo	Development Bond Stress Psi	Crack (1) Dist. Y in.	Crack (2) Dist. Y in.
760	0.002				28500	1.432	558		
2130	0.012	5			29130	1.472	571	11	
3120	0.021	8			29910	1.512	586		
3920	0.027	11			30530	1.547	595	11.5	
4970	0.035	14			31110	1.575	604		
5970	0.043	17			31650	1.604	610		
6840	0.051	20			32510	1.642	619		
7780	0.062	24			33130	1.682	631		
8620	0.070	27			33850	1.712	639		
9520	0.077	30			34550	1.752	648		
10460	0.086	34			35190	1.782	652		
12420	0.112	43			35910	1.817	660		
13330	0.127	49			36390	1.854	666		
14160	0.152	59			37030	1.892	674		
14880	0.182	71			37860	1.930	679		
15130	0.249	97	3.5		38510	1.972	690		
15700	0.400	156	5.5		39050	1.992	694		6.5
16230	0.474	184	7		39310	2.023	696		
16870	0.517	201			39880	2.052	696		
17670	0.572	224			40460	2.097	708		
18260	0.632	246			40760	2.122	708		
18860	0.691	270			41090	2.152	713		
19300	0.748	290			41330	2.180	720		
19700	0.802	312			41900	2.212	724		
20080	0.832	324			42360	2.237	724		8.5
20600	0.862	336			42510	2.272	730		
21080	0.907	352			43030	2.310	731		
21640	0.952	371			43220	2.332	732		
22290	0.997	389			43600	2.362	736		
22730	1.042	406	10		44080	2.407	741		
23410	1.092	425			44510	2.452	745		
23940	1.132	440			44840	2.502	749		
24520	1.162	452			45050	2.547	752		
25000	1.207	469			45340	2.592	758		
25800	1.257	488	10.5		45630	2.637	758		
26220	1.297	502			45940	2.687	761		
26710	1.324	516			46160	2.722	766		
27420	1.365	532			46340	2.772	766		
27960	1.397	543			46580	2.822	772		
					46740	2.862	772		

\* See fig CI

Machine Load Lbs	Strain o/oo	Development Bond Stress Psi	Crack (1) Dist. Y in.	Crack (2) Dist. Y in.
46980	2.917	773		
47300	2.972	777		
47520	3.017	777		
47720	3.065	780		
47980	3.132	782		
47980	3.187	786		
48060	3.232	786		
48160	3.262	786		
48540	3.332	788		
48660	3.382	791		
48700	3.417	791		
49000	3.462	794		
49210	3.512	794		
49390 **	3.572	794		
49650	3.652	800	12	
49740	3.712	800		
49870	3.752	800		

\*\* Appearance of first split

Beam D  
I7-4-1

Table C 6

Machine Load Lbs	Strain o/oo	Development Bond Stress Psi	Crack (1) Dist. Y in.	Crack (2) Dist. Y in.	Machine Load Lbs	Strain o/oo	Development Bond Stress Psi	Crack (1) Dist. Y in.	Crack (2) Dist. Y in.
940	0.005	2			31720	1.789	575		
1840	0.011	4			32250	1.841	581		
2460	0.020	7			32930	1.892	592		
3850	0.029	10			33480	1.948	601		
5370	0.046	16			33880	1.990	610		
6720	0.060	20			34650	2.050	617		
7930	0.072	25			35040	2.098	621		
9350	0.090	31			35280	2.131	625		
10580	0.100	34			35650	2.170	630		
11520	0.126	43			35920	2.219	636		
12640	0.155	53			36430	2.266	641		
13190	0.172	59			36800	2.319	643		
14100	0.195	67			37170	2.361	646		
14770	0.250	86			37690	2.440	652		
15120	0.400	136	5		38070	2.501	659		
15590	0.460	157			38560	2.560	664		
16260	0.530	161	6		38920	2.640	668		
16970	0.600	206	7		39390	2.705	670		
17370	0.660	226			39780	2.770	673		
18110	0.715	244			40090	2.845	678		
18750	0.765	261	9		40410	2.895	680		
19310	0.820	280			40750	2.952	681		
20250	0.882	302			40850	2.920	682		
20780	0.928	316			40960**	2.920	682		
21280	0.980	335							
22350	1.045	358						11	
22770	1.090	373							
23190	1.130	386	10						
23650	1.160	396							
24370	1.207	413	10.5						
24790	1.240	424							
25450	1.291	441							
26110	1.339	457							
26510	1.374	468							
27040	1.411	481							
27590	1.467	498							
28290	1.510	514							
28850	1.560	527							
29350	1.606	535							
29950	1.648	545							
30520	1.684	552							
31250	1.740	566		4					

\* See fig CI

\*\* Appearance of first split

Beam D<sub>20-4-1</sub>

Table C 7

Machine Load Lbs	Strain o/oo	Development Bond Stress Psi	Crack (1) Dist. Y* in.	Crack (2) Dist. Y in.	Machine Load Lbs	Strain o/oo	Development Bond Stress Psi	Crack (1) Dist. Y in.	Crack (2) Dist. Y in.
1400	0.008	2			28730	2.172	532		
2290	0.018	5							
3150	0.027	8			29160	2.250	541		
3930	0.040	12							
5155	0.051	15			29735	2.342	545		
6610	0.070	20							
7640	0.083	24			30400	2.410	552		
8950	0.110	32							
0140	0.138	40			30950	2.528	559		
2640	0.430	124	6.5						
3630	0.610	176			3 0970				
4210	0.710	205	7.5						
4750	0.775	224							
5600	0.870	251							
6440	0.970	281	10						
7280	1.062	306							
7930	1.150	332							
8870	1.244	360							
9500	1.315	380							
0300	1.390	401							
0500	1.412	407							
1240	1.465	424							
1900	1.512	434							
2350	1.550	441							
3040	1.607	455	11						
3640	1.654	460							
4210	1.700	471							
4710	1.756	480							
5340	1.801	489							
5890	1.861	496							
6470	1.911	502							
7010	1.972	514							
7580	2.030	519							
8170	2.100	524							

\* See fig C1

Table C 8

Machine Load Lbs	Strain o/oo	Development Bond Stress Psi	Crack (1) Dist. Y* in.	Crack (2) Dist. Y in.	Machine Load Lbs	Strain o/oo	Development Bond Stress Psi	Crack (1) Dist. Y in.	Crack (2) Dist. Y in.
2090	0.010	7			29520	0.550	414		
2930	0.016	12			30200	0.598	450	8	
5030	0.025	19			30750	0.630	475		
5750	0.032	24			31480	0.676	509		
8820	0.042	32			32690	0.725	545	8.5	
9920	0.050	37			33460	0.772	581		9
12750	0.062	47			34730	0.830	624	9.5	
15830	0.074	56			35590	0.890	671	10	
19970	0.084	63			36580	0.960	721	10.5	
26680	0.092	69			37250	1.016	761		
35520	0.108	81			38040	1.060	799		
46320	0.118	87			38940	1.012	830		
59780	0.130	98			39530	1.140	858		
76190	0.142	107			40240	1.176	881		
9710	0.162	122			40890	1.222	921		
13030	0.206	156	3.5		41990	1.280	965		
17550	0.258	194			42600	1.324	1000		
23000	0.332	250	7.5		43210	1.370	1030	11	10
30440	0.432	325		8	43730	1.420	1065		
4010	0.500	376			44330	1.460	1100		
					45030	1.506	1125		
					46520*				

See fig CI

\*\* Appearance of first split.

Table C 9

Machine	Strain	Development Bond Stress	Crack (1) Dist. Y*	Crack (2) Dist. Y	Machine Load Lbs	Strain	Development Bond Stress	Crack (1) Dist. Y	Crack (2) Dist. Y
	‰	psi	in.	in.		‰	psi	in.	in.
20	0.013	6			24360	0.647	316		
60	0.020	10			25370	0.710	349		
90	0.031	15			26290	0.765	375		5.5
20	0.040	20			27150	0.823	403		
10	0.051	25			28150	0.875	429	10.5	6.5
30	0.061	30			28780	0.925	454		
00	0.071	35			29360	0.965	473		
90	0.079	39			30790	1.025	502		8
00	0.087	43			31830	1.085	534	11	
40	0.103	51			32960	1.140	560		
60	0.115	56			33940	1.197	587		
90	0.129	64			34880	1.245	610		9
70	0.147	72			36050	1.303	640		
30	0.161	79			37370	1.371	671		
10	0.180	88	5		38330	1.425	699		
00	0.235	115			39080	1.467	719		
70	0.325	159	6		40240	1.521	740		
00	0.417	205	8	3.5	41070	1.561	753		
40	0.499	245	10	4	41570	1.585	763		
00	0.595	292			42590	1.633	778	11.5	
					43630	1.681	794		
					44470	1.723	809		
					44760	1.753	815		
					45420	1.785	820		
					45840	1.815	830		
					46780	1.855	837		
					47350	1.895	850		
					47900	1.935	863		
					48660	1.980	870		
					49090	2.017	873		
					49350	2.053	880		
					49960	2.091	886		
					50350 **	2.131	895		

\* See fig CI

\*\* Appearance of first split



Machine Load Lbs	Strain ‰	Development Bond Stress Psi	Crack (1) Dist. Y in.	Crack (2) Dist. Y in.	Machine Load Lbs	Strain ‰	Development Bond Stress Psi	Crack (1) Dist. Y in.	Crack (2) Dist. Y in.
2570	0.010	5			26070	1.152	563		
3960	0.022	11			27280	1.222	598		
5990	0.035	17			28520	1.295	635		
7810	0.050	24			29720	1.371	671		6
9780	0.062	30			30870	1.450	711		
1500	0.080	39			32140	1.530	745		
2040	0.092	45			33380	1.600	769		
3870	0.110	54			34640	1.672	790		
5000	0.140	69			35270	1.715	803	10	7.5
5950	0.205	100			36640	1.795	825		
6620	0.410	200	4.5		38320	1.880	846		
7580	0.500	245			39480	1.970	870		
8660	0.540	265	7		41170	2.098	877		
9570	0.665	326			42250	2.180	906		
10320	0.775	380	7.5		43650	2.290	920		
1310	0.835	409			44540	2.400	933		
1300	0.908	445	9	3	45290	2.502	946		
1630	0.992	486			46360**				
1110	1.072	522							

\* See fig CI

\*\* Appearance of first split

Machine Load Lbs.	Strain o/oo	Development Bond Stress Psi	Crack (1) Dist. Y in.	Crack (2) Dist. Y in.	Machine Load Lbs	Strain o/oo	Development Bond Stress Psi	Crack (1) Dist. Y in.	Crack (2) Dist. Y in.
1730	0.007	3			26360	0.955	469	9	7
2440	0.015	7			27010	0.993	486		
4640	0.025	12			27900	1.035	508		
6650	0.035	17			28780	1.085	532		
8450	0.047	23			29820	1.133	552		
10220	0.059	28			30860	1.183	581		8
12160	0.063	31			31590	1.217	595		
13670	0.083	41			32090	1.235	605		
15030	0.095	47			32570	1.253	613		
16440	0.110	54			33130	1.277	623	9.5	8.5
17370	0.123	60			33740	1.303	640		
18510	0.135	66			34630	1.333	652		
19700	0.155	76			35440	1.367	670		
20400	0.170	83			35930	1.385	680		
21440	0.195	95	3.5		36650	1.407	690		
21880	0.435	213	6.5		37330	1.433	699		9
21880	0.595	291	7	6	38380	1.470	720		
22340	0.646	316			39180	1.500	735		
23220	0.707	346			39790	1.515	740	10	
24110	0.785	385			40650	1.541	746		
25150	0.847	415	7.5		41460	1.570	758		
					42010	1.593	762		
					42710	1.605	770		
					43330	1.630	781		
					44060	1.655	782		
					44850 **				

\* See fig CI

\*\* Appearance of first split

Beam D<sub>15-4-2</sub>

Table C 12

Machine Load lbs	Strain ‰	Development Bond Stress Psi	Crack (1) Dist. Y in.	Crack (2) Dist. Y in.	Machine Load Lbs	Strain ‰	Development Bond Stress Psi	Crack (1) Dist. Y in.	Crack (2) Dist. Y in.
510	0.015	6			22190	1.200	468	10	2.5
570	0.025	10			23150	1.260	491		
770	0.035	14			24800	1.340	521		
840	0.050	20			25000	1.415	550		
900	0.065	25			25815	1.485	576		
980	0.080	31			26660	1.560	599		
1040	0.090	35			27780	1.630	611	11	
1100	0.115	44			28690	1.700	635		
1160	0.140	54			29580	1.775	649		
1190	0.270	105	4.5		30165	1.840	661		
1270	0.370	144	6		31490	1.930	679		
1350	0.460	178	8		32500	2.002	692		
1490	0.700	274	9		33130	2.058	702		
1560	0.778	303			34225	2.130	711		
1640	0.860	324			35080	2.195	721		
1750	0.925	360			35820	2.260	730		
1820	0.998	389			36825	2.330	731		
1900	1.060	413			37520	2.390	748		
1980	1.125	439			38210	2.460	750		
					39215	2.530	751		
					39620	2.570	756		
					40360	2.640	759		
					41030	2.705	761		
					41790	2.740	766		
					42620	2.840	771		
					43340 **	3.000	777		

\* See fig. CI

\*\* Appearance of first split

Machine Load lbs	Strain %	Development Bond Stress psi	Crack (1) Dist. Y in.	Crack (2) Dist. Y in.	Machine Load	Strain %	Development Bond Stress psi	Crack (1) Dist. Y in.	Crack (2) Dist. Y in.
1910	0.015	5			35400	2.130	530		
2700	0.022	6			36340	2.180	535		
4090	0.032	9			37430	2.250	541		
5350	0.047	14			38360	2.340	548		
6770	0.060	17			38800	2.390	550		11
8390	0.075	22			39430	2.475	555		
9750	0.090	26			40050	2.540	560		
1060	0.110	32			40320	2.630	564		
2150	0.128	37			40920	2.725	568		
3360	0.250	73	6		41620	2.840	574		
4340	0.315	91	7		41880	2.930	576		
4910	0.695	200	9		42480	3.110	581		
5520	0.770	223			43040	3.260	584		
6290	0.820	237			43710	3.480	590		
7340	0.915	265	10		44200	3.680	590		
8380	1.010	293			44520	3.770	590		
9480	1.090	316	10.5		45170	3.995	590		
10760	1.178	340	11		45670	4.275	590		
11950	1.252	362			45890	4.425			
12900	1.345	390			46320	4.670			
14040	1.375	396			46700	4.795			
15330	1.500	433			47030	4.990			
16440	1.590	450			47310	5.135			
17700	1.665	466			47580	5.295			
18940	1.740	480			47900	5.545			
20100	1.790	488		9	48570	6.235			
20780	1.860	498	12		48900	6.505			
21730	1.920	505			49530	7.255			
22710	1.985	516			49910	7.695			
23700	2.050	521			50090	7.935			
24400	2.100	527			50320	8.275			
					50590	8.585			
					50840	8.895			
					50960	9.115			
					51130	9.255			
					51380	9.345			
					52290	9.905			
					52620	10.395			
					52900	11.075			
					55940	**			

\* See fig CI

\*\* Appearance of first split

Beam D<sub>8-4-3</sub>

Table C 14

Machine Load Lbs	Strain o/oo	Development Bond Stress Psi	Crack (1) Dist. Y* in.	Crack (2) Dist. Y in.
980	0.008	5		
900	0.015	10		
400	0.020	13		
770	0.028	19		
100	0.030	20		
440	0.040	27		
240	0.048	32		
180	0.060	40		
060	0.075	50		
890	0.085	57		
860	0.108	72		
700	0.130	87		
910	0.155	104		5
040	0.182	122		
070	0.245	165	7	6
040	0.510	344	11	
300	0.652	440		
100	0.810	545		
320	0.940	634	11.5	
370	1.075	721		
370	1.235	830		
110	1.345	907		8
030	1.458	978		
790	1.560	1050		
430	1.640	1100		
900**	1.725	1150		
510	1.860	1220		

\* See fig CI

\*\* Appearance of first split

Beam D<sub>10-4-3</sub>

Table C 15

Machine Load Lbs	Strain o/oo	Development Bond Stress Psi	Crack (1) Dist. Y in.	Crack (2) Dist. Y in.
1540	0.008	4		
3750	0.020	11		
5950	0.030	16		
9060	0.050	26		
11120	0.062	33		
13310	0.078	41		
14820	0.092	49		
16870	0.110	59		
18300	0.128	68		
19850	0.160	86	2	3
20600	0.190	101		
22050	0.282	150		
23320	0.490	260	3	6
24580	0.600	318		8
26710	0.700	375	6.5	
27870	0.790	420		
30000	0.880	470		10.5
31500	0.960	511		11
33260	1.035	550	7.5	
35000	1.118	593		
36700	1.190	632		
38480	1.260	670		
41000**				

\* See fig. CI

Machine Load Lbs	Strain o/oo	Development Bond Stress Psi	Crack (1) Dist. Y* in.	Crack (2) Dist. Y in.
1970	0.010	5		
3760	0.020	11		
5770	0.030	16		
7210	0.038	20		
10350	0.055	30		
11150	0.060	32		
12480	0.070	37		
14430	0.082	44		
15390	0.095	50		
16350	0.100	53		
17740	0.115	61		
19330	0.135	72		
20460	0.180	96		
21180	0.245	130		
22090	0.410	217		
23170	0.480	255	6	
24100	0.550	293	7	
25530	0.620	330	8	9
26620	0.690	367		
27820	0.750	397		
29210	0.815	430		
30160	0.865	460		
31590	0.930	495		11
32700	0.990	526		
34000	1.065	568	9	
35270	1.135	603		
36670	1.215	646	10.5	
38060	1.300	690		
39350	1.360	722		
40400	1.420	755		
41480	1.482	790		
42860	1.558	829	11	12
43660	1.632	861		
45000	1.738	911		
45920 **	1.860	970		

\* See fig CI.

\*\* Appearance of first split

Machine Load Lbs	Strain ‰	Development Bond Stress Psi	Crack (1) Dist. Y* in.	Crack (2) Dist. Y in.	Machine Load Lbs	Strain ‰	Development Bond Stress Psi	Crack (1) Dist. Y in.	Crack (1) Dist. Y in.
2580	0.025	11			54960	2.545	948		
5060	0.040	18							
6350	0.050	22			55410	2.640	967		
8150	0.062	27							
9660	0.078	34			55820	2.720	975		
11750	0.090	40							
12750	0.102	45			56470	2.810	982		
14700	0.120	53							
16220	0.140	62			57030	2.910	995		
17620	0.200	88							
18150	0.350	154	6.5		57510	2.990	1002		
19600	0.432	190	7.5						
21060	0.505	221	8.5		57750	3.10	1010		
22220	0.520	229							
23230	0.630	276			58030**				
24480	0.690	303							
26110	0.768	370							
27420	0.825	382	10						
28700	0.890	391		7					
30320	0.960	421							
31420	1.018	455							
32730	1.070	471	11						
34040	1.140	501							
35510	1.210	541							
36770	1.275	560							
38040	1.335	586							
39260	1.395	613	12						
40520	1.460	641							
41670	1.520	668							
42840	1.580	694							
44080	1.645	720							
45100	1.700	741							
46220	1.758	760							
47350	1.825	784							
48280	1.895	806							
49260	1.962	830							
50240	2.040	850							
51060	2.100	865							
51850	2.168	879							
52270	2.232	890							
52880	2.300	805							
53380	2.355	916							
54070	2.440	930							

\* See fig CI

\*\* Appearance of first split



Machine Load lbs	Strain o/oo						
	Gage 1	Gage 4	Gage 5	Gage 6	Gage 7	Gage 8	Gage 9
1990	0.010	0.015	0.010	0.015	0.019	0.002	0.000
4340	0.025	0.030	0.025	0.030	0.022	0.002	0.002
6140	0.030	0.050	0.040	0.035	0.025	0.015	0.010
8950	0.050	0.055	0.050	0.052	0.040	0.015	0.015
10570	0.060	0.080	0.065	0.060	0.050	0.030	0.018
12590	0.070	0.100	0.080	0.072	0.058	0.030	0.025
14770	0.092	0.130	0.110		0.072	0.048	0.036
16280	0.110	0.150	0.150	0.080	0.105	0.060	0.047
18650	0.210	0.260	0.280	0.210	0.220	0.160	0.110
19790	0.268	0.330	0.375	0.285	0.295	0.205	0.155
21230	0.311	0.382	0.460	0.370	0.358	0.242	0.184
23020	0.365	0.442	0.560	0.460	0.430	0.280	0.220
24500	0.410	0.500	0.635	0.500	0.489	0.298	0.252
25890	0.450	0.532	0.705	0.632	0.555	0.300	0.265
27710	0.490	0.650	0.695	0.750	0.652	0.300	0.280
28550	0.540	0.670	0.842	0.812	0.700	0.285	0.280

Machine Load lbs	Bond Stress Psi					
	Between	Between	Between	Between	Between	Between
	4-5	5-6	6-7	7-8	8-9	9-end
1990	40	28	16	93	12	0
4340	44	24	48	117	0	6
6140	93	32	61	60	28	30
8950	65	- 4	69	150	0	44
10570	141	32	61	121	73	52
12590	182	56	81	170	73	73
14770	202	380	-145	150	73	105
16280	93	432	-149	270	110	123
18650	40	444	- 65	371	295	325
19790	-61	565	- 60	545	299	456
21230	-240	585	60	615	343	540
23020	-365	648	181	909	364	645
24500	-521	648	242	1210	266	740
25890	-685	485	465	1550	198	780
27710	-443	325	585	2130	105	822
28550	-605	242	688	2480	28	822

Beam S<sub>2</sub>

Table C 20

Machine Load Lbs	Strain o/oo				
	Gage 2	Gage 4	Gage 6	Gage 11	Gage 12
2330	0.000	0.002	0.005	0	-0.015
5200	0.000	0.002	0.010	-0.01	-0.030
7210	0.000	0.010	0.025	-0.01	-0.03
9450	0.010	0.020	0.045	-0.01	-0.03
11500	0.012	0.032	0.060	-0.01	-0.03
13870	0.018	0.046	0.090	-0.005	-0.03
15670	0.025	0.057	0.110	0	-0.03
17870	0.030	0.070	0.145	0	-0.03
19770	0.042	0.098	0.190	0.005	-0.025
21810	0.070	0.195	0.280	0.055	-0.005
22830	0.120	0.30	0.375	0.080	0.02
23500	0.22	0.38	0.330	0.005	0.06

APPENDIX D

Photographs of Beams after Failure

## MODE OF FAILURE OF BEAMS

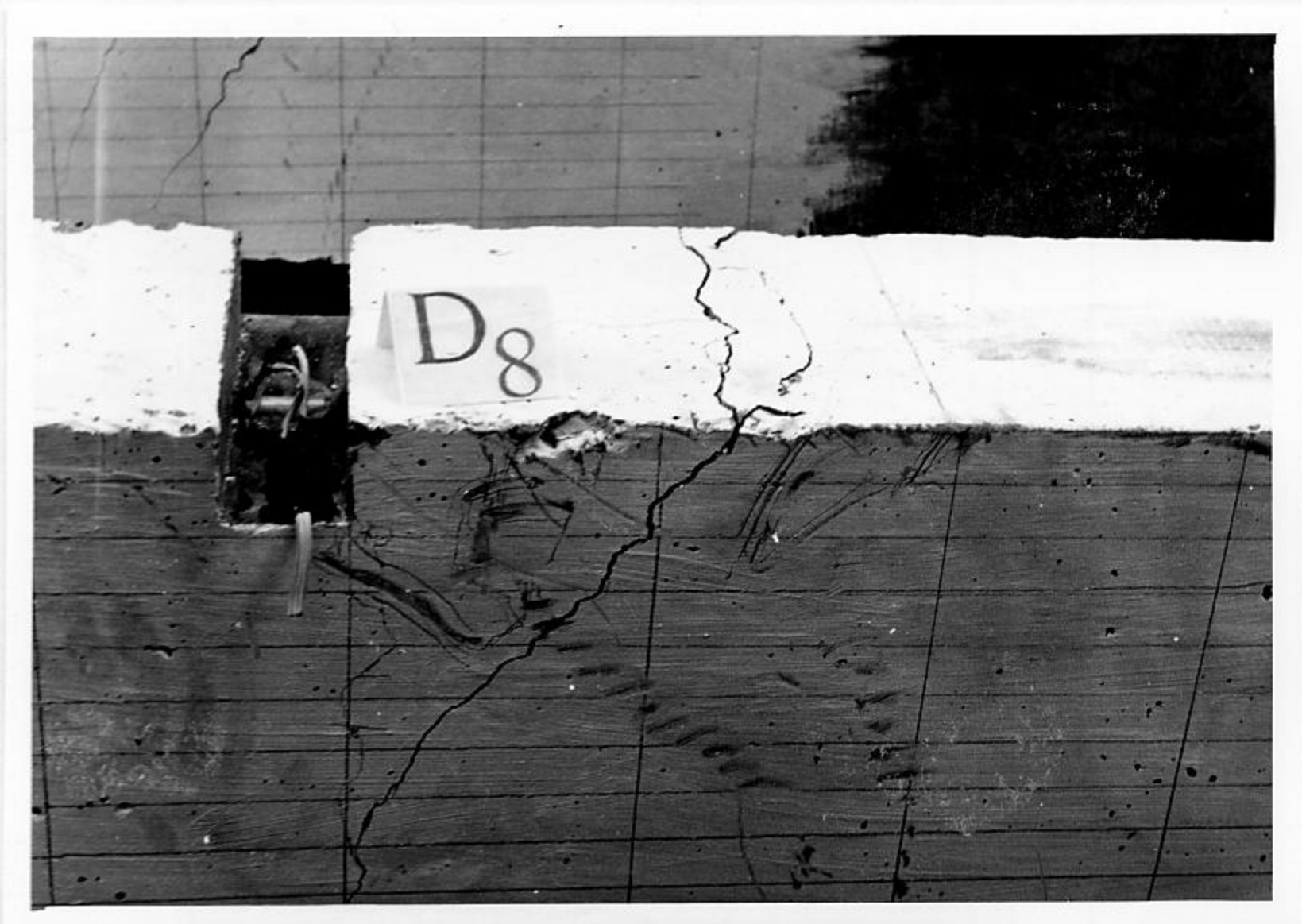
Beam Notation	Mode of Failure
D <sub>12-4-1</sub>	<b>Yielding of Steel and Splitting</b>
D <sub>8-4-1</sub>	Diagonal Tension
D <sub>12-2-1</sub>	Diagonal Tension and Splitting
D <sub>12-1-1</sub>	Diagonal Tension and Splitting
D <sub>15-4-1</sub>	<b>Yielding of Steel and Splitting</b>
D <sub>17-4-1</sub>	<b>Yielding of Steel and Splitting</b>
D <sub>20-4-1</sub>	Tension at inflection point
D <sub>8-4-2</sub>	Diagonal Tension
D <sub>12-4-2</sub>	Splitting
D <sub>12-2-2</sub>	Yielding of Steel and Splitting
D <sub>12-1-2</sub>	Diagonal Tension and Splitting
D <sub>15-4-2</sub>	Yielding of Steel and Splitting
D <sub>20-4-2</sub>	Yielding of Steel and Splitting
D <sub>8-4-3</sub>	Splitting
D <sub>12-4-3</sub>	Yielding of Steel and Splitting
D <sub>10-4-3</sub>	Splitting and Diagonal Tension
D <sub>10-2-3</sub>	Splitting and Diagonal Tension
S <sub>1</sub>	Splitting
S <sub>2</sub>	Splitting

Beam D<sub>8-4-1</sub> at failure

Fig.



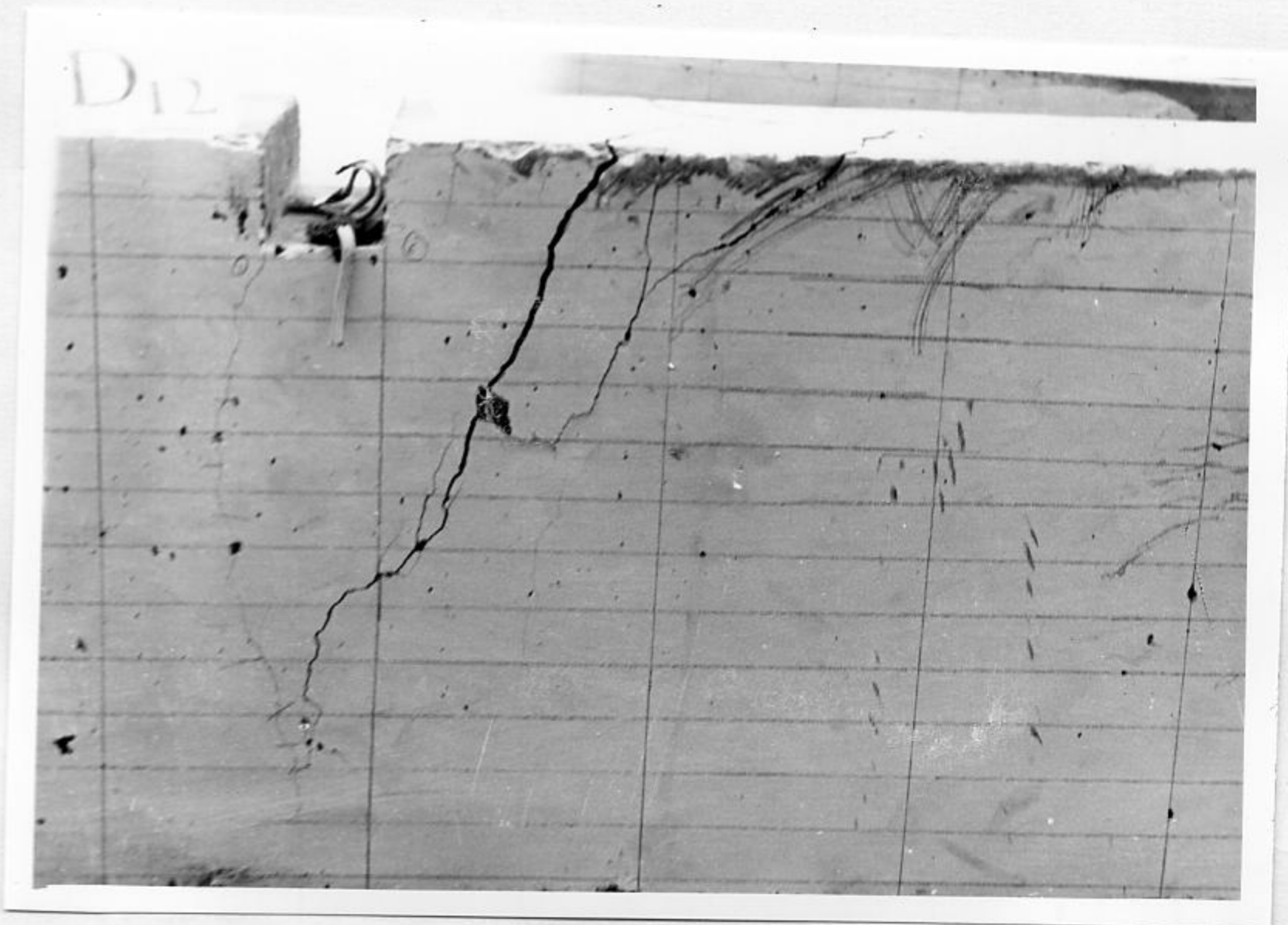
Top View



Pictorial View



Top View



Side View

Beam D15-4-1 at failure



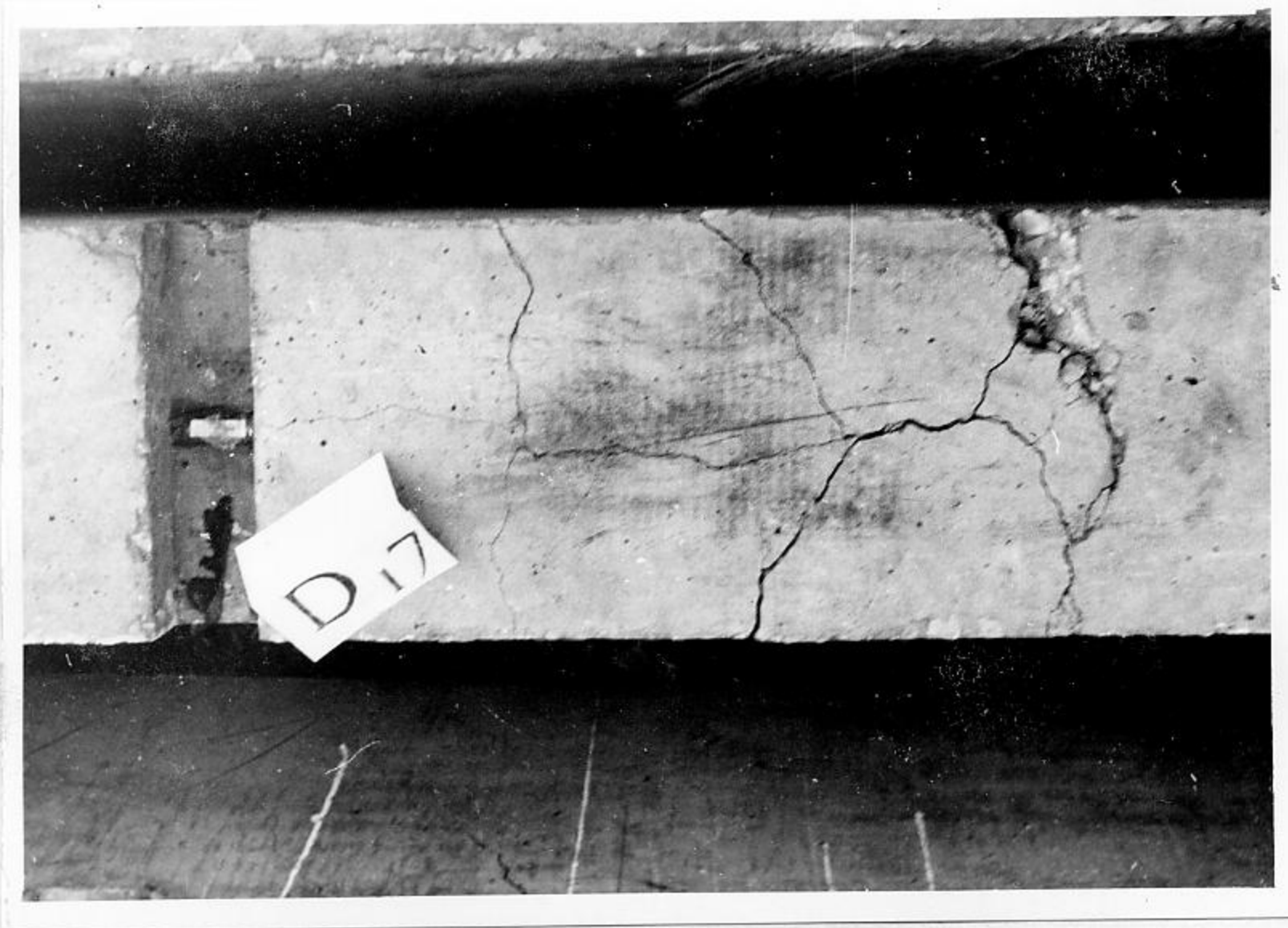
Top View



Pictorial View



D<sub>17-4-1</sub> at failure



Top View

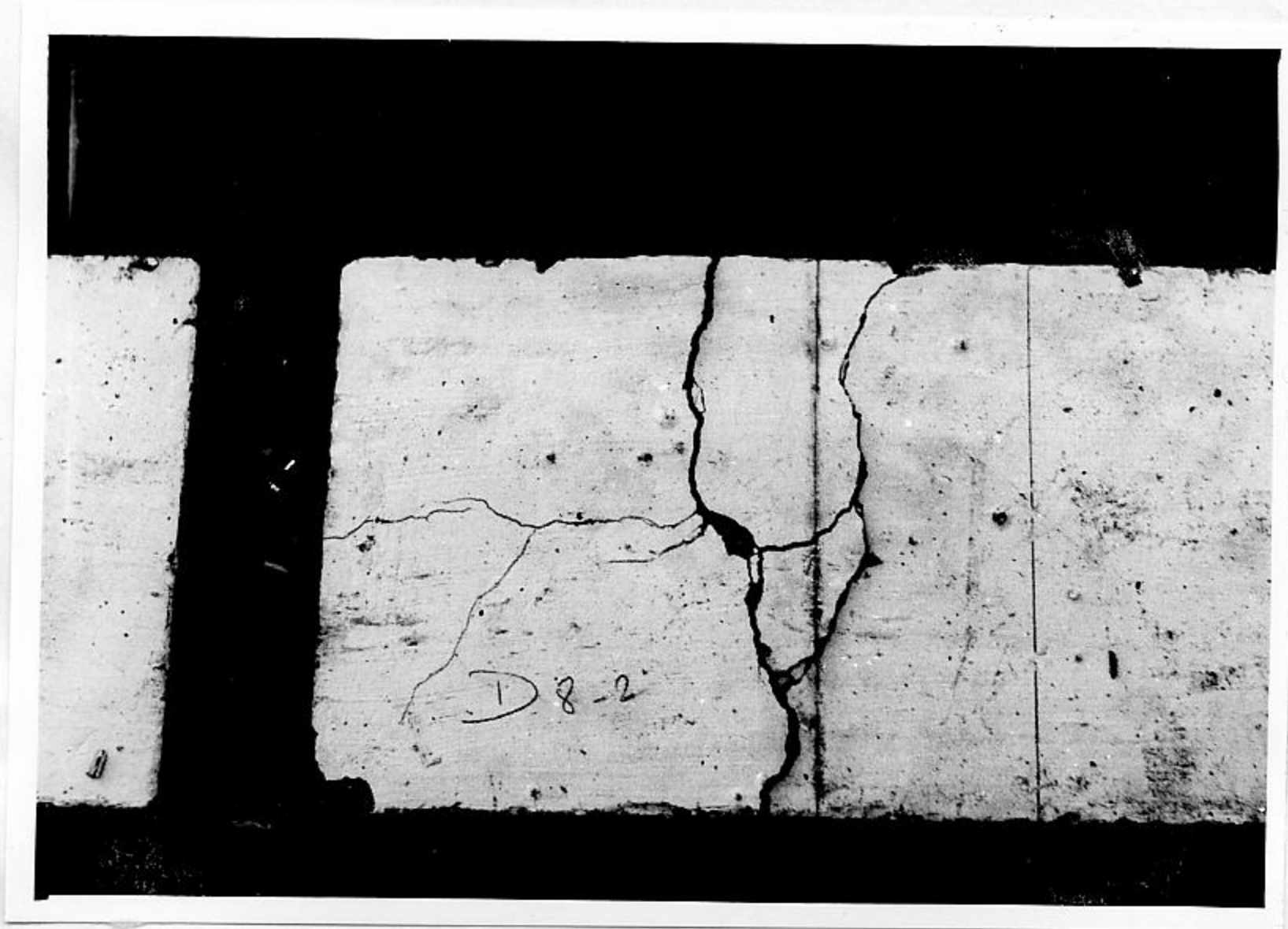
Beam D<sub>20</sub>-4-1 at failure



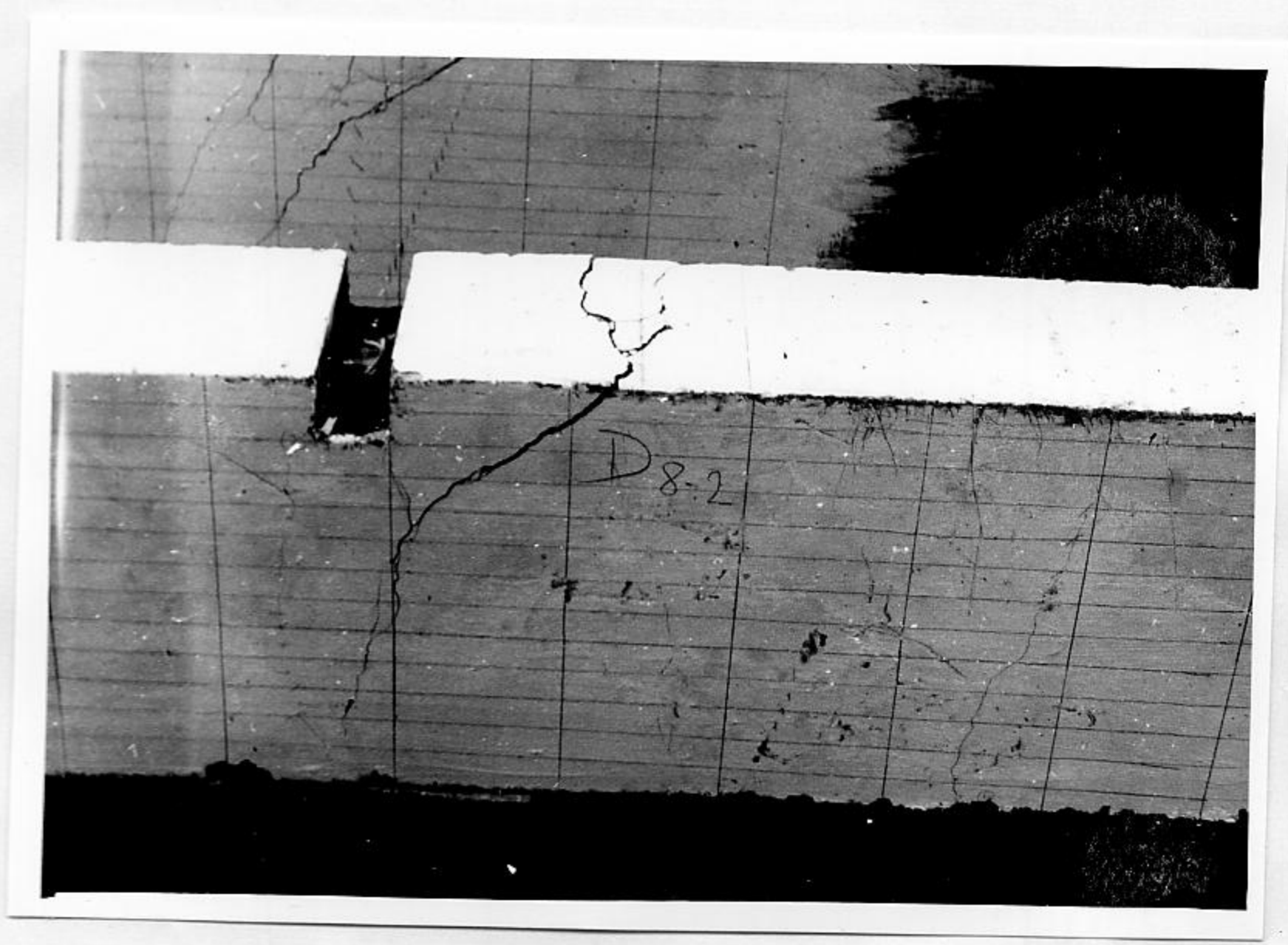
Pictorial View

Beam D<sub>8-4-2</sub> at failure

39



Top View

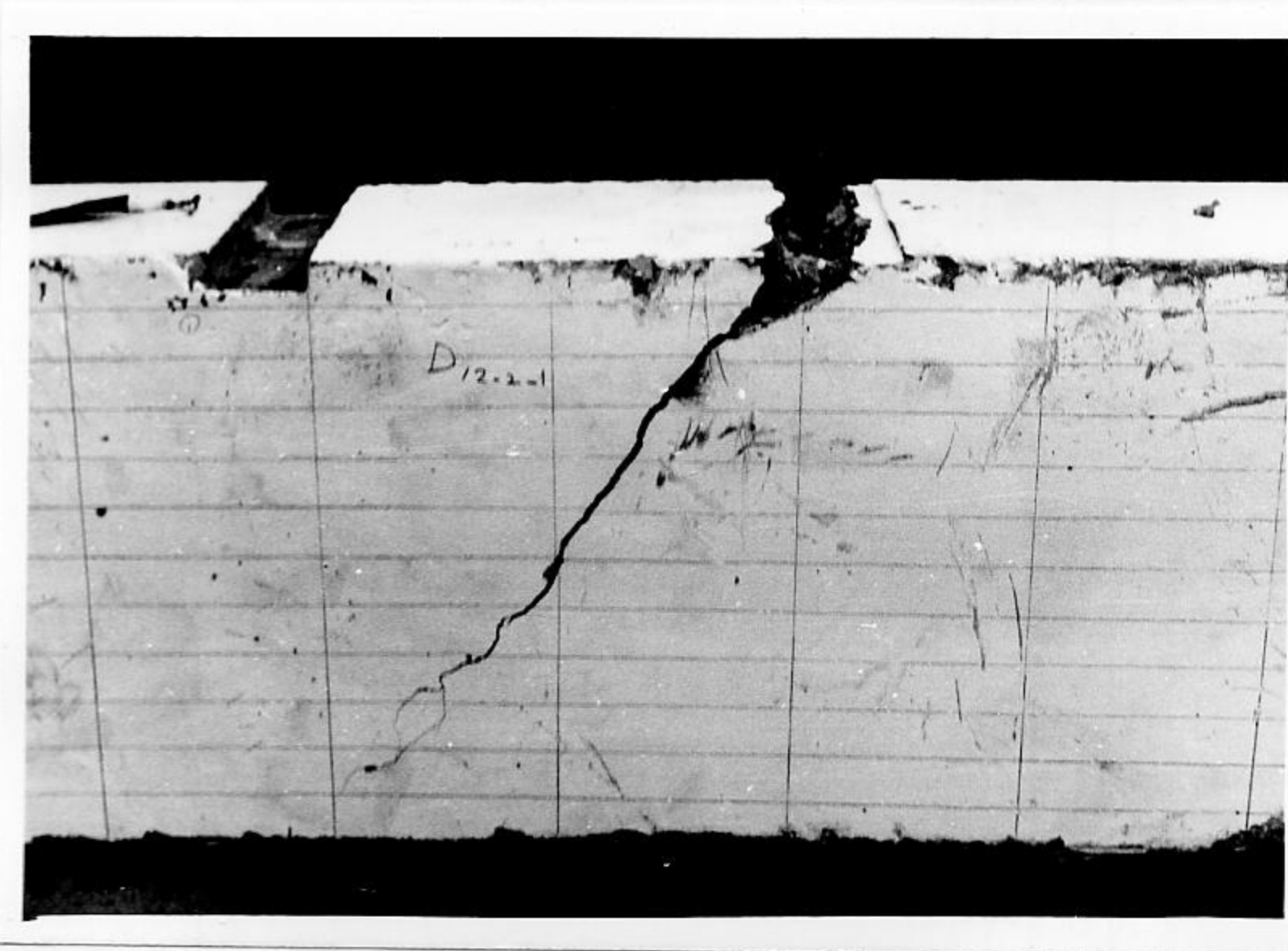


Pictorial View

Beam D<sub>12-1-2</sub> at failure

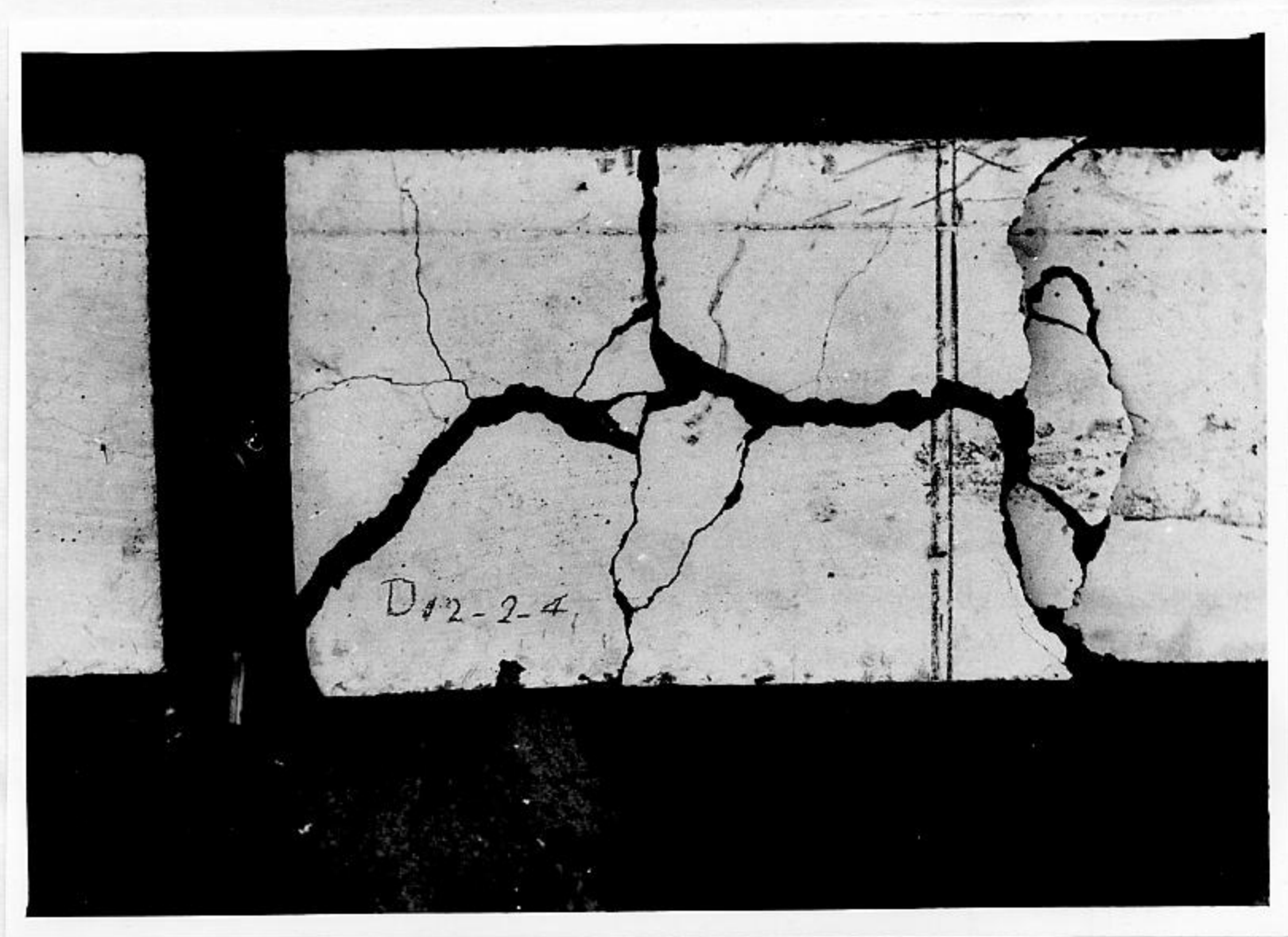


Top View



Side View

Beam D<sub>12-4-2</sub> at failure



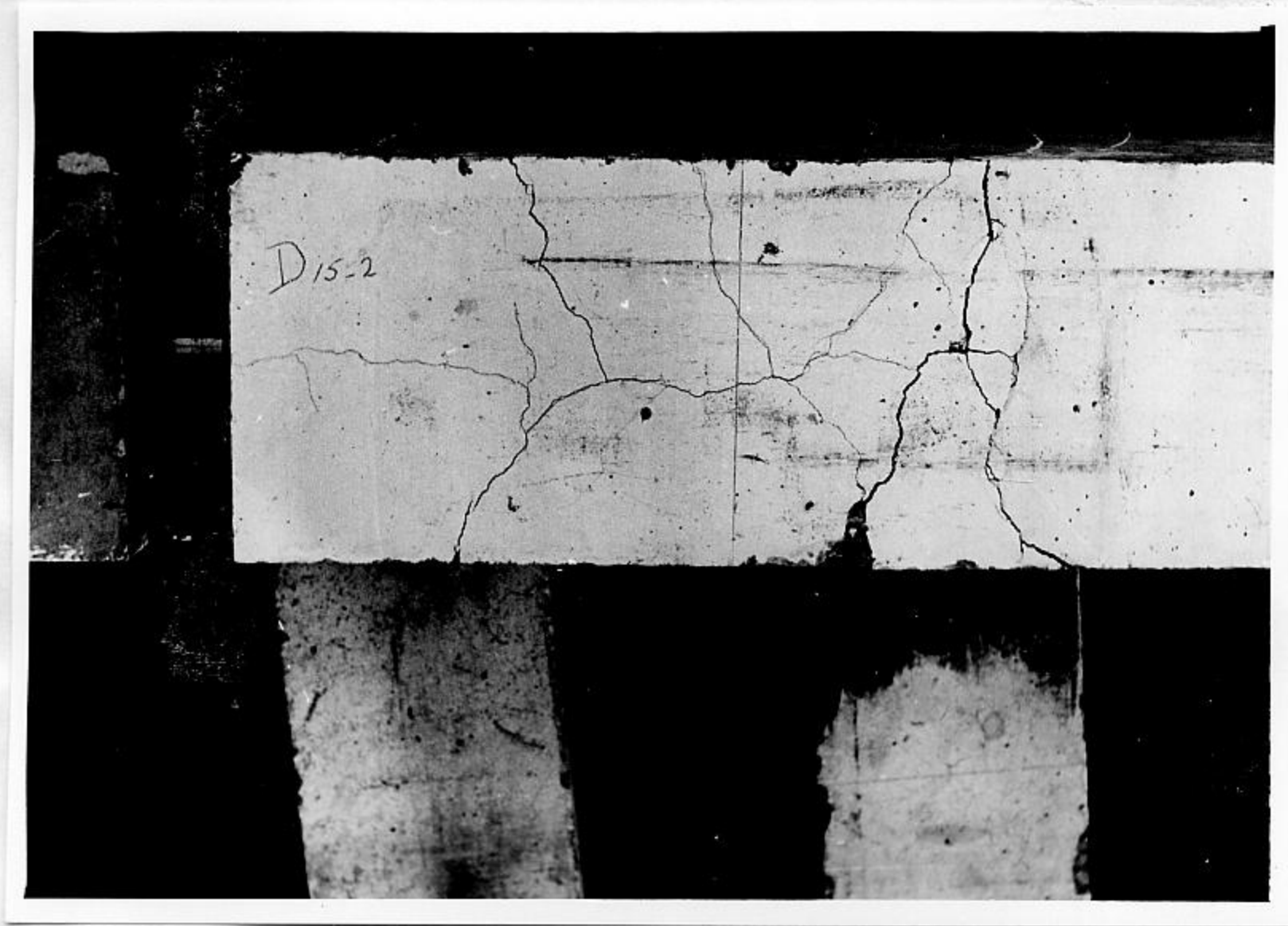
Top View



Side View

Beam D<sub>15-4-2</sub> at failure

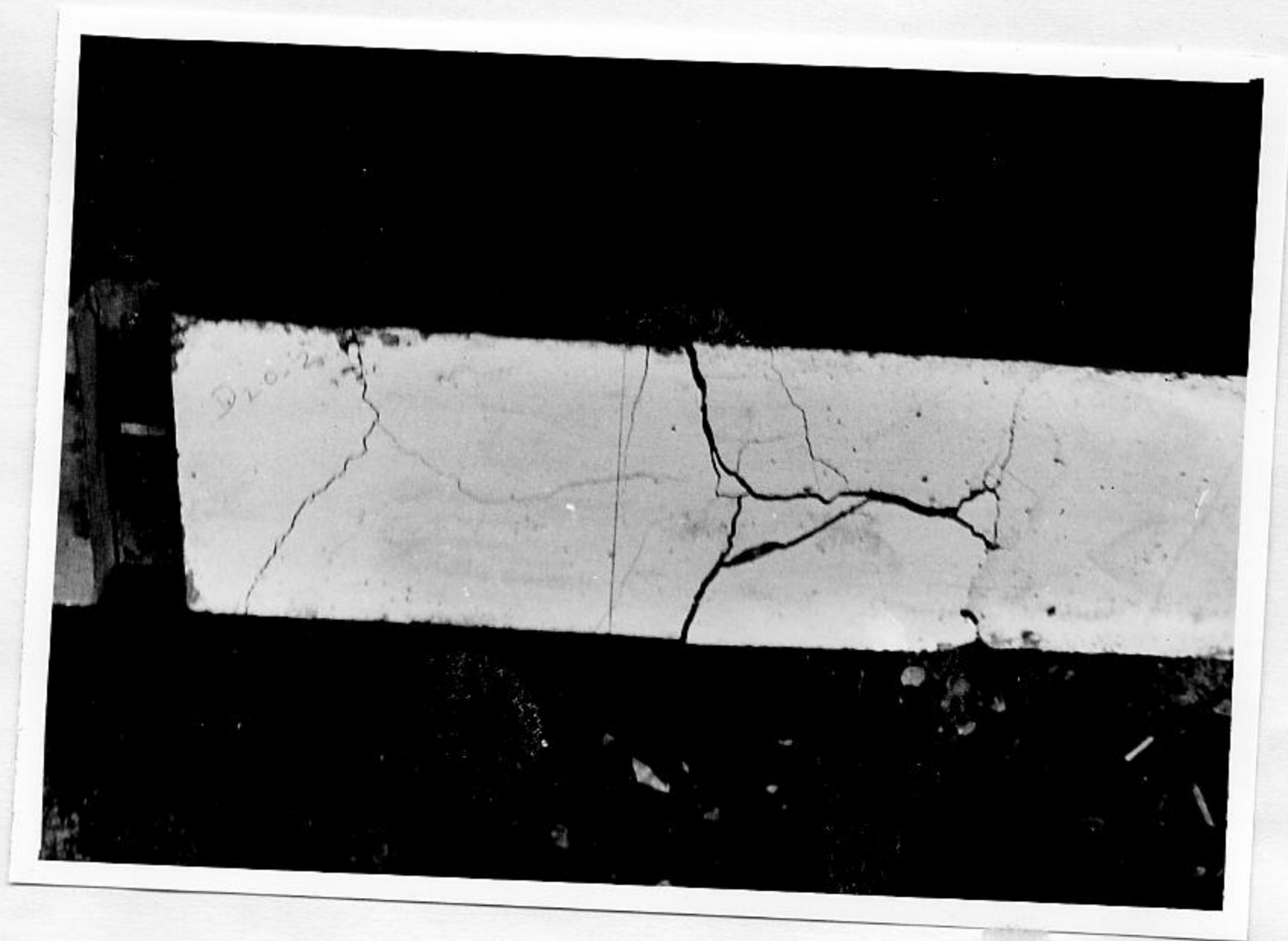
42



Top View

Beam D<sub>20-4-2</sub> at failure

13

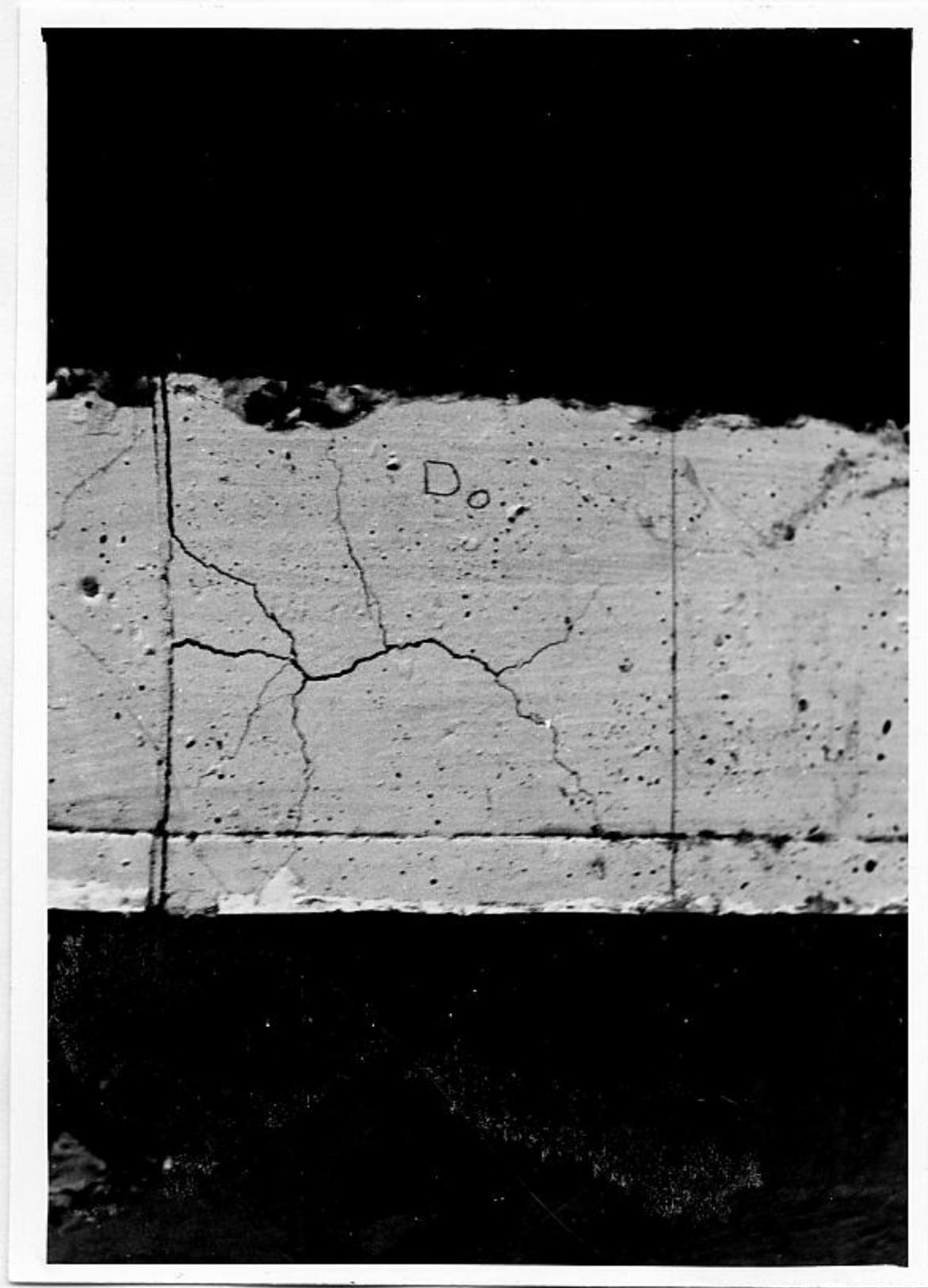


Top View

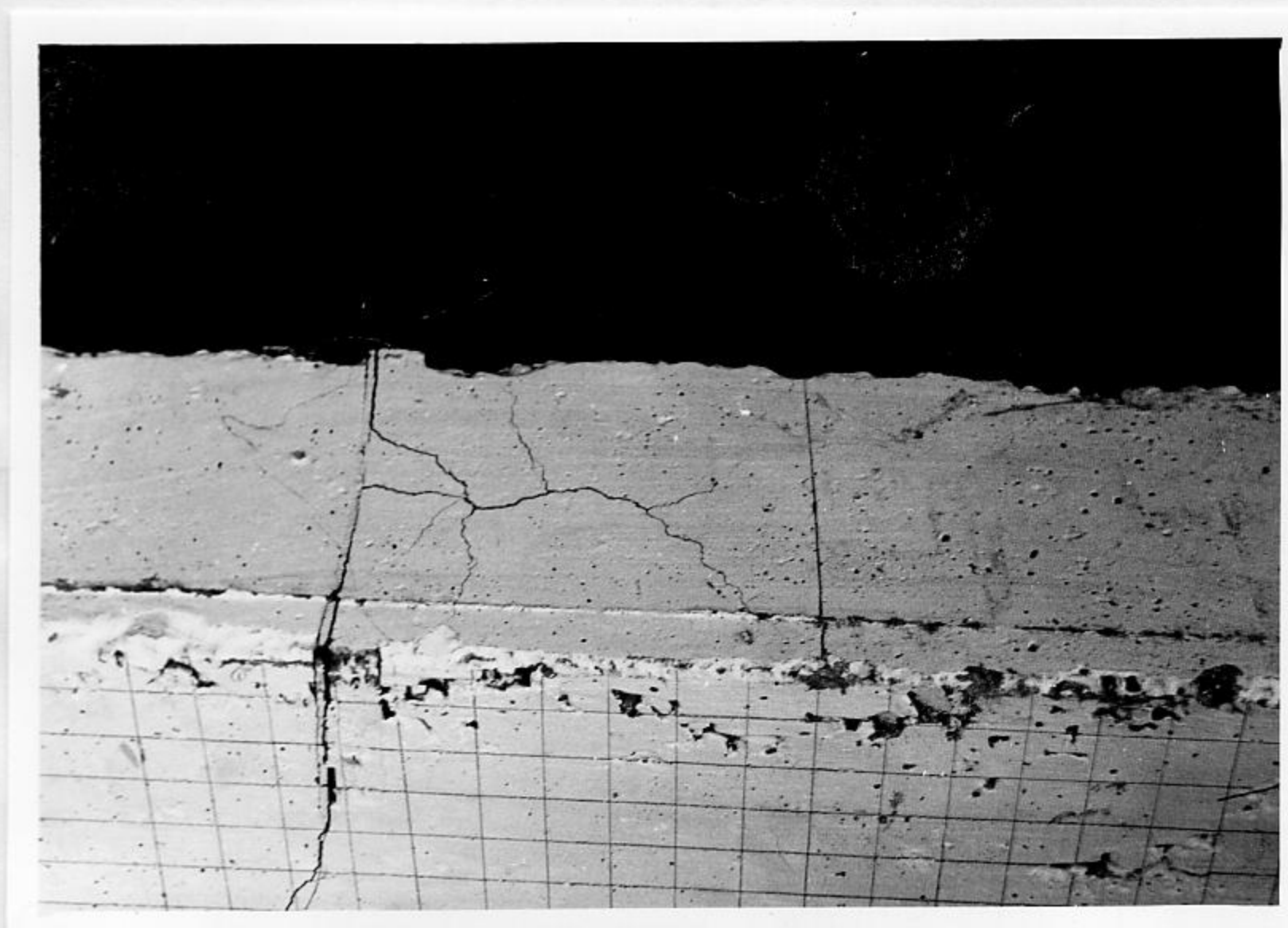


Pictorial View

S  
Beam S<sub>1</sub> at failure



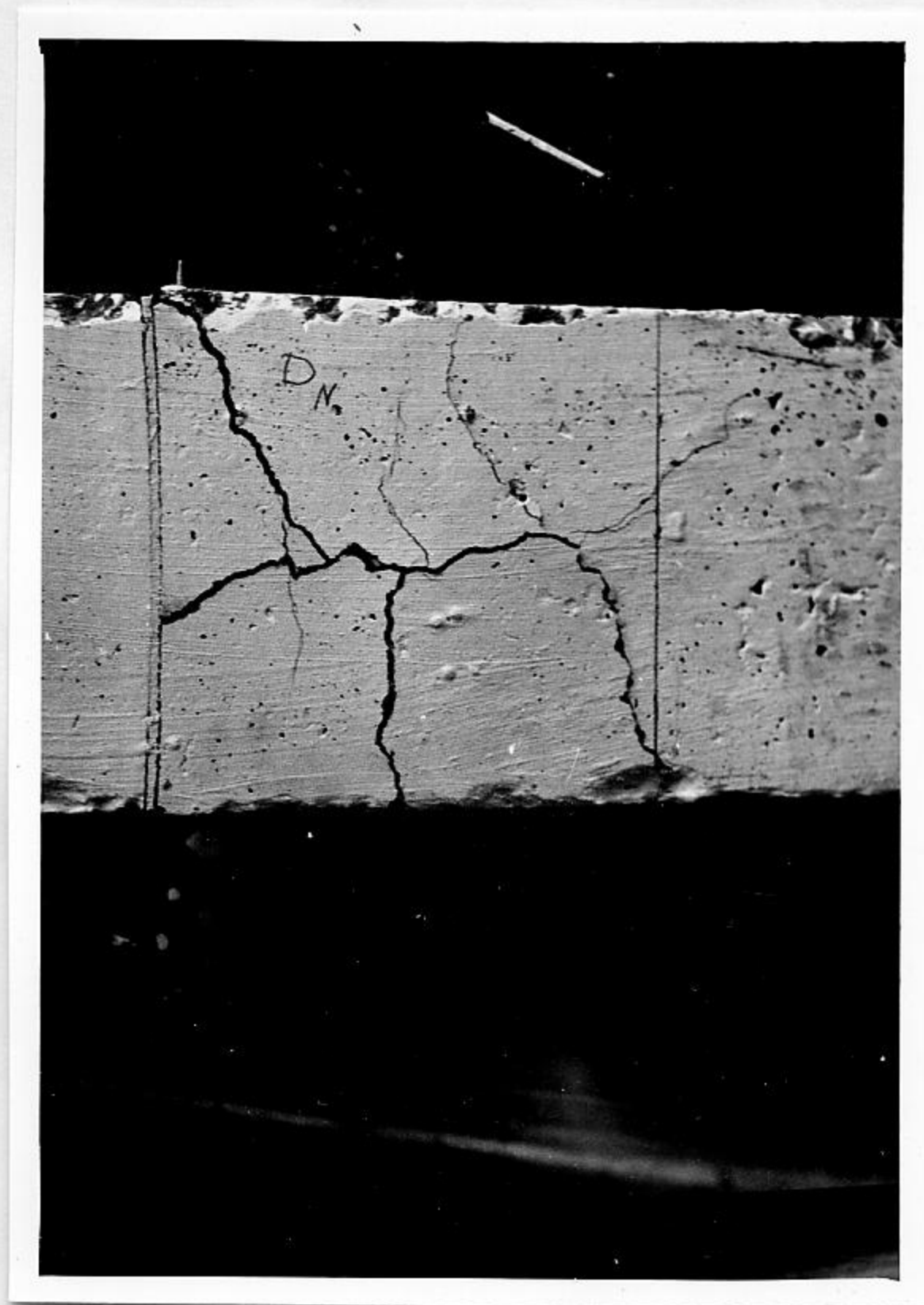
Top View



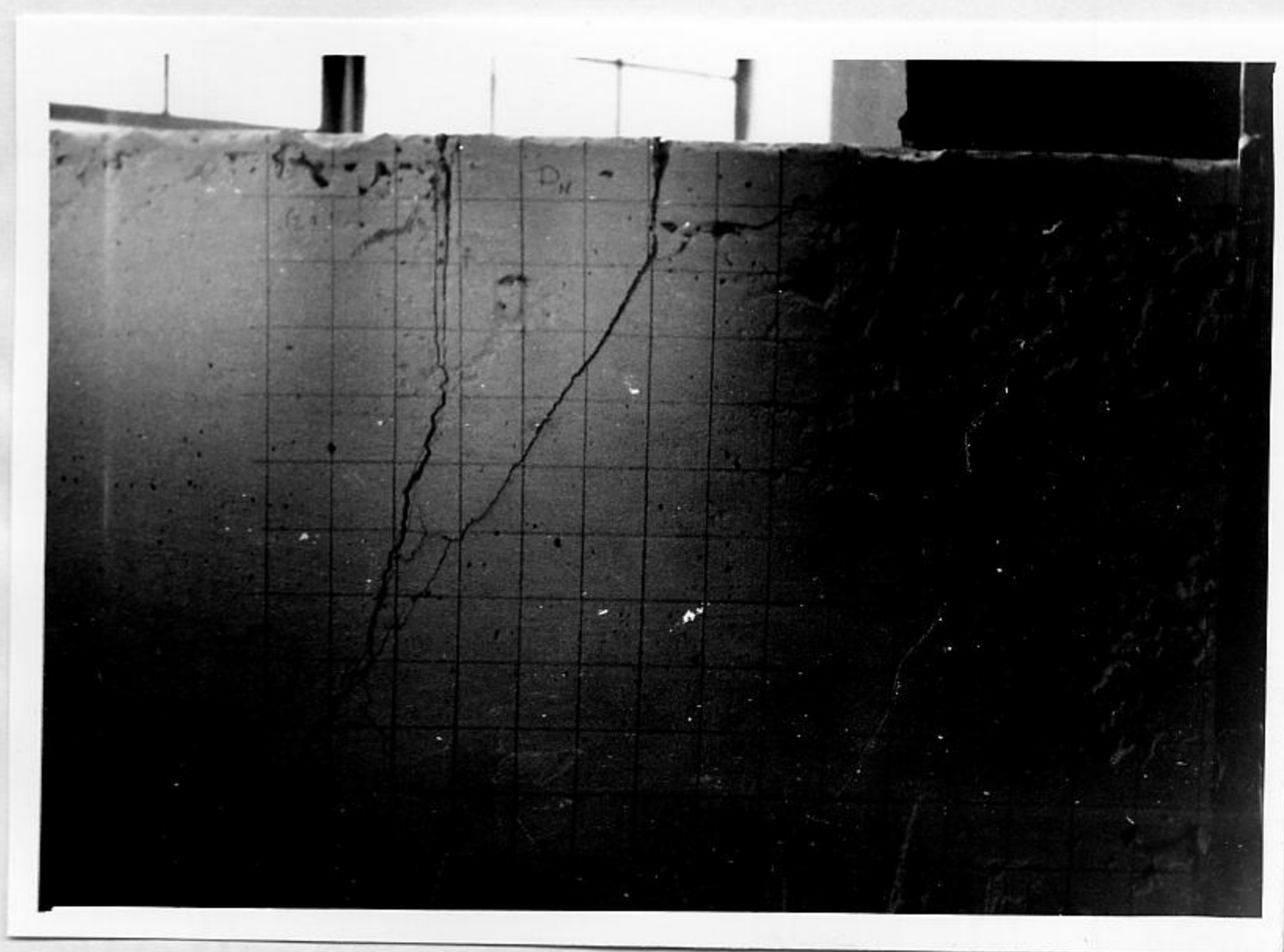
Pictorial View



Beam S<sub>2</sub> at failure



Top View



Side View

## BIBLIOGRAPHY

1. Ferguson, Phil. M. and Thompson, J. Neils: "Development Length of High Strength Reinforcing Bars in Bond," J. ACI, vol. 59, July 1962, p.887.
2. Mathey, Robert G. and Wotstein, David: "Investigation of Bond in Beam and Pullout Specimens with High-Yield-Strength Deformed Bars," J. ACI, vol. 32, March 1961, p. 1071.
3. Regle pour le Calcule et L'execution des Construction en Beton Arme (Regles BA 1960) by Documentation Techniques du Batiment et des Travaux Publics, Article 1,121.
4. Mains, R.M. "Measurement of the Distribution of Tensile and Bond Stresses along Reinforcing Bars," J. ACI, vol. 48, November 1951, p.225.
5. Winter G., Urquhart, L.C., O'Rourke C.E. and Nilson, Arthur H. Design of Concrete Structures. Seventh Edition. McGraw-Hill Book Company.
6. ACI Standard, Building Code Requirements for Reinforced Concrete. (ACI 318-63) June 1963. American Concrete Institute Publication.

ADDITIONAL BIBLIOGRAPHY

not referred to in this work

1. Ferguson, Phil. M. and Thompson, J. Neils. "Development Length for Large High Strength Reinforcing Bars," J. ACI, vol. 62, January 1965, p.71.
2. Ferguson, Phil. M. and Matloob Farid N. "Effect of Bar Cutoff on Bond and Shear Strength of Reinforced Concrete Beams", J. ACI, vol. 31, July 1959, p.5.
3. Ferguson, Phil. M. Reinforced Concrete Fundamentals. Second Edition. Copyright 1965, by John Wiley & Sons, Inc.
4. Makhlof, Hanna M. "The Effect of Bond Stresses upon the Interval of Cracking in Reinforced Concrete Beams". Thesis.
5. Perry, Ervin S. and Thompson J. Neils. " Bond Stress Distribution on Reinforcing Steel in Beams and Pullout Specimens". J. ACI, vol.63, August 1966, p.865.